Delay and Capacity Studies for Mobile Ad Hoc Networks with Transmission-Group Based MAC Protocol

by

Juntao Gao

A dissertation submitted in partial fulfillment
of the requirements for the degree of
Doctor of Philosophy
(The School of Systems Information Science)
in Future University Hakodate
March 2014

To my family

ABSTRACT

Delay and Capacity Studies for Mobile Ad Hoc Networks with Transmission-Group Based MAC Protocol

by

Juntao Gao

As an advanced wireless networking technology, mobile ad hoc networks (MANETs) represent a class of self-configuring and infrastructureless networks with wireless mobile nodes. As MANETs can be rapidly deployed, reconfigured and extended at low cost, they are appealing for many critical application scenarios, like disaster relief, emergency rescue, battle field communications, environment monitoring, etc.

To facilitate the application of MANETs in providing Quality of Service (QoS) guaranteed services for the above scenarios, understanding the end-to-end delay performance of these networks is of fundamental importance. Available works on end-to-end delay in MANETs reported either its upper bounds, or its approximations, both of which will introduce noticeable errors to end-to-end delay evaluations in these networks. However, the analytic end-to-end delay modeling for MANETs still remains elusive, which significantly hinders the development and application of such networks. To this end, this thesis devotes to the study on analytic end-to-end delay modeling for MANETs, where the commonly used Transmission-Group Based MAC protocol (MAC-TG) is adopted to address wireless channel access issues in these networks. Be-

sides delay performance analysis for MAC-TG MANETs, we also provide the study on their throughput capacity.

To analyze the overall end-to-end delay for MAC-TG MANETs, we first study one part of it, i.e., the time a packet experiences in its source node (called source delay hereafter). A powerful theoretical framework based on Quasi-Birth-and-Death (QBD) theory is developed to capture source delay behaviors in highly dynamical MANETs, with which we derive the cumulative distribution function as well as mean and variance of the source delay. By extending the QBD-based theoretical framework, we then study the end-to-end delay performance in the considered MANETs, where a typical two-hop relay routing protocol is employed to deliver packets. Based on the extended theoretical framework, we analytically model the expected end-to-end delay. Extensive simulations are further provided to validate the efficiency of our QBD-based models and end-to-end delay results.

Regarding the throughput capacity for the concerned MAC-TG MANETs, we first determine a general throughput capacity upper bound for these networks, which holds for any feasible packet routing algorithm in such networks. We then prove that the upper bound we determined is just the exact throughput capacity for this class of MANETs by showing that for any traffic input rate within the throughput capacity upper bound, there exists a corresponding two-hop relay algorithm to stabilize such networks. A closed-form upper bound on end-to-end delay is further derived for any traffic input rate within the throughput capacity under the corresponding two-hop relay algorithm. Finally, based on the exact network capacity result, we examine the impacts of transmission range and node density upon network capacity.

ACKNOWLEDGEMENTS

Upon completing this PhD thesis summarizing my three-year research journey in Future University Hakodate, I want to express my thousands of thanks to all who give me generous love, help and encouragement during my studies, which definitely lightens my life of this period and eases research difficulties I have encountered.

First and foremost, I am indebted to my supervisor Professor Xiaohong Jiang. During my PhD pursuit, he gave me a lot of help in both research and life. For research, he introduced me to the fantastic and advanced networking technique Mobile Ad Hoc Networks, guided me to indentify interesting research problems, discussed with me about promising problem solutions and helped me revise research manuscripts. Only with his kindly guidance could I make some research achievements. For life, he also gave me great advices regarding my research career and Japanese learning. It is definitely a great pleasure having Professor Jiang as my supervisor.

I owe my sincere gratitude to Professor Osamu Takahashi. Professor Takahashi organized a wonderful weekly discussion group, in which I reported my research progress to others and received many meaningful suggestions from colleagues as to improve my research work. This discussion group offered me a great chance to practice my English presentation skills. Furthermore, Professor Takahashi gave me financial support for working as his research assistant, which greatly helped to relieve my living expenses.

My thanks also go to my research colleagues under the supervision of Professor

Jiang: Yin Chen, Jinxiao Zhu, Jia Liu, Bin Yang and Yuanyu Zhang. They act as my dear brothers and sisters in life, who accompanied me to spend a lot of pleasing times. I will never forget the parties we held together and the lunches prepared by Yin Chen and Jinxiao Zhu. I want to thank Bin Yang and Yuanyu Zhang for their generous help in moving my home. I really cherish the friendship between me and Jia Liu. It is them who make my life in Japan colorful.

Finally, I want to express my thanks to my family. Words always lose power when it comes to deliver my thanks to my parents. My parents raised me up from a baby to an adult, act as my life mentor, give me unconditional love and continuous support for my life and research. It is them who give me power to carry on when I am faced with challenges and difficult choices. I thank also my young brother who keeps reminding me there is at least one man in the world to back me up. I love them forever.

TABLE OF CONTENTS

LIST OF FIGURES

Figure

CHAPTER I

Introduction

In this chapter, we first introduce mobile ad hoc networks (MANETs) and their critical role in communication networks. We then outline the open problems to be resolved for these networks. Finally, we introduce the organization of this thesis.

1.1 Background of Mobile Ad Hoc Networks

As wireless networking techniques can connect mobile users, extend the distance of cabling services and overcome connecting difficulties of conventional cabling networks, wireless networks have found a lot of applications in our daily life in the past decades, such as the popular cellular data networks (GSM, WiMAX, 3G), local area networks (Wi-Fi, Bluetooth), and satellite communications (GPS, television) [1, 2]. However, wireless networks rely heavily on centralized control systems to function, like base stations and satellites, which are vulnerable to nature disasters and artificial attacks. Motivated by this, a novel distributed wireless networking technique has been proposed recently, termed as mobile ad hoc networks [3–5].

A mobile ad hoc network (MANET) as illustrated in Fig. 1.1 is a collection of mobile node peers which could freely join, move around and leave the network. All these nodes are connected by a wireless channel, through which they autonomously exchange control and management information to form a network. In such a network,

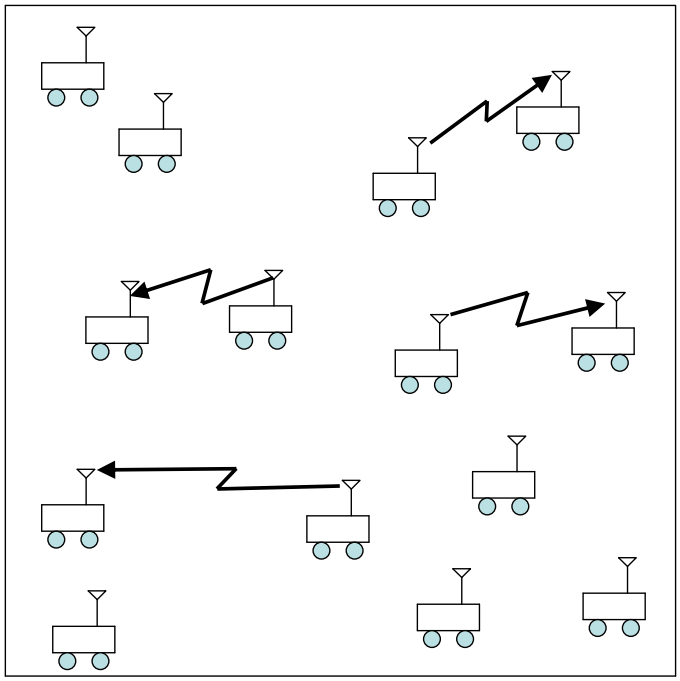

Figure 1.1: An example for a mobile ad hoc network.

nodes transmit their own data to as well as relay data from other node peers such that they manage to deliver their data to destinations in a cooperative and distributed way without the help from any pre-established infrastructures. In a MANET, data typically goes through a multi-hop route of nodes to reach its destination, along which once an intermediate node or more fail, the data could turn to an alternative node to continue its delivery rather than terminates its delivery as in a centralized network.

Due to the distributed structure of MANETs, they possess many appealing features:

- MANETs can be rapidly deployed. Since mobile devices that could function as mobile nodes in a MANET are easy to access in our daily life, like portable computers, mobile phones, PDAs, wireless sensors, etc., they can be easily collected and a MANET could be quickly ready to set up. With plenty of mobile devices, they could be rapidly deployed in many ways, like being scattered by a plane, being distributed by animals or rivers, and being handed out by people.

- MANETs can be quickly reconfigured. As mobile nodes in a MANET could freely roam around over the whole network, once the network configuration is changed in one or several nodes, the reconfigure-control information could be quickly spread like a disease, i.e., whenever a node carrying such information moves into the transmission range of another node who does not have a copy of such information, they would immediately exchange the reconfigure-control information.

- MANETs can be flexibly extended. First, all mobile nodes in a MANET could easily join or leave the network due to mobility, which makes the network physically expandable. Second, the dynamic reconfigure process of the network enables newly joined nodes to quickly function as a node peer, which makes the network logically extendable.

- MANETs are highly robust to node failures. Since mobile nodes are connected through wireless channel which instinctively has the broadcast feature, the ongoing data transmission could be overheard simultaneously by several nodes in the broadcast region and thus one node failure in the region has no impact on the data transmission. On the other hand, if all next-hop nodes fail, the data could also be forwarded to other nodes when such an opportunity arises as the data carrying node move around.

Thanks to these attractive features of MANETs, these networks hold great promises for a lot of critical network application scenarios, such as tactical networks used for military communications, sensor networks used for environment monitoring, emergency rescue for disaster relief, entertainment, etc. MANETs are so promising that they intrigue extensive attentions in either industries or academics, as evident from several ongoing national-scale projects in the USA and Europe, see, for example [6,7]. In USA, DARPA has invested millions of dollars to fund a research group called

IT-MANET to advance Information Theory for Mobile Ad Hoc Networks. The IT-MANET group is composed of the most sophisticated researchers in networking techniques from top universities, like MIT, Northwest, Stanford, UCLA, UC Davis and USC.

1.2 Questions to Be Answered

To facilitate the application of MANETs, researchers have devoted enormous efforts to investigating the performance limits of these networks, like delay [8–11], capacity [12–16], energy [13, 17], of which network delay and capacity are two most fundamental metrics. Network delay is the time it takes a packet to reach its destination after it is generated at its source node. Network capacity is defined as the maximum traffic input rate a MANET could stably support. Both network delay and capacity performance analysis play crucial roles in the development of MANETs. Network capacity provides not only an upper bound on the achievable throughput of a network against which the performance of existing protocols could be compared, but also a guideline for engineers and practitioners to improve network designs [5]. As for network delay, it serves as an essential performance metric for time sensitive applications, like VoIP service, real-time broadcasting and online videos [18,19], based on whose analysis delay guaranteed services could be provided.

However, the study of network delay and capacity in highly dynamic MANETs are challenging. This is because their analysis involve complex cross-layer network dynamics (like those in physical layer, medium access control (MAC) layer and network layer), which will significantly affect data delivery processes and thus the capacity and delay performances in a compound and complicated way. Regarding the dynamics in physical layer, they mainly result from the inherent complex physical characteristics of MANETs, i.e., node mobility, channel fading and interference [15, 20–22]. Since nodes in a MANET could freely roam around over the whole network, two nodes

may meet together at some time and keep their contact for some time duration and then move apart from each other randomly. As a result, mobility dynamics have profound impact on higher layer performances as for whether two nodes are within the transmission range of each other and thus connected to conduct data communication. Even if such connection between two nodes are established, there still exists channel fading issues that may fail the already vulnerable data exchange process. In wireless communications, channel fading comes from attenuation of transmission medium, shadowing caused by obstacles and multipath fading, which can never be ruled out. All these factors may make the transmitted data hardly decoded and thus cause transmission failures. Besides node mobility and channel fading, interference from other concurrent transmissions also plays an important role in disturbing the ongoing data exchange process in the term of signal-to-noise-and-interference ratio.

Regarding the dynamics in MAC layer, they are mainly related to the wireless channel access and interference avoidance issues [23]. In a MANET, data transmissions are conducted through one common wireless channel for all mobile nodes and thus one major issue is to handle how mobile peers access the common wireless channel in a fair and efficient way. As there is no pre-established infrastructure acting as a central controller to coordinate all node transmissions, these mobile nodes have to access the wireless channel in a distributed and possibly cooperative way. In that matter, all nodes will be blind to the situation of other transmissions, which may cause collisions for an ongoing transmission node pairs if a neighboring node also decides to transmit at the same time. On the other hand, the interference caused by simultaneous transmissions may also result in failures for the ongoing transmission. Thus, an MAC protocol for MANETs should carefully deal with wireless channel access and interference avoidance issues, and the resulting randomness from the corresponding MAC protocols will impact higher layer data transmissions.

For the dynamics in network layer, traffic pattern, scheduling policy and routing

protocol are involved. In a MANET, traffic pattern, derived from applications, defines the mapping relationships between source nodes and destination nodes, such as unicast (one source node sends data to a unique destination), multicast (one source node sends data to several selected destinations) and broadcast (one source node sends data to all possible destinations). Under different traffic patterns, the data packets at one source node will create different traffic burdens on network. For any traffic pattern, when multiple packets are present in one mobile node, they are first queued up at that node and once the node accesses the wireless channel, the packets are then scheduled to be transmitted to the next node according to some scheduling policy, like First-In-First-Out, Last-In-First-Out [24], Max-Weight scheduling [25,26], etc. For a scheduled packet, it is left for the routing protocol to decide which node it should be handed over to. Obviously, all above factors of traffic pattern, scheduling policy and routing protocol will affect the whole network delay and capacity performances.

Besides the complex dynamics in each layer, they are actually correlated and have compound effects on network capacity and delay performances [27, 28]. All these dynamics together make the analysis of network delay and capacity challenging. In the past decades, delay analysis for MANETs mainly focused on asymptotic delay analysis (order sense rather than analytic results on network delay). While asymptotic delay results only explore delay scaling trends as network size scales up, it is helpless for engineers to refer to for delay guaranteed protocol design, which can be done only under analytic delay results. On the other hand, network capacity results have been known only for small networks such as two-node network (i.e., Shannon capacity) and for large MANETs, asymptotic capacity (order sense rather than exact results on capacity) were reported [12, 14, 29–31]. Exact network capacity for general MANETs still remains elusive. This is mainly because there lacks powerful theoretical frameworks that could efficiently captures those network dynamics.

1.3 Thesis Organization

This thesis is devoted to analytic delay and capacity studies for MANETs. By adopting the powerful Quasi-Birth-and-Death (QBD) theory and Lyapunov theory, we show that the above cross-layer network dynamics could be nicely incorporated into analytic delay and capacity analysis for MANETs. The rest of this thesis is organized as follows:

Chapter II MANETs Preliminaries. This chapter introduces some preliminaries regarding MANET physical layer models and MAC layer models involved in our delay and capacity studies. We first introduce MANET physical layer models regarding what kind of network structure we consider (network model), how nodes move in our considered MANET (node mobility model) and how two nodes conduct one-hop communication (communication model). After establishing basic physical layer models, we then introduce the MAC protocol which is adopted by mobile nodes in the considered MANET to access wireless channel. Specifically, we employ the commonly used Transmission-Group (TG) based MAC protocol (MAC-TG for short).

Chapter III Source Delay for MAC-TG MANETs. In this chapter, we focus on the study of source delay which constitutes an essential part of end-to-end delay and thus serves as a fundamental quantity for delay performance analysis in networks. We first review the available works on partial delay studies, and then introduce a general packet dispatching scheme with dispatch limit f (PD-f for short) for source nodes to dispatch packets. We then apply the Quasi-Birth-and-Death (QBD) theory to develop a theoretical framework to capture the complex packet dispatching process in PD-f MANETs. With the help of the theoretical framework, we derive the cumulative distribution function as well as mean and variance of the source delay in such networks. Finally, extensive simulation and theoretical results are provided to validate our source delay analysis and illustrate how source delay in

MANETs are related to network parameters, such as packet dispatch limit, buffer size and packet dispatch probability.

Chapter IV End-to-End Delay for MAC-TG MANETs. In this chapter, we study the fundamental end-to-end delay performance in MANETs. We first summarize available works on end-to-end delay analysis in MANETs and point out their limitations, and then introduce the traffic pattern under which we conduct our end-to-end delay study. We then extend the QBD theory-based theoretical framework in Chapter III to efficiently capture the complex dynamics in the considered MANETs. We show that with the help of this theoretical framework, analytic results can be derived for expected end-to-end delay and also per node throughput capacity for MANETs. Simulation and numerical results are further provided to illustrate the efficiency of these QBD theory-based models as well as our theoretical findings.

Chapter V Throughput Capacity for MAC-TG MANETs. In this chapter, we analyze the throughput capacity for MAC-TG MANETs. First, related works on throughput capacity analysis for MANETs are reviewed and their limitations are outlined. We first introduce assumptions about the traffic pattern we consider for throughput capacity study of MANETs. Starting with the condition of network stability, we then determine a throughput upper bound for the network throughput in the considered MAC-TG MANETs. Then, we prove that the determined throughput upper bound is just the throughput capacity for the considered MANETs.

Chapter VI Conclusion. This chapter concludes the whole thesis, summarizing the contributions made by this thesis towards analytic delay and capacity studies in MANETs. We also discuss possible directions that merit future study.

CHAPTER II

MANETs Preliminaries

In this chapter, we introduce the models of MANETs under which the delay and capacity studies are conducted. We introduce first the basic network physical layer models, regarding network structure, node mobility and node communication in MANETs, and then the Transmission-Group Based Medium Access Control (MAC-TG) Protocol for transmission scheduling to resolve wireless channel access and interference issues in the concerned MANETs.

2.1 Physical Layer Models

2.1.1 Network Model

We consider a MANET of unit square area as illustrated in Fig. 2.1, in which there are n nodes roaming around randomly and independently. All these nodes conduct data transmission through one common wireless channel.

In such a square MANET, when a node arrives at its border, it can no longer move forward along its moving direction. Such phenomenon is called border effect, which will introduce more complexity for performance analysis while bringing less insight. Thus, similar to previous works [11, 32, 33], we assume the square area in Fig. 2.1 to be a torus, i.e., the square area being wrapped up with each border connecting to its

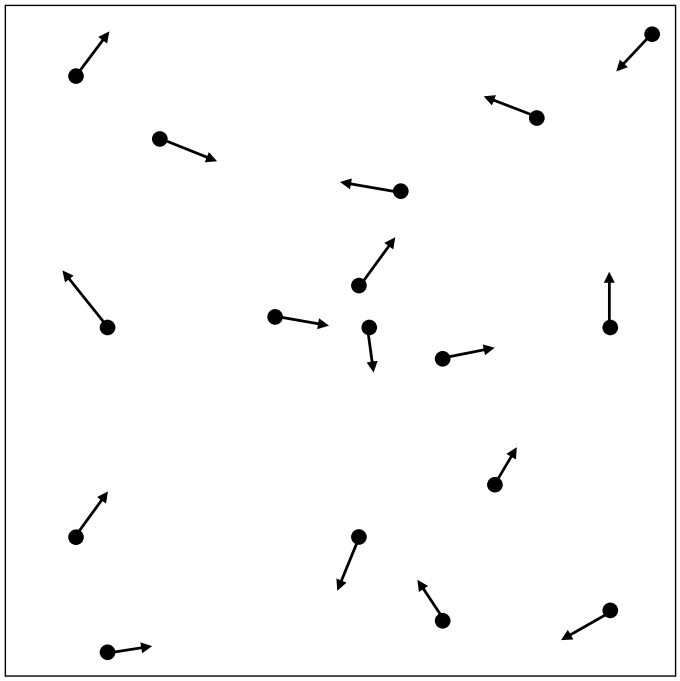

Figure 2.1: An example for a MANET, in which mobile nodes are represented by dots.

opposite border, such that a node could move seamlessly around the whole network without borders.

To facilitate the operation of the torus MANET like node mobility and data transmission, we discretize the network both in time and in space [11, 16, 32–36]. As for time, it is divided into discrete time slots with equal duration, and for space, the network area is partitioned into $m \times m$ square cells shown in Fig. 2.3 [1]. In such a MANET with discretized time and space, all nodes move from time slot to time slot and from cell to cell, and they contend for wireless channel based on time slots also. The events happening in MANETs based on discrete time slots are illustrated in Fig. 2.2. As indicated in [11, 16, 32–36], such discretized time and network area could also ease theoretical performance analysis in MANETs.

[1]Notice that a discretized network serves as an approximation to the real continuous network, and the approximation accuracy could be flexibly controlled by properly setting the length of time slot durations and the size of square cells.

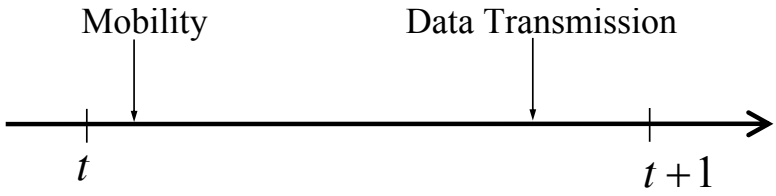

Figure 2.2: Illustration of events happening in a MANET.

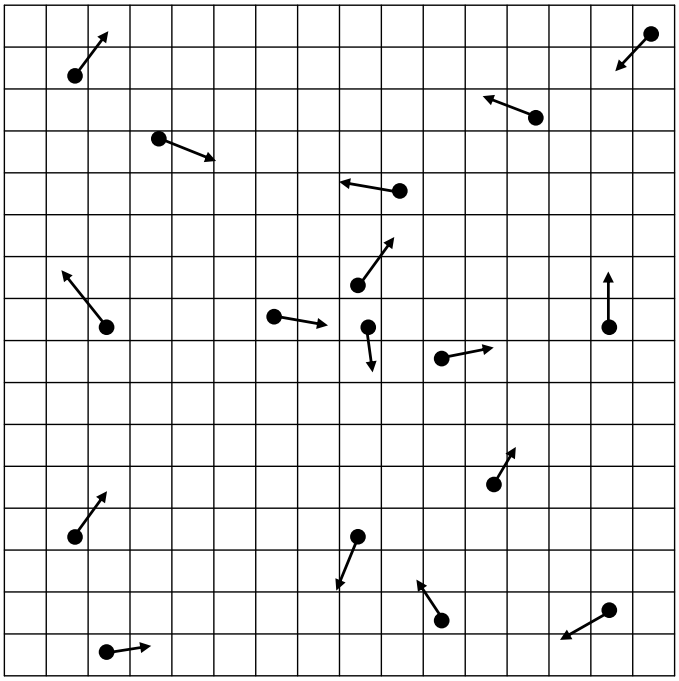

Figure 2.3: Illustration of the partition for a MANET.

2.1.2 Mobility Model

In the discrete MANET, we assume all nodes move following the Independent and Identically Distributed (i.i.d.) mobility model, which has been widely adopted in the literature [15, 16, 35–38]. According to the i.i.d. mobility model, every node moves independently from others, and at the beginning of every time slot, each node first chooses a cell randomly and uniformly from all cells in the network as its destination cell, and then moves into that chosen cell and stays in it for the whole time slot. Under such i.i.d. mobility model, all nodes change their cell positions drastically from time slot to time slot, resulting in uniform distribution of nodes in the network every time slot. Such network topology changes under i.i.d. mobility model represent the sample

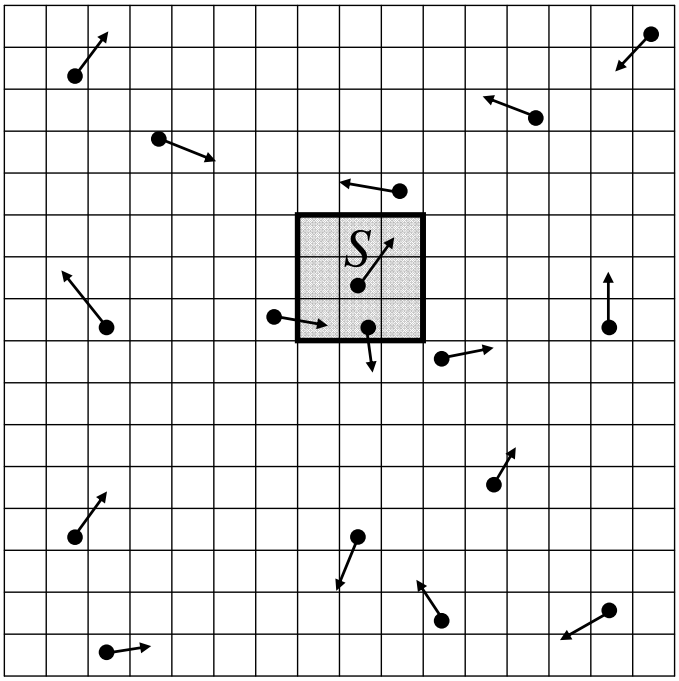

Figure 2.4: Transmission range of a node in a MANET.

points of any long-run network topology changes under other mobility models with the same uniform distribution. Thus, the analysis conducted under i.i.d. mobility model serves as a meaningful performance bound for other mobility models [16].

2.1.3 Communication Model

In a time slot, after nodes move according to the i.i.d. mobility model, they will conduct data transmissions through one common wireless channel. We assume that all nodes transmit data through one common wireless channel, and each node (say S in Fig. 2.4) employs the same transmission range $r = \sqrt{8}/m$ to cover 9 cells, including S's current cell and its 8 neighboring cells.

It is notable that multiple nodes may transmit data simultaneously in the current time slot, which may cause mutual interference and thus transmission interruption. To account for mutual interference and interruption among concurrent transmissions, the commonly used protocol model is adopted here as illustrated in Fig. 2.5 [12,32,36,39].

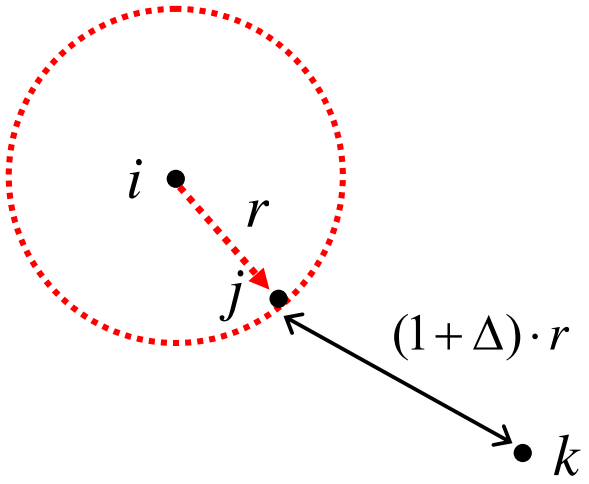

Figure 2.5: Protocol model in a MANET.

According to the protocol model, node i could successfully transmit to another node j if and only if $d_{ij} \leq r$, where r denotes the common transmission range employed by nodes, and for another simultaneously transmitting node $k \neq i, j$, $d_{kj} \geq (1+\Delta)\cdot r$, where d_{ij} denotes the Euclidean distance between node i and node j and $\Delta \geq 0$ is the guard factor to prevent interference. In a time slot, the data that can be transmitted during a successful transmission is normalized to one packet.

2.2 MAC Layer Models

In a time slot, we adopt a commonly used MAC protocol to address wireless medium access issue in the considered MANET, which is based on the concept of Transmission-Group (MAC-TG for short) [32, 33, 36, 39].

2.2.1 TG Definition

As illustrated in Fig. 2.6 that a Transmission-Group (TG) consists of a group of cells with any two of them being separated by a horizontal and vertical distance of some integer multiple of α ($1 \leq \alpha \leq m$) cells. In Fig. 2.6, each TG is labeled with a unique number and all shaded cells belong to the same TG 1. The whole network

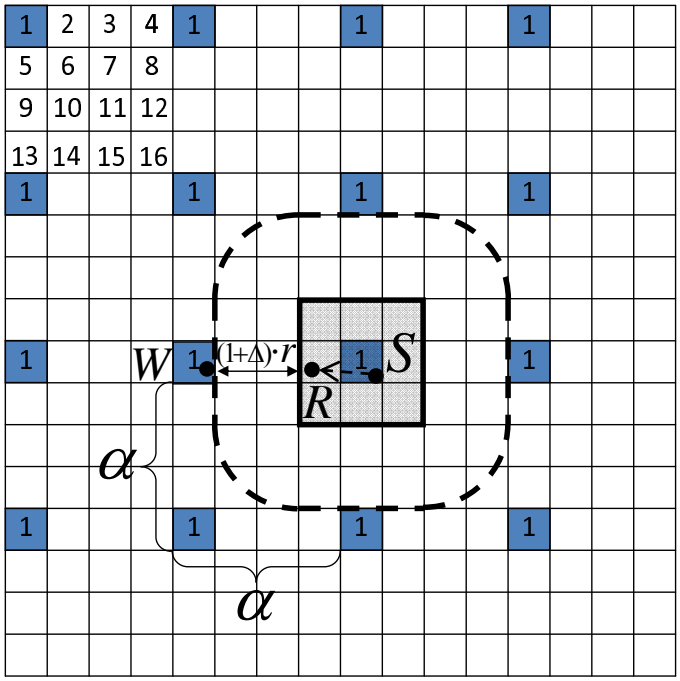

Figure 2.6: Illustration of MAC-TG protocol.

cells are then divided into α^2 TGs and each TG consists of $K = \lfloor m^2/\alpha^2 \rfloor$ cells, where $\lfloor \cdot \rfloor$ is the floor function.

2.2.2 MAC-TG Operations

Under the MAC-TG protocol, TGs are activated alternatively from time slot to time slot, i.e., each TG is activated every α^2 time slots to schedule data transmissions. We call cells in an activated TG as active cells, and only a node in an active cell could access the wireless channel and do packet transmission. If there are multiple nodes in an active cell, one of them is selected randomly to have a fair access to wireless channel.

To avoid interference among concurrent transmissions under the MAC-TG protocol, the parameter α should be set properly. Suppose a node (say S in Fig. 2.6) in an active cell is transmitting to node R at the current time slot, and another node W in one adjacent active cell is also transmitting simultaneously. As required by

the protocol model, the distance d_{WR} between W and R should satisfy the following condition to guarantee successful transmission from S to R,

$$d_{WR} \geq (1 + \Delta) \cdot r \tag{2.1}$$

Notice that $d_{WR} \geq (\alpha - 2)/m$, we have

$$(\alpha - 2)/m \geq (1 + \Delta) \cdot r \tag{2.2}$$

Since $\alpha \leq m$ and $r = \sqrt{8}/m$, α should be set as

$$\alpha = \min\{\lceil (1 + \Delta) \cdot \sqrt{8} + 2 \rceil, m\}, \tag{2.3}$$

where the function $\lceil x \rceil$ returns the least integer value greater than or equal to x.

Remark 1 *It is notable that the Transmission-Group based scheduling scheme has been widely adopted for distributed MANETs [32, 33, 35, 39], whose implementation involves acquiring the information of what time slot it is currently and which cell a node stays within at that time slot. Such information could be obtained by each node through the Global Positioning System (GPS), which provides accurate time and location information [40] and thus facilitates the operation of distributed MANETs [3, 41]. With the help of GPS, the group-based scheduling can be easily implemented as follows. Based on GPS, we know the current time slot t and thus can easily determine the index of current active group as $|t|_{\alpha^2} + 1$, where $|\cdot|_h$ denotes the modulus-h operation and α^2 is just the number of groups in a MANET. With the active group index, a node can then tell whether it stays within an active cell at current time slot t based on its cell location information from GPS. If the node is in an active cell, then it has opportunities to transmit data.*

2.3 Summary

In this chapter, we establish the essential MANET models for the following delay and capacity performance analysis. The models include physical layer models and MAC layer model. For physical layer, we introduce the network structures regarding time and space, node mobility model and communication model. For MAC layer, we introduce the TG based MAC protocol to address channel access issues.

CHAPTER III

Source Delay for MAC-TG MANETs

Source delay, the time a packet experiences in its source node, is an indispensable behavior in any network. Since the source delay is a delay quantity common to all MANETs, it serves as a fundamental quantity for delay performance analysis in MANETs. For MANETs without packet redundancy [15, 16] and with one-time broadcast based packet redundancy [42], the source delay actually serves as a practical lower bound for and thus constitutes an essential part of overall end-to-end delay in those networks. The source delay is also an indicator of packet lifetime, i.e., the maximum time a packet could stay in a network; in particular, it lower bounds the lifetime of a packet and thus serves as a crucial performance metric for MANETs with packet lifetime constraint. We conduct a thorough source delay study in this chaper.

3.1 Related Works and Their Limitations

The available works on partial delay study (with respect to overall end-to-end delay) in MANETs mainly focus on the delivery delay analysis [8, 36, 43–48] and local delay analysis [49–51].

The delivery delay, defined as the time it takes a packet to reach its destination after its source starts to deliver it, has been extensively studied in the literature. For sparse MANETs without channel contentions, the Laplace-Stieltjes transform of

delivery delay was studied in [8]; later, by imposing lifetime constraints on packets, the cumulative distribution function and n-th order moment of delivery delay were examined in [43, 47]; the delivery delay was also studied in [44, 45, 48] under different assumptions on inter-meeting time among mobile nodes. For more general MANETs with channel contentions, closed-form results on mean and variance of delivery delay were recently reported in [36].

Regarding the local delay, i.e. the time it takes a node to successfully transmit a packet to its next-hop receiver, it was reported in [49] that some MANETs may suffer from a large and even infinite local delay. The work [50] indicates that the power control serves as a very efficient approach to ensuring a finite local delay in MANETs. It was further reported in [51] that by properly exploiting node mobility in MANETs it is possible for us to reduce local delay there. Despite much research activity on delay performance analysis in MANETs, the source delay performance of such networks is still largely unknown by now.

3.2 System Assumptions

In a MAC-TG MANET, we further introduce the following assumptions for our source delay study, including traffic pattern regarding packet generating in the network and a packet dispatch scheme for source nodes to dispatch generated packets.

3.2.1 Traffic Pattern

We consider the widely adopted permutation traffic model [32, 36, 38], where there are n distinct traffic flows in the network as illustrated in Fig. 3.1. Under such traffic model, each node acts as the source of one traffic flow and at the same time the destination of another traffic flow. The packet generating process in each source node is assumed to be a Bernoulli process, where a packet is generated by its source node with probability λ in a time slot [16].

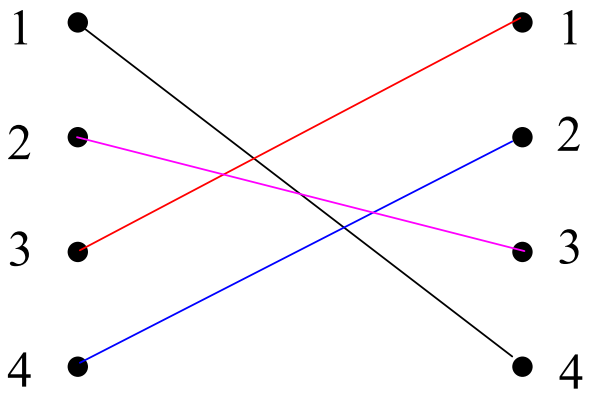

Figure 3.1: An example for permutation traffic in a MANET with 4 nodes.

We assume that each source node has a first-come-first-serve queue (called source-queue hereafter) with limited buffer size $M > 0$ to store its locally generated packets. Each locally generated packet in a source node will be inserted into the end of its source-queue if the queue is not full, and dropped otherwise.

3.2.2 Packet Dispatch Scheme

In a MAC-TG MANET, once a node (say S) got access to the wireless channel according to the MAC-TG protocol in a time slot, it then executes a general packet dispatch scheme with dispatch limit f (PD-f for short) summarized in Algorithm 1 for packets dispatch, where a same packet will be dispatched out up to f times by its source node such that packet dispatching process can be flexibly controlled through a proper setting of f.

Remark 2 *The PD-f scheme is general and covers many widely used packet dispatching schemes as special cases, like the ones without packet redundancy [15, 16, 34] when $f = 1$ and only unicast transmission is allowed, the ones with controllable packet redundancy [35, 36, 44] when $f > 1$ and only unicast transmission is allowed, and the ones with uncontrollable packet redundancy [42, 52] when $f \geq 1$ and broadcast transmission is allowed.*

Algorithm 1 PD-f scheme

```
1: if S has packets in its source-queue then
2:    S checks whether its destination D is within its transmission range;
3:    if D is within its transmission range then
4:       S transmits the head-of-line (HoL) packet in its source-queue to D; {source-
         destination transmission}
5:       S removes the HoL packet from its source-queue;
6:       S moves ahead the remaining packets in its source-queue;
7:    else
8:       With probability q (0 < q < 1), S dispatches the HoL packet;
9:       if S conducts packet dispatch then
10:         S dispatches the HoL packet for one time; {packet-dispatch transmission}
11:         if S has already dispatched the HoL packet for f times then
12:            S removes the HoL packet from its source-queue;
13:            S moves ahead the remaining packets in its source-queue;
14:         end if
15:      end if
16:   end if
17: else
18:   S remains idle;
19: end if
```

3.3 Source Delay Modeling

In this section, a QBD-based theoretical framework is developed to capture the packet dispatching process in a MAC-TG MANET with PD-f scheme (PD-f MANET for short). This framework will help us to analyze source delay in Section 3.4.

3.3.1 QBD-Based Theoretical Framework

Due to the symmetry of source nodes, we only focus on a source node S in our analysis. We adopt a two-tuple $\mathbf{X}(t) = (L(t), J(t))$ to define the state of the source-queue in S at time slot t, where $L(t)$ denotes the number of packets in the source-queue at slot t and $J(t)$ denotes the number of packet dispatches that have been conducted for the current head-of-line packet by slot t, here $0 \leq L(t) \leq M$, $0 \leq J(t) \leq f-1$ when $1 \leq L(t) \leq M$, and $J(t) = 0$ when $L(t) = 0$.

Suppose that the source-queue in S is at state (l, j) in the current time slot, all

the possible state transitions that may happen at the next time slot are summarized in Fig. 3.2, where

- $I_0(t)$ is an indicator function, taking value of 1 if S conducts source-destination transmission in the current time slot, and taking value of 0 otherwise;
- $I_1(t)$ is an indicator function, taking value of 1 if S conducts packet-dispatch transmission in the current time slot, and taking value of 0 otherwise;
- $I_2(t)$ is an indicator function, taking value of 1 if S conducts neither source-destination nor packet-dispatch transmission in the current time slot, and taking value of 0 otherwise;
- $I_3(t)$ is indicator function, taking value of 1 if S locally generates a packet in the current time slot, and taking value of 0 otherwise.

From Fig. 3.2 we can see that as time evolves, the state transitions of the source-queue in S form a two-dimensional QBD process [53]

$$\{\mathbf{X}(t), t = 0, 1, 2, \cdots\}, \tag{3.1}$$

on state space

$$\big\{\{(0,0)\} \cup \{(l,j)\}; 1 \leq l \leq M, 0 \leq j \leq f-1\big\}. \tag{3.2}$$

Based on the transition scenarios in Fig. 3.2, the overall transition diagram of above QBD process is illustrated in Fig. 3.3.

Remark 3 *The QBD framework is powerful in the sense it enables main network dynamics to be captured, like the dynamics involved in the packet generating process and these involved in the source-destination and packet-dispatch transmissions (i.e., node mobility, medium contention, interference and packet transmitting).*

3.3.2 Transition Matrix and Some Basic Results

As shown in Fig. 3.3 that there are in total $1 + M \cdot f$ two-tuple states for the source-queue in S. To construct the transition matrix of the QBD process, we arrange all these $1 + M \cdot f$ states in a left-to-right and top-to-down way as follows: $\{(0,0),(1,0),(1,1),\cdots,(1,f-1),(2,0),(2,1),\cdots,(2,f-1),\cdots,(M,0),\cdots,(M,f-1)\}$. Under such state arrangement, the corresponding state transition matrix $\mathbf{P}$ of the QBD process can be determined as

$$\mathbf{P} = \begin{bmatrix} \mathbf{B_1} & \mathbf{B_0} & & & \\ \mathbf{B_2} & \mathbf{A_1} & \mathbf{A_0} & & \\ & \mathbf{A_2} & \ddots & \ddots & \\ & & \ddots & \mathbf{A_1} & \mathbf{A_0} \\ & & & \mathbf{A_2} & \mathbf{A_M} \end{bmatrix}, \tag{3.3}$$

where the corresponding sub-matrices in matrix $\mathbf{P}$ are defined as follows:

- $\mathbf{B_0}$: a matrix of size $1 \times f$, denoting the transition probabilities from $(0,0)$ to $(1,j)$, $0 \le j \le f-1$.

- $\mathbf{B_1}$: a matrix of size 1×1, denoting the transition probability from $(0,0)$ to $(0,0)$.

- $\mathbf{B_2}$: a matrix of size $f \times 1$, denoting the transition probabilities from $(1,j)$ to $(0,0)$, $0 \le j \le f-1$.

- $\mathbf{A_0}$: a matrix of size $f \times f$, denoting the transition probabilities from (l,j) to $(l+1,j')$, $1 \le l \le M-1, 0 \le j,j' \le f-1$.

- $\mathbf{A_1}$: a matrix of size $f \times f$, denoting the transition probabilities from (l,j) to (l,j'), $1 \le l \le M-1, 0 \le j,j' \le f-1$.

- $\mathbf{A_2}$: a matrix of size $f \times f$, denoting the transition probabilities from (l, j) to $(l-1, j')$, $2 \leq l \leq M, 0 \leq j, j' \leq f-1$.

- $\mathbf{A_M}$: a matrix of size $f \times f$, denoting the transition probabilities from (M, j) to (M, j'), $0 \leq j, j' \leq f-1$.

Some basic probabilities involved in the above sub-matrices are summarized in the following Lemma.

Lemma 1 *For a given time slot, let p_0 be the probability that S conducts a source-destination transmission, let p_1 be the probability that S conducts a packet-dispatch transmission, and let p_2 be the probability that S conducts neither source-destination nor packet-dispatch transmission. Then, we have*

$$p_0 = \frac{1}{\alpha^2}\left\{\frac{9n-m^2}{n(n-1)} - \left(\frac{m^2-1}{m^2}\right)^{n-1}\frac{8n+1-m^2}{n(n-1)}\right\}, \tag{3.4}$$

$$p_1 = \frac{q(m^2-9)}{\alpha^2(n-1)}\left\{1 - \left(\frac{m^2-1}{m^2}\right)^{n-1}\right\}, \tag{3.5}$$

$$p_2 = 1 - p_0 - p_1. \tag{3.6}$$

Proof 1 *The proof is given in Appendix A.1.*

3.4 Source Delay Analysis

Based on the QBD-based theoretical framework developed above, this section conducts analysis on the source delay defined as follow.

Definition 1 *In a PD-f MANET, the source delay U of a packet is defined as the time the packet experiences in its source-queue after it is inserted into the source-queue.*

To analyze the source delay, we first examine the steady state distribution of the source-queue, based on which we then derive the CDF and mean/variance of the source delay.

3.4.1 State Distribution of Source-Queue

We adopt a row vector $\boldsymbol{\pi}^*_\omega = [\pi^*_{\omega,0}\ \boldsymbol{\pi}^*_{\omega,1} \cdots \boldsymbol{\pi}^*_{\omega,M}]$ of size $1 + M \cdot f$ to denote the steady state distribution of the source-queue, here $\pi^*_{\omega,0}$ is a scalar value representing the probability that the source-queue is in the state $(0, 0)$, while $\boldsymbol{\pi}^*_{\omega,l} = (\pi^*_{\omega,l,j})_{1\times f}$ is a sub-vector with $\pi^*_{\omega,l,j}$ being the probability that the source-queue is in state (l, j), $1 \le l \le M, 0 \le j \le f - 1$.

For the analysis of source delay, we further define a row vector $\boldsymbol{\pi}^*_\Omega = [\pi^*_{\Omega,0}\ \boldsymbol{\pi}^*_{\Omega,1} \cdots \boldsymbol{\pi}^*_{\Omega,M}]$ of size $1+M\cdot f$ to denote the conditional steady state distribution of the source-queue under the condition that a new packet has just been inserted into the source-queue, here $\pi^*_{\Omega,0}$ is a scalar value representing the probability that the source-queue is in the state $(0, 0)$ under the above condition, while $\boldsymbol{\pi}^*_{\Omega,l} = (\pi^*_{\Omega,l,j})_{1\times f}$ is a sub-vector with $\pi^*_{\Omega,l,j}$ being the probability that the source-queue is in state (l, j) under the above condition, $1 \le l \le M, 0 \le j \le f - 1$. Regarding the evaluation of $\boldsymbol{\pi}^*_\Omega$, we have the following lemma.

Lemma 2 *In a PD-f MANET, its conditional steady source-queue state distribution* $\boldsymbol{\pi}^*_\Omega$ *is given by*

$$\boldsymbol{\pi}^*_\Omega = \frac{\boldsymbol{\pi}^*_\omega \mathbf{P_2}}{\lambda \boldsymbol{\pi}^*_\omega \mathbf{P_1 1}}, \tag{3.7}$$

where $\mathbf{1}$ *is a column vector with all elements being* 1*. The matrix* $\mathbf{P_1}$ *in (3.7) is determined based on (3.3) by setting the corresponding sub-matrices as follows:*

For $M = 1$,

$$\mathbf{B_0} = \mathbf{0}, \tag{3.8}$$

$$\mathbf{B_1} = [1], \tag{3.9}$$

$$\mathbf{B_2} = \mathbf{c}, \tag{3.10}$$

$$\mathbf{A_M} = \mathbf{0}. \tag{3.11}$$

For $M \geq 2$,

$$\mathbf{B_0} = \mathbf{0}, \tag{3.12}$$

$$\mathbf{B_1} = [1], \tag{3.13}$$

$$\mathbf{B_2} = \mathbf{c}, \tag{3.14}$$

$$\mathbf{A_0} = \mathbf{0}, \tag{3.15}$$

$$\mathbf{A_1} = \mathbf{Q}, \tag{3.16}$$

$$\mathbf{A_2} = \mathbf{c} \cdot \mathbf{r}, \tag{3.17}$$

$$\mathbf{A_M} = \mathbf{0}. \tag{3.18}$$

where $\mathbf{0}$ *is a matrix of proper size with all elements being* 0,

$$\mathbf{c} = [p_0 \quad \cdots \quad p_0 \quad p_0 + p_1]^T, \tag{3.19}$$

$$\mathbf{r} = [1 \quad 0 \quad \cdots \quad 0], \tag{3.20}$$

$$\mathbf{Q} = \begin{bmatrix} p_2 & p_1 & & & \\ & p_2 & p_1 & & \\ & & \ddots & \ddots & \\ & & & p_2 & p_1 \\ & & & & p_2 \end{bmatrix}. \tag{3.21}$$

The matrix $\mathbf{P_2}$ *in (3.7) is also determined based on (3.3) by setting the corresponding sub-matrices as follows:*

For $M = 1$*,*

$$\mathbf{B_0} = [\lambda \quad 0 \quad \cdots \quad 0], \tag{3.22}$$

$$\mathbf{B_1} = [0], \tag{3.23}$$

$$\mathbf{B_2} = \mathbf{0}, \tag{3.24}$$

$$\mathbf{A_M} = \lambda \mathbf{c} \cdot \mathbf{r}. \tag{3.25}$$

For $M \geq 2$*,*

$$\mathbf{B_0} = [\lambda \quad 0 \quad \cdots \quad 0], \tag{3.26}$$

$$\mathbf{B_1} = [0], \tag{3.27}$$

$$\mathbf{B_2} = \mathbf{0}, \tag{3.28}$$

$$\mathbf{A_0} = \lambda \mathbf{Q}, \tag{3.29}$$

$$\mathbf{A_1} = \lambda \mathbf{c} \cdot \mathbf{r}, \tag{3.30}$$

$$\mathbf{A_2} = \mathbf{0}, \tag{3.31}$$

$$\mathbf{A_M} = \lambda \mathbf{c} \cdot \mathbf{r}. \tag{3.32}$$

Proof 2 *See Appendix A.2 for the proof.*

The result in (3.7) indicates that for the evaluation of $\boldsymbol{\pi}^*_{\Omega}$, we still need to determine the steady state distribution $\boldsymbol{\pi}^*_{\omega}$ of the source-queue.

Lemma 3 *In a PD-f MANET, its steady state distribution* $\boldsymbol{\pi}^*_{\omega}$ *of the source-queue is determined as follows:*

For $M = 1$,

$$\pi^*_{\omega,0} = \pi^*_{\omega,0}\mathbf{B_1} + \boldsymbol{\pi}^*_{\omega,1}\mathbf{B_2}, \tag{3.33}$$

$$\boldsymbol{\pi}^*_{\omega,1} = \pi^*_{\omega,0}\mathbf{B_0} + \boldsymbol{\pi}^*_{\omega,1}\mathbf{A_M}, \tag{3.34}$$

$$\boldsymbol{\pi}^*_{\omega} \cdot \mathbf{1} = 1. \tag{3.35}$$

For $M = 2$,

$$\pi^*_{\omega,0} = \pi^*_{\omega,0}\mathbf{B_1} + \boldsymbol{\pi}^*_{\omega,1}\mathbf{B_2}, \tag{3.36}$$

$$\boldsymbol{\pi}^*_{\omega,1} = \pi^*_{\omega,0}\mathbf{B_0} + \boldsymbol{\pi}^*_{\omega,1}\mathbf{A_1} + \boldsymbol{\pi}^*_{\omega,2}\mathbf{A_2}, \tag{3.37}$$

$$\boldsymbol{\pi}^*_{\omega,2} = \boldsymbol{\pi}^*_{\omega,1}\mathbf{A_0} + \boldsymbol{\pi}^*_{\omega,2}\mathbf{A_M}, \tag{3.38}$$

$$\boldsymbol{\pi}^*_{\omega} \cdot \mathbf{1} = 1. \tag{3.39}$$

For $M \geq 3$,

$$[\pi^*_{\omega,0}, \boldsymbol{\pi}^*_{\omega,1}] = [\pi^*_{\omega,0}, \boldsymbol{\pi}^*_{\omega,1}] \begin{bmatrix} \mathbf{B_1} & \mathbf{B_0} \\ \mathbf{B_2} & \mathbf{A_1} + \mathbf{RA_2} \end{bmatrix}, \tag{3.40}$$

$$\boldsymbol{\pi}^*_{\omega,i} = \boldsymbol{\pi}^*_{\omega,1}\mathbf{R}^{i-1}, \quad 2 \leq i \leq M-1, \tag{3.41}$$

$$\boldsymbol{\pi}^*_{\omega,M} = \boldsymbol{\pi}^*_{\omega,1}\mathbf{R}^{M-2}\mathbf{R_M}, \tag{3.42}$$

$$\boldsymbol{\pi}^*_{\omega} \cdot \mathbf{1} = 1, \tag{3.43}$$

where

$$\mathbf{B_0} = [\lambda \quad 0 \quad \cdots \quad 0], \tag{3.44}$$

$$\mathbf{B_1} = [1-\lambda], \tag{3.45}$$

$$\mathbf{B_2} = (1-\lambda)\mathbf{c}, \tag{3.46}$$

$$\mathbf{A_0} = \lambda\mathbf{Q}, \tag{3.47}$$

$$\mathbf{A_1} = (1-\lambda)\mathbf{Q} + \lambda\mathbf{c}\cdot\mathbf{r}, \tag{3.48}$$

$$\mathbf{A_2} = (1-\lambda)\mathbf{c}\cdot\mathbf{r}, \tag{3.49}$$

$$\mathbf{A_M} = \mathbf{A_1} + \mathbf{A_0}, \tag{3.50}$$

$$\mathbf{R} = \mathbf{A_0}[\mathbf{I} - \mathbf{A_1} - \mathbf{A_0}\cdot\mathbf{1}\cdot\mathbf{r}]^{-1}, \tag{3.51}$$

$$\mathbf{R_M} = \mathbf{A_0}[\mathbf{I} - \mathbf{A_M}]^{-1}, \tag{3.52}$$

here $\mathbf{c}$, $\mathbf{r}$ *and* $\mathbf{Q}$ *are given in (3.19), (3.20) and (3.21), respectively;* $\mathbf{I}$ *is an identity matrix of size* $f \times f$*, and* $\mathbf{1}$ *is a column vector of proper size with all elements being* 1*.*

Proof 3 *See Appendix A.3 for the proof.*

3.4.2 CDF, Mean and Variance of Source Delay

Based on the conditional steady state distribution $\boldsymbol{\pi}^*_\Omega$ of the source-queue, we are now ready to derive the CDF as well as mean and variance of the source delay, as summarized in the following theorem.

Theorem III.1 *In a PD-f MANET, the probability mass function* $Pr\{U = u\}$*, CDF*

$Pr\{U \leq u\}$, mean $\overline{U}$ and variance σ_U^2 of the source delay U of a packet are given by

$$Pr\{U = u\} = \boldsymbol{\pi}_{\Omega}^{-}\mathbf{T}^{u-1}\mathbf{c}^{+}, \quad u \geq 1, \tag{3.53}$$

$$Pr\{U \leq u\} = 1 - \boldsymbol{\pi}_{\Omega}^{-}\mathbf{T}^{u}\mathbf{1}, \quad u \geq 0, \tag{3.54}$$

$$\overline{U} = \boldsymbol{\pi}_{\Omega}^{-}(\mathbf{I} - \mathbf{T})^{-2}\mathbf{c}^{+}, \tag{3.55}$$

$$\sigma_U^2 = \boldsymbol{\pi}_{\Omega}^{-}(\mathbf{I} + \mathbf{T})(\mathbf{I} - \mathbf{T})^{-3}\mathbf{c}^{+} - \overline{U}^2, \tag{3.56}$$

where $\boldsymbol{\pi}_{\Omega}^{-} = [\boldsymbol{\pi}_{\Omega,1}^{*}\ \boldsymbol{\pi}_{\Omega,2}^{*} \cdots \boldsymbol{\pi}_{\Omega,M}^{*}]$ is a sub vector of $\boldsymbol{\pi}_{\Omega}^{*}$, $\mathbf{c}^{+}$ is a column vector of size $M \cdot f$ and $\mathbf{T}$ is a matrix of size $(M \cdot f) \times (M \cdot f)$ determined as follows:

For $M = 1$,

$$\mathbf{c}^{+} = \mathbf{c}, \tag{3.57}$$

$$\mathbf{T} = \mathbf{Q}. \tag{3.58}$$

For $M \geq 2$,

$$\mathbf{c}^{+} = [\mathbf{c} \quad 0 \quad \cdots \quad 0]^{T}, \tag{3.59}$$

$$\mathbf{T} = \begin{bmatrix} \mathbf{A_1} & \mathbf{A_0} & & & \\ \mathbf{A_2} & \mathbf{A_1} & \mathbf{A_0} & & \\ & \ddots & \ddots & \ddots & \\ & & \mathbf{A_2} & \mathbf{A_1} & \mathbf{A_0} \\ & & & \mathbf{A_2} & \mathbf{A_M} \end{bmatrix}, \tag{3.60}$$

where

$$\mathbf{A_0} = \mathbf{0}, \tag{3.61}$$

$$\mathbf{A_1} = \mathbf{Q}, \tag{3.62}$$

$$\mathbf{A_2} = \mathbf{c} \cdot \mathbf{r}, \tag{3.63}$$

$$\mathbf{A_M} = \mathbf{Q}, \tag{3.64}$$

here $\mathbf{c}$, $\mathbf{r}$ *and* $\mathbf{Q}$ *are given in (3.19), (3.20) and (3.21), respectively, and* $\mathbf{0}$ *is a matrix of proper size with all elements being* 0.

Proof 4 *See Appendix A.4 for the proof.*

3.5 Numerical Results

In this section, we first provide simulation results to validate the efficiency of our QBD-based theoretical framework and source delay models, and then illustrate how source delay in a PD-f MANET is related to network parameters.

3.5.1 Source Delay Validation

To validate the theoretical framework and source delay models, a customized C++ simulator was developed to simulate the packet generating and dispatching processes in PD-f MANETs [54], in which network parameters, such as the number of network nodes n, network partition parameter m, source-queue buffer size M, packet dispatch limit f, packet dispatch probability q and packet generating probability λ, can be flexibly adjusted to simulate source delay performance under various network scenarios. Based on the simulator, extensive simulations have been conducted to validate our our QBD-based source delay models. For three typical network scenarios of $n = 100$ (small network), $n = 200$ (medium network) and $n = 400$ (large

network) with $m = 8, M = 7, f = 2, q = 0.4$ and $\lambda = 0.001$, the corresponding simulation/theoretical results on the CDFs of source delay are summarized in Fig. 3.4.

We can see from Fig. 3.4 that for all three network scenarios considered here, the theoretical results on the CDF of source delay match nicely with the corresponding simulated ones, indicating that our QBD-based theoretical framework is highly efficient in modeling the source delay behaviors of PD-f MANETs. We can also see from Fig. 3.4 that the source delay in a small network (e.g. $n = 100$ here) is very likely smaller than that of a large network (e.g. $n = 200$ or $n = 400$ here). This is because that for a given network area and a fixed partition parameter m, as network size in terms of n decreases the channel contention becomes less severe and thus each source node has more chances to conduct packet dispatch, leading to a shorter source delay one packet experiences in its source node.

3.5.2 Source Delay Performance Illustration

With our QBD-based theoretical framework, we then illustrate how source delay performance, in terms of its mean $\overline{U}$ and standard deviation $\sigma_U = \sqrt{\sigma_U^2}$, is related to some main network parameters like packet generating probability λ, source-queue buffer size M, packet dispatch limit f and packet dispatch probability q.

We first illustrate in Figs. 3.5 how $\overline{U}$ and σ_U vary with λ and M for a network scenario of $n = 200, m = 16, q = 0.6$ and $f = 3$. We see from Fig. 3.5a that for any given M, $\overline{U}$ first increases as λ increases until λ reaches some threshold value and then $\overline{U}$ remains almost a constant as λ increases further beyond that threshold. On the other hand, for a given $\lambda \in [0.0005, 0.002]$, as M increases $\overline{U}$ first increases and then remains constant, while for a given $\lambda \in [0.002, 0.01]$, $\overline{U}$ always increases as M increases. Regarding the standard deviation σ_U of source delay, we see from Fig. 3.5b that for given M, as λ increases from 0.0005 to 0.01 σ_U first increases sharply to a peak value, then decreases sharply, and finally converges to a constant. It is interesting to

see that the peak values of σ_U under different settings of M are all achieved at the same $\lambda = 0.0025$. The results in Fig. 3.5b further indicate that for fixed λ, as M increases σ_U always first increases and then gradually converges to a constant.

We then illustrate in Figs. 3.6 how $\overline{U}$ and σ_U vary with packet dispatch parameters q and f under the network scenario of $n = 300, m = 16, M = 7$ and $\lambda = 0.002$. From Fig. 3.6a and Fig. 3.6b we can see that although both $\overline{U}$ and σ_U always decrease as q increases for a fixed f, their variations with q change dramatically with the setting of f. On the other hand, for a given $q \in [0.05, 0.2]$, as f increases both $\overline{U}$ and σ_U first increase and then tend to a constant, while for a given $q \in [0.2, , 1.0]$, both $\overline{U}$ and σ_U always monotonically increase as f increases.

3.6 Summary

This chapter conducted a thorough study on the source delay in MANETs, a new and fundamental delay metric for such networks. A QBD-based theoretical framework was developed to model the source delay behaviors under a general packet dispatching scheme, based on which the cumulative distribution function as well as the mean and variance of source delay were derived. As validated through extensive simulation results that our QBD-based framework is highly efficient in modeling the source delay performance in MANETs. Numerical results were also provided to illustrate how source delay is related with and thus can be controlled by some key network parameters, like source-queue buffer size, packet dispatch limit, and packet dispatch probability. It is expected that our source delay analysis and the related QBD-based theoretical framework will solidly contribute to the study of end-to-end delay behavior in MANETs.

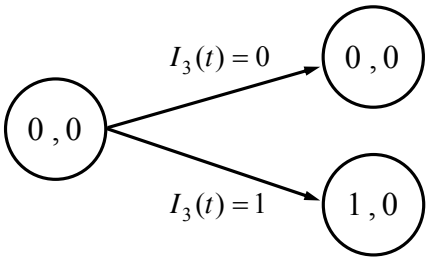

(a) State transition when $l = 0$.

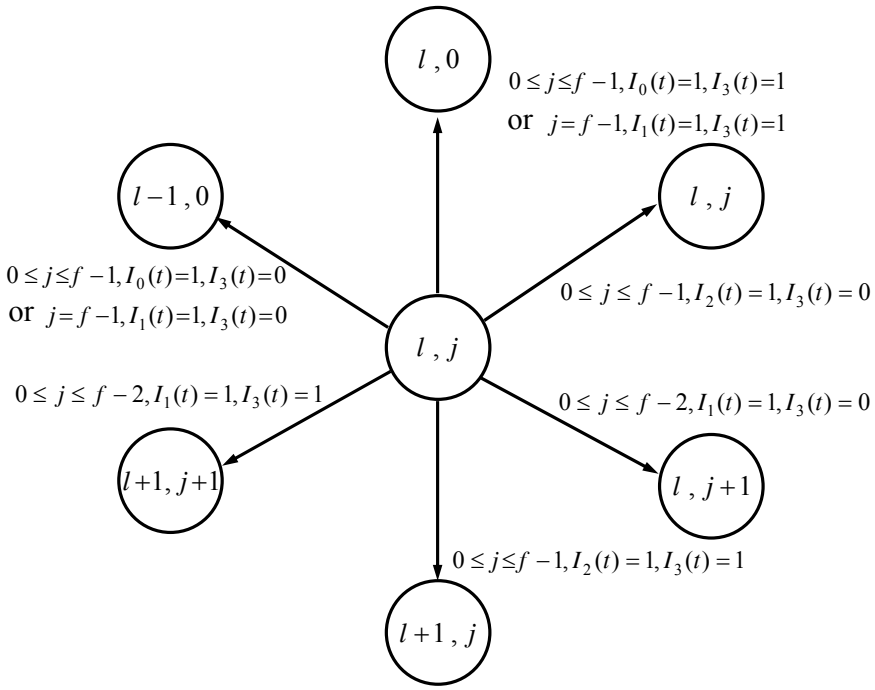

(b) State transition when $1 \le l \le M - 1$.

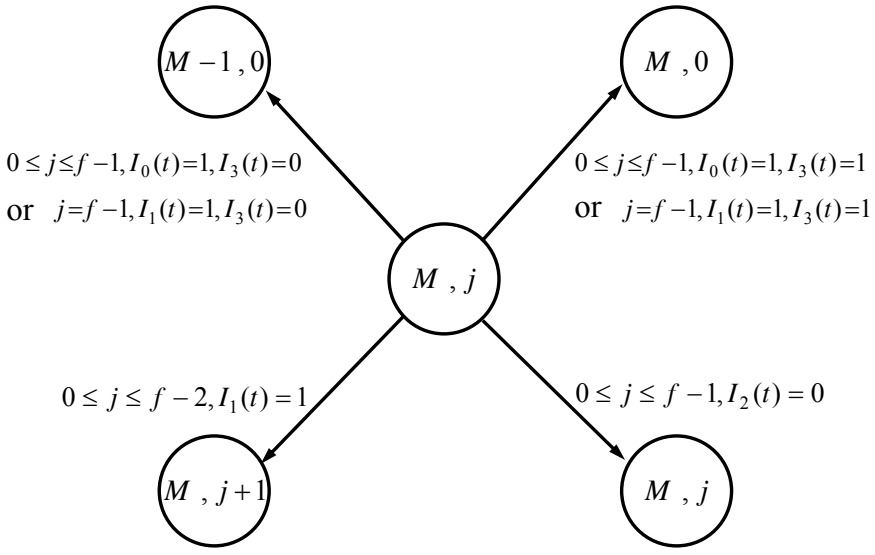

(c) State transition when $l = M$.

Figure 3.2: State transitions from state (l, j) of the source-queue.

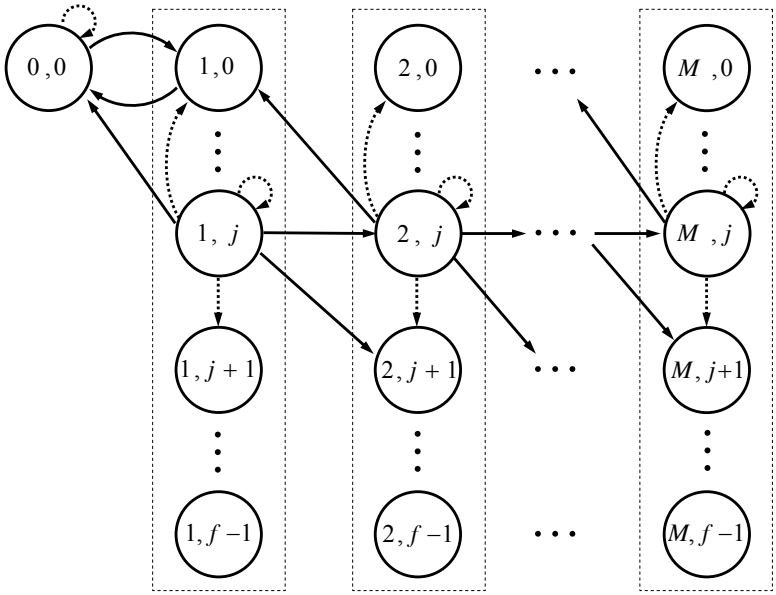

Figure 3.3: State transition diagram for the QBD process of source-queue. For simplicity, only transitions from typical states (l, j) are illustrated for $1 \leq l \leq M$, while other transitions are the same as that shown in Fig. 3.2.

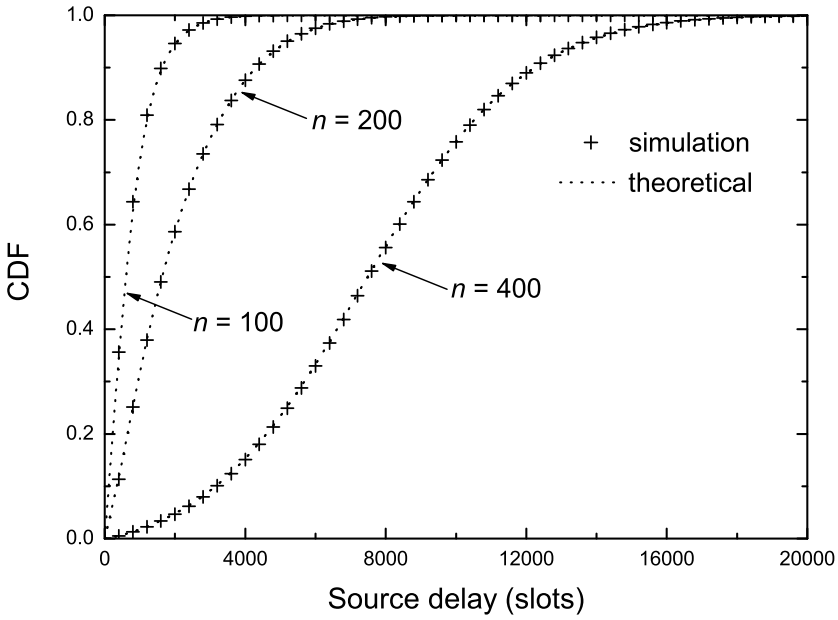

Figure 3.4: The simulation and theoretical results on cumulative distribution function (CDF) of source delay.

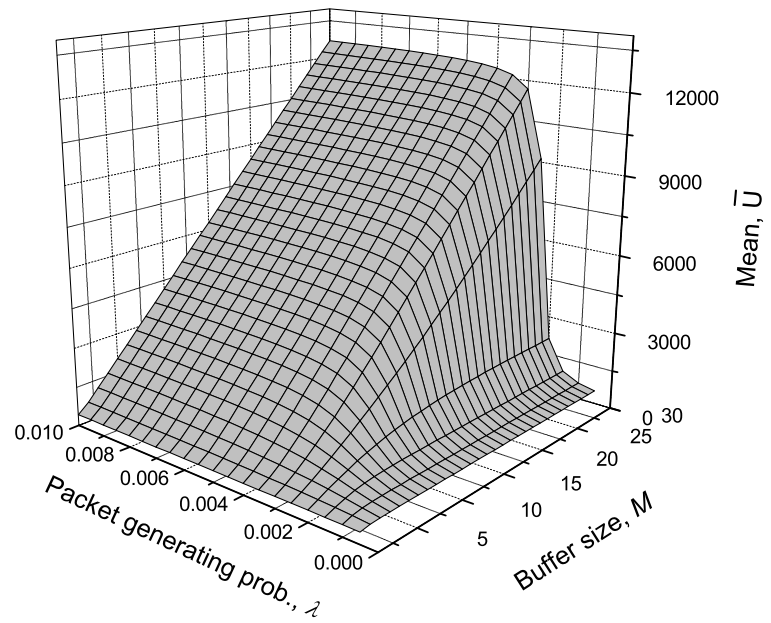

(a) $\overline{U}$ versus (λ, M)

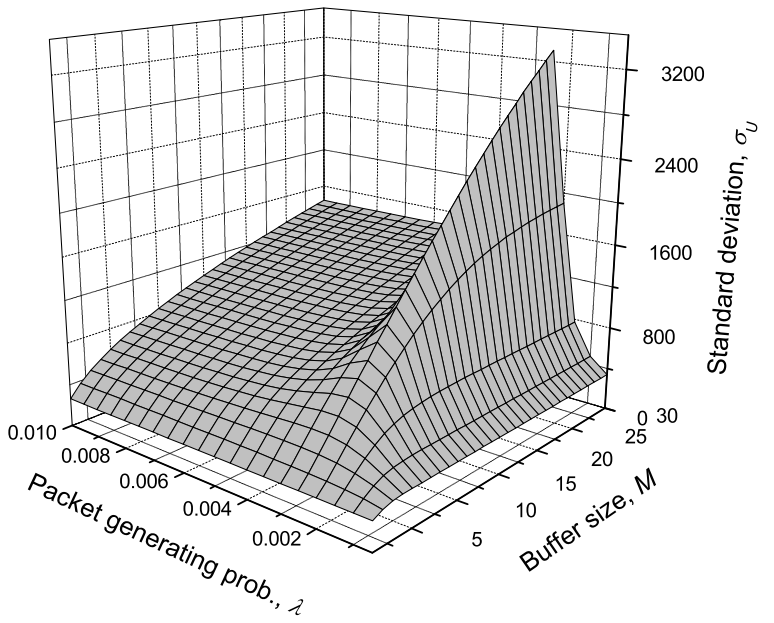

(b) σ_U versus (λ, M)

Figure 3.5: Source delay performance versus packet generating probability λ and source-queue buffer size M.

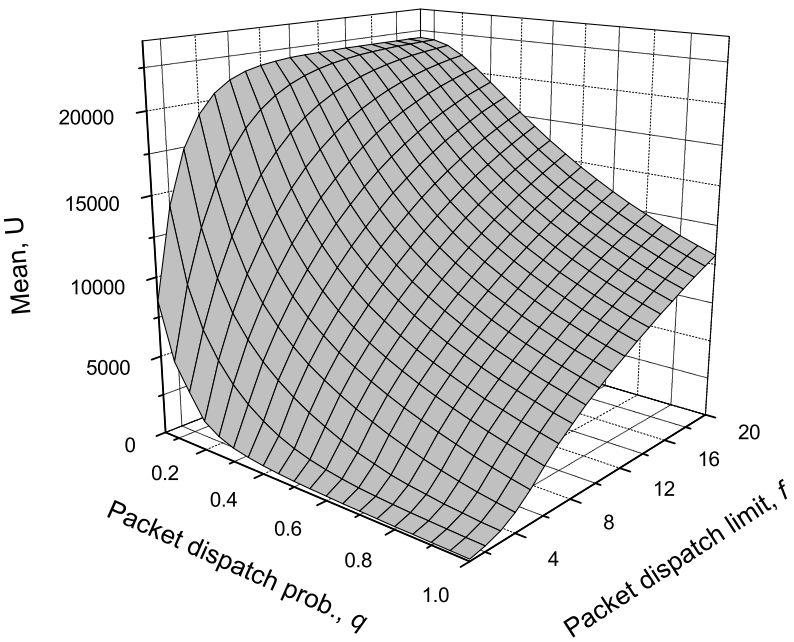

(a) $\overline{U}$ versus (q, f)

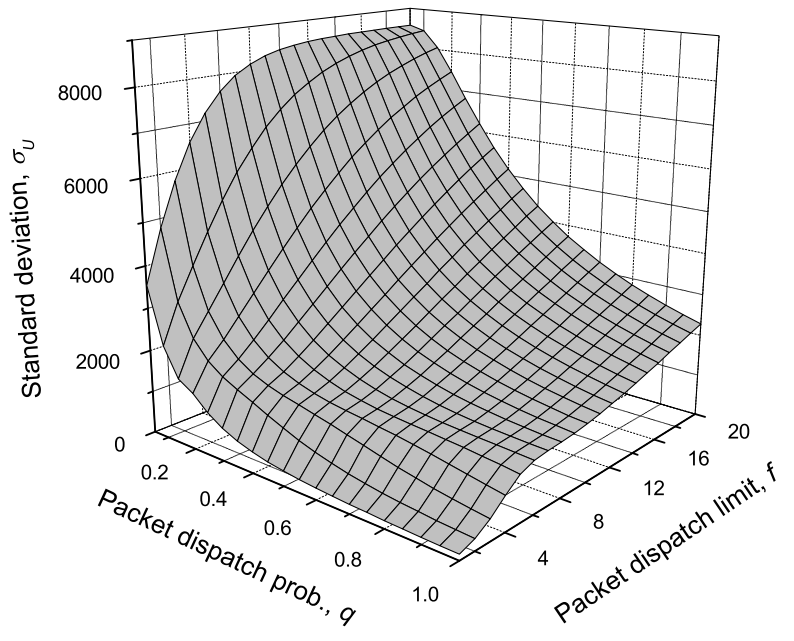

(b) σ_U versus (q, f)

Figure 3.6: Source delay performance versus packet dispatch probability q and packet dispatch limit f.

CHAPTER IV

End-to-End Delay for MAC-TG MANETs

To facilitate the applications of MANETs in providing Quality of Service (QoS) guaranteed services, understanding the end-to-end delay performance of such networks is of fundamental importance. However, the analytical modeling of practical end-to-end delay in MANETs remains a technical challenge. This is due to the highly dynamical behaviors of MANETs in terms of node mobility, interference, wireless channel/traffic contention, queueing process of a packet at its source node and the complicated delivery process of the packet among mobile nodes. By extending the former QBD-based theoretical framework, we incorporate these complex network dynamics into end-to-end delay analysis and derive the expected end-to-end delay in this chapter.

4.1 Related Works and Their Limitations

Available works on end-to-end delay analysis in MANETs mainly focus on deriving upper bounds or approximations for such delay. Based on the $M/G/1$ queueing model, Neely et al. [16] derived some closed-form upper bounds on the expected end-to-end delay in MANETs with two-hop relay routing. Later, Liu et al. [35] extended the model in [16] to obtain upper bounds on expected end-to-end delay in MANETs with a variant of two-hop relay routing and limited packet redundancy. For MANETs

with multi-hop back-pressure routing, Alresaini et al. [55] adopted the Lyapunov drift model to derive an upper bound on the expected end-to-end delay there. For MANETs with multi-hop linear routing, Ciucu et al. [56, 57] proposed a network calculus approach to derive upper bounds on end-to-end delay distribution.

In addition to the delay upper bound results, approximations to end-to-end delay in MANETs have also been explored recently [9, 38, 58, 59]. By adopting the polling model, Hanbali et al. [58] provided an approximation to expected end-to-end delay for a simple two-hop relay MANET consisting of only one source node, one relay node and one destination node. For more general two-hop relay MANETs with multiple source-destination pairs and multiple relay nodes, Liu et al. [9,38] adopted the $M/M/1$ queue model to obtain approximations to the expected end-to-end delay there. For MANETs with multi-hop relay routing, Jindal et al. [59] developed approximations to corresponding end-to-end delay based on the elementary probability theory.

It is notable that the results in [9, 16, 35, 38, 55–59] indicate that although above upper bound and approximation results are helpful for us to understand the general delay behaviors in MANETs, they usually introduce significant errors in end-to-end delay analysis. This is mainly due to the lack of an efficient theoretical framework to capture the complex network dynamics and thus the corresponding network state transitions in MANETs. This chapter extends the former QBD-based theoretical framework to capture the network state transitions and thus to tackle the challenging end-to-end delay modeling issue in MANETs.

4.2 System Assumptions

In this section, we introduce first the traffic pattern, and then the two-hop relay routing scheme that deals with packet delivery, under which we conduct the end-to-end delay study.

4.2.1 Traffic Pattern

Similar to previous works [32, 35, 36], we consider the permutation traffic pattern in which each node acts as the source of a traffic flow and at the same time the destination of another traffic flow. Thus, there are in total n distinct traffic flows in the MANET. Each source node exogenously generates packets for its destination according to an Bernoulli process with average rate λ (packets/slot) [16].

4.2.2 Two Hop Relay Routing Protocol

In a MAC-TG MAENT, once a node (say S) succeeds in wireless channel contention and becomes a transmitter, it executes the popular two-hop relay (2HR) routing protocol defined in Algorithm 2 for packet delivery [36, 60, 61]. With the 2HR routing, each exogenously generated packet at S is first distributed out to relays through wireless broadcast [60, 62], and it is then delivered to its destination D via these relays.

Algorithm 2 2HR Routing Protocol

1: Transmitter S selects to conduct packet-broadcast with probability q, $0 < q < 1$, and to conduct packet-delivery with probability $1 - q$;
2: **if** S selects packet-broadcast **then**
3: S executes Procedure 1.1;
4: **else**
5: S executes Procedure 1.2;
6: **end if**

To facilitate the operation of the 2HR routing protocol, each node, say S, is equipped with three types of First In First Out (FIFO) queues: one source-queue, one broadcast-queue and $n - 2$ parallel relay-queues (no relay-queue is needed for node S itself and its destination node D).

Source-queue: Source-queue stores packets exogenously generated at S and destined for D. These exogenous packets will be distributed out to relay nodes later in FIFS way.

Procedure 1.1 packet-broadcast

1: **if** S has packets in its source-queue **then**
2: S distributes out the head-of-line (HoL) packet of source-queue through wireless broadcast to all nodes in its coverage cells;
3: Any node, say R, in the coverage cells of S reserves a copy of that packet;
4: **if** R is not the destination D **then**
5: R inserts the HoL packet into the end of its relay-queue associated with D;
6: **else**
7: **if** R is currently requesting the HoL packet **then**
8: R keeps the HoL packet and increases $ACK(D)$ by 1;
9: **else**
10: R discards that packet;
11: **end if**
12: **end if**
13: S moves that HoL packet out of source-queue and inserts it into the end of its broadcast-queue;
14: S moves ahead the remaining packets in its source-queue;
15: **else**
16: S remains idle;
17: **end if**

Procedure 1.2 packet-delivery

1: S randomly selects a node U as its receiver from nodes in its coverage cells. Denote the source of U as V;
2: S initiates a handshake with U to acquire the packet number $ACK(U) + 1$ and thus to know which packet U is currently requesting;
3: S checks its corresponding relay-queue/broadcast-queue whether it bears a packet with $ID(V) = ACK(U) + 1$;
4: **if** S bears such packet **then**
5: S delivers that packet to U;
6: S clears all packets with $ID(V) \leq ACK(U)$ from its corresponding relay-queue/broadcast-queue;
7: S moves ahead the remaining packets in its corresponding relay-queue/broadcast-queue;
8: U increases $ACK(U)$ by 1;
9: **end if**

Broadcast-queue: Broadcast-queue stores packets from source-queue that have already been distributed out by S but have not been acknowledged yet by D the reception of them.

Relay-queue: Each node other than S and D is assigned with a relay-queue in

S to store redundant copies of packets distributed out by the source of that node.

To ensure the in-order packet reception at D, similar to previous works [16, 35, 36] that S labels every exogenously generated packet with a unique identification number $ID(S)$, which increases by 1 every time a packet is generated; destination D also maintains an acknowledgment number $ACK(D)$ indicating that D is currently requesting the packet with $ID(S) = ACK(D) + 1$ (i.e, the packets with $ID(S) \leq ACK(D)$ have already been received by D).

4.3 End-to-End Delay Modeling

In this section, we first present some basic results, and then develop a novel theoretical framework based on the QBD theory to efficiently capture the complex network state transitions under network dynamics.

4.3.1 Basic Results

We focus on one specific traffic flow from source S to destination D in our analysis. Notice that once a packet is generated at S, it first experiences a queueing process in the source-queue of S before being distributed out (served), and it then experiences a network delivery process after being distributed out into the network by S and before being successfully received by D. Since D requests packets in order according to $ACK(D)$, all packets distributed out by S will be also delivered (served) in order. Thus, we can treat the network delivery process as a queueing process of one virtual network-queue. Notice also that the departure process of source-queue is just the arrival process of network-queue.

To fully depict the two queueing processes in both source-queue and network-queue, we define following probabilities for a time slot.

- p_b : probability that S becomes transmitter and also selects to do packet-

broadcast.

- $p_c(j)$: probability that j copies of a packet exist in the network (including the one in S) after the packet is distributed out by S in the current time slot, $1 \leq j \leq n-1$.

- $p_r(j)$: probability that D receives the packet it is currently requesting given that j copies of the packet exist in the network, $1 \leq j \leq n-1$.

- $p_0(j)$: probability that j copies of a packet exist in the network after S becomes transmitter and selects to do packet-broadcast for this packet, given that D is out of the coverage cells of S and network-queue is empty, $1 \leq j \leq n-1$.

- $p_0(0)$: $p_0(0) = 1 - \sum_{j=1}^{n-1} p_0(j)$.

- $p_b^+(j)$: probability that S becomes transmitter, selects to do packet-broadcast and also successfully conducts packet-broadcast for one packet; at the same time, D receives the packet it is requesting given that j copies of that packet exist in the network, $1 \leq j \leq n-1$.

- $p_b^-(j)$: probability that S becomes transmitter, selects to do packet-broadcast and also successfully conducts packet-broadcast for one packet; at the same time, D does not receive the packet it is requesting given that j copies of that packet exist in the network, $1 \leq j \leq n-1$.

- $p_f^+(j)$: probability that S does not successfully conduct packet-broadcast for any packet; at the same time, D receives the packet it is requesting given that j copies of that packet exist in the network, $1 \leq j \leq n-1$.

- $p_f^-(j)$: probability that S does not successfully conduct packet-broadcast for any packet; at the same time, D does not receive the packet it is requesting given that j copies of that packet exist in the network, $1 \leq j \leq n-1$.

The following lemma reveals a nice property about the source-queue and network-queue, which will help us to evaluate the above probabilities in Lemma 5.

Lemma 4 *For the considered MANET with MAC-TG protocol for transmission scheduling and 2HR protocol for packet delivery, the arrival process of network-queue is a Bernoulli process with probability λ and it is independent of the state of source-queue.*

Proof 5 *We know from Section 4.2.1 that the arrival process of source-queue in S is a Bernoulli process with probability λ. The service process of source-queue is actually also a Bernoulli process, because in every time slot S gets a chance with constant probability p_b to do packet-broadcast to distribute out a packet in source-queue (or equivalently, the source-queue is served with probability p_b in every time slot). Thus, the source-queue in S follows a Bernoulli/Bernoulli queue, and in equilibrium the packet departure process of source-queue is also a Bernoulli process with probability λ, which is independent of the state of source-queue (i.e., the number of packets in source-queue) [63]. Because the arrival process of network-queue is just the departure process of source-queue, this finishes the proof of this Lemma.*

Lemma 5

$$p_b = \frac{qm^2}{\alpha^2 n}\left\{1 - \left(\frac{m^2-1}{m^2}\right)^n\right\} \tag{4.1}$$

$$p_c(j) = \frac{n\binom{n-2}{j-1}(m^2-9)^{n-1-j}}{m^{2n}-(m^2-1)^n}\Big\{(m^2-9)f(j)+f(j+1)\Big\} \tag{4.2}$$

$$p_r(j) = \frac{j(1-q)m^2}{\alpha^2 n(n-1)}\left\{1-\left(\frac{m^2-1}{m^2}\right)^n - \frac{n}{m^2}\left(\frac{m^2-9}{m^2}\right)^{n-1}\right\} \tag{4.3}$$

$$p_0(j) = \frac{\lambda\cdot q\cdot\binom{n-2}{j-1}(m^2-9)^{n-j}}{\alpha^2 m^{2n-2}p_b} f(j) \tag{4.4}$$

$$p_0(0) = 1 - \frac{\lambda\cdot q\cdot(m^2-9)}{\alpha^2(n-1)p_b}\left\{1-\left(\frac{m^2-1}{m^2}\right)^{n-1}\right\} \tag{4.5}$$

$$\begin{aligned} p_b^+(j) = {} & (j-1)\frac{\lambda(q-q^2)(m^4-m^2\alpha^2)}{\alpha^4 n(n-1)(n-2)p_b} \\ & \cdot\left\{1-2\left(\frac{m^2-1}{m^2}\right)^n + \left(\frac{m^2-2}{m^2}\right)^n \right. \\ & \left. - \frac{n}{m^2}\left(\frac{m^2-9}{m^2}\right)^{n-1} + \frac{n}{m^2}\left(\frac{m^2-10}{m^2}\right)^{n-1}\right\} \end{aligned} \tag{4.6}$$

$$p_b^-(j) = \lambda - p_b^+(j) \tag{4.7}$$

$$p_f^+(j) = p_r(j) - p_b^+(j) \tag{4.8}$$

$$p_f^-(j) = 1 - p_b^+(j) - p_b^-(j) - p_f^+(j) \tag{4.9}$$

where

$$f(x) = \frac{9^x - 8^x}{x} \tag{4.10}$$

Proof 6 *The proof of Lemma 5 is given in Appendix B.1.*

Remark 4 *The complex network dynamics of node mobility, interference, wireless channel and traffic contention are incorporated into the calculation of the above probabilities as shown in Appendix B.1.*

4.3.2 Extended QBD Theoretical Framework

To capture network dynamics of packet distributing, packet queueing and delivering processes and corresponding network state transitions, we use $L(t) \geq 0$ to denote the number of local packets distributed out from S but not received yet by D until time slot t, and use $J(t)$ to denote the number of copies of the packet D is currently requesting at time slot t in the network, $0 \leq J(t) \leq n-1$. As time t evolves, the queueing process of network-queue follows a two-dimensional QBD process [53, 64]

$$\{(L(t), J(t)), t = 0, 1, 2, \cdots\}, \tag{4.11}$$

on state space

$$\big\{\{(0,0)\} \cup \{(l,j)\}; l \geq 1, 1 \leq j \leq n-1\big\} \tag{4.12}$$

where $(0,0)$ corresponds to the empty network-queue state. $L(t)$ increases by 1 if S distributes out a packet from its source-queue while D does not receive the packet it is requesting at slot t, $L(t)$ decreases by 1 if S does not distribute out a packet from its source-queue while D receives the packet it is requesting at slot t, and $L(t)$ keeps unchanged, otherwise.

All states in (4.12) can be divided into the following subsets

$$N(0) = \{(0,0)\} \tag{4.13}$$

$$N(l) = \big\{\{(l,j)\}, 1 \leq j \leq n-1\big\}, l \geq 1 \tag{4.14}$$

where subset $N(0)$ is called level 0 and subset $N(l)$ is called level l. It is notable that when network-queue is in some state of level l ($l \geq 1$) at a time slot, the next state of one-step state transitions could only be some state in the same level l or in its adjacent levels $l-1$ and $l+1$.

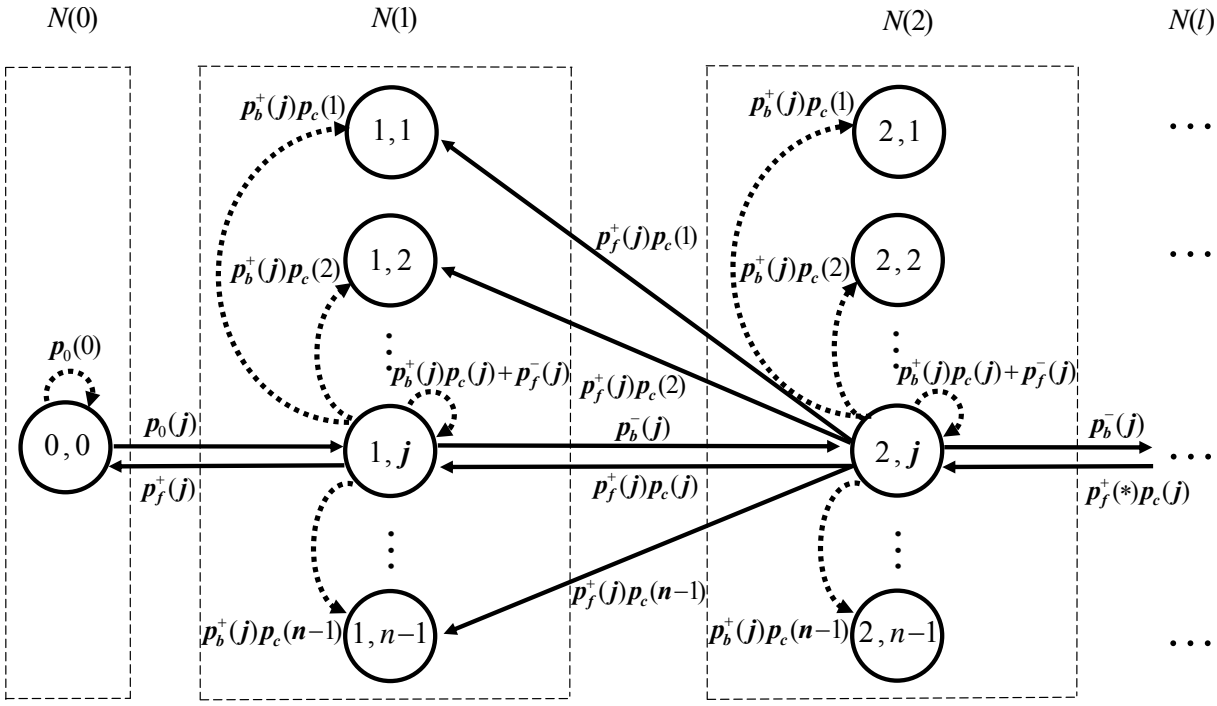

Figure 4.1: State transition diagram for the QBD process of network-queue.

Based on the queueing process of network-queue and the definitions of probabilities in Lemma 5, the underlying QBD process of the network-queue has state transition diagram shown in Fig. 4.1. In Fig. 4.1, $p_f^+(*)p_c(j)$ denotes the probability of the transition from some state $(3,*)$ in level 3 to the state $(2,j)$ in level 2, where the asterisk '$*$' means some eligible copy number in $\{1,2,\cdots,n-1\}$.

To facilitate our discussion, we calssify the state transitions in Fig. 4.1 as **intra-level transition** (denoted by dotted arrows in Fig. 4.1) and **inter-level transition** (denoted by solid arrows in Fig. 4.1).

Intra-level Transition: There are two cases regarding the intra-level transitions, namely, the state transition inside level 0 and the state transitions inside level l ($l \geq 1$). For level 0, it has only one state $(0,0)$, which could only transit to itself. For levels $l \geq 1$, they all follow the same intra-level transitions, i.e., a state (l,j) in level l could transit to any state (including itself) in the same level, $1 \leq j \leq n-1$.

Inter-level Transition: There are also two cases regarding the inter-level tran-

sitions, namely, transitions between level 0 and level 1, and transitions between level l and level $l+1$ ($l \geq 1$). The inter-level transitions between level 0 and level 1 are simply bi-transitions between state $(0,0)$ and any state $(1,j)$, $1 \leq j \leq n-1$. For adjacent levels l and $l+1$ ($l \geq 1$), they all follow the same inter-level transitions, i.e., a state (l,j) in level l could only transit to the corresponding state $(l+1,j)$ in level $l+1$, while a state $(l+1,j)$ in level $l+1$ could transit to any state in level l, $1 \leq j \leq n-1$.

4.4 End-to-End Delay Analysis

With the help of the theoretical framework, we finally derive the expected end-to-end delay and also per node throughput capacity for the concerned MANETs.

Definition 2 *End-to-end delay T_e of a packet is the time elapsed between the time slot the packet is generated at its source and the time slot it is delivered to its destination.*

Definition 3 *Per node throughput capacity μ is defined as the maximum packet arrival rate λ every node in the concerned MANET can stably support.*

Before presenting our main result on the expected end-to-end delay, we first derive the per node throughput capacity, with which the input rate the MANET can stably support and the corresponding end-to-end delay can then be determined.

Theorem IV.1 *For the considered MANET, its per node throughput capacity μ is given by*

$$\mu = \min\left\{p_b, \frac{1}{\sum_{j=1}^{n-1} \frac{p_c(j)}{p_r(j)}}\right\} \tag{4.15}$$

Proof 7 *In equilibrium, the service rate μ_s of source-queue is*

$$\mu_s = p_b \tag{4.16}$$

and the service rate μ_d of network-queue, i.e., the rate D receives its requesting packets, is

$$\mu_d = \frac{1}{\sum_{j=1}^{n-1} \frac{p_c(j)}{p_r(j)}}. \tag{4.17}$$

To ensure network stability, packet generation rate λ at S should satisfy

$$\lambda < \min\{\mu_s, \mu_d\} \tag{4.18}$$

Thus, the per node throughput capacity μ is determined as

$$\mu = \min\{\mu_s, \mu_d\} \tag{4.19}$$

Based on above per node throughput capacity result and the QBD-based theoretical framework, we now establish the following theorem on the expected end-to-end delay of the concerned MANET.

Theorem IV.2 *For the concerned MANET, where each source node exogenously generates packets according to a Bernoulli process with probability λ ($\lambda < \mu$), the expected end-to-end delay $\mathbb{E}(T_e)$ of a packet is determined as*

$$\mathbb{E}(T_e) = \frac{\overline{L}_1 + \overline{L}_2}{\lambda}, \tag{4.20}$$

where

$$\overline{L}_1 = \frac{\lambda - \lambda^2}{p_b - \lambda} \tag{4.21}$$

$$\overline{L}_2 = \frac{\mathbf{y_1}(\mathbf{I} - \mathbf{R})^{-2}\mathbf{1}}{\phi} \tag{4.22}$$

$$\mathbf{R} = \mathbf{A_0}(\mathbf{I} - \mathbf{A_1} - \mathbf{A_0 1 v_0})^{-1} \tag{4.23}$$

$$[y_0, \mathbf{y_1}] = [y_0, \mathbf{y_1}] \begin{bmatrix} \mathbf{B_1} & \mathbf{B_0} \\ \mathbf{B_2} & \mathbf{A_1} + \mathbf{R A_2} \end{bmatrix} \tag{4.24}$$

$$\phi = y_0 + \mathbf{y_1}(\mathbf{I} - \mathbf{R})^{-1}\mathbf{1} \tag{4.25}$$

$$\mathbf{v_0} = \begin{bmatrix} p_c(1) & p_c(2) & \cdots & p_c(j) & \cdots & p_c(n-1) \end{bmatrix} \tag{4.26}$$

$$\mathbf{A_0} = \text{diag}\left(p_b^-(1), p_b^-(2), \cdots, p_b^-(j), \cdots, p_b^-(n-1)\right) \tag{4.27}$$

$$\begin{aligned} \mathbf{A_1} = &\text{diag}\left(p_f^-(1), p_f^-(2), \cdots, p_f^-(j), \cdots, p_f^-(n-1)\right) + \\ &\begin{bmatrix} p_b^+(1) & p_b^+(2) & \cdots & p_b^+(j) & \cdots & p_b^+(n-1) \end{bmatrix}^T \mathbf{v_0} \end{aligned} \tag{4.28}$$

$$\mathbf{A_2} = \mathbf{B_2 v_0} \tag{4.29}$$

$$\mathbf{B_0} = \begin{bmatrix} p_0(1) & p_0(2) & \cdots & p_0(j) & \cdots & p_0(n-1) \end{bmatrix} \tag{4.30}$$

$$\mathbf{B_1} = [p_0(0)] \tag{4.31}$$

$$\mathbf{B_2} = \begin{bmatrix} p_f^+(1) & p_f^+(2) & \cdots & p_f^+(j) & \cdots & p_f^+(n-1) \end{bmatrix}^T \tag{4.32}$$

here $\mathbf{I}$ *denotes an identity matrix of size* $(n-1) \times (n-1)$, $\mathbf{1}$ *denotes a column vector of size* $(n-1) \times 1$ *with all elements being* 1, y_0 *is a scalar value, and* $\mathbf{y_1}$ *is a row vector of size* $1 \times (n-1)$.

Proof 8 *From Lemma 4 we know that we can analyze queueing processes of source-queue and network-queue separately.*

First, for the source-queue at S, *since it follows a Bernoulli/Bernoulli queue, we know from [16, 64] that the expected number of packets* $\overline{L}_1$ *in the queue is determined as*

$$\overline{L}_1 = \frac{\lambda - \lambda^2}{p_b - \lambda} \tag{4.33}$$

Then, for the network-queue, its queueing process follows a QBD process shown

in Fig. 4.1. The corresponding state transition matrix $\mathbf{Q}$ *of the transition diagram in Fig. 4.1 is given by*

$$\mathbf{Q} = \begin{bmatrix} \mathbf{B_1} & \mathbf{B_0} & \mathbf{0} & \mathbf{0} & \cdots \\ \mathbf{B_2} & \mathbf{A_1} & \mathbf{A_0} & \mathbf{0} & \cdots \\ \mathbf{0} & \mathbf{A_2} & \mathbf{A_1} & \mathbf{A_0} & \cdots \\ \mathbf{0} & \mathbf{0} & \mathbf{A_2} & \mathbf{A_1} & \cdots \\ \vdots & \vdots & \vdots & \vdots & \ddots \end{bmatrix} \tag{4.34}$$

where $\mathbf{B_1}$ *defined in (4.31) represents the state transition from* $(0,0)$ *to* $(0,0)$*;* $\mathbf{B_0}$ *defined in (4.30) represents the state transitions from* $(0,0)$ *to* $(1,j)$*,* $1 \leq j \leq n-1$*;* $\mathbf{B_2}$ *defined in (4.32) represents the state transitions from* $(1,j)$ *to* $(0,0)$*,* $1 \leq j \leq n-1$*;* $\mathbf{A_1}$ *defined in (4.28) represents the state transitions from* (l,j) *to* (l,i)*,* $l \geq 1$*,* $1 \leq j,i \leq n-1$*;* $\mathbf{A_0}$ *defined in (4.27) represents the state transitions from* (l,j) *to the corresponding* $(l+1,j)$*,* $l \geq 1$*,* $1 \leq j \leq n-1$*;* $\mathbf{A_2}$ *defined in (4.29) represents the state transitions from* (l,j) *to* $(l-1,i)$*,* $l \geq 2$*,* $1 \leq j,i \leq n-1$*.*

Based on the QBD process theory [53, 64], the queueing process of the network-queue can be analyzed through two related matrices $\mathbf{R}$ *and* $\mathbf{G}$ *determined as:*

$$\mathbf{R} = \mathbf{A_0}(\mathbf{I} - \mathbf{A_1} - \mathbf{A_0}\mathbf{G})^{-1} \tag{4.35}$$

$$\mathbf{G} = \mathbf{A_2} + \mathbf{A_1}\mathbf{G} + \mathbf{A_0}\mathbf{G}^2 \tag{4.36}$$

where $\mathbf{R} = (r_{ij})_{(n-1)\times(n-1)}$*, the entry* r_{ij} *(*$1 \leq i,j \leq n-1$*) of matrix* $\mathbf{R}$ *is the expected number that the QBD of network-queue visits state (*$l+1$*,* j*) before it returns to states in* $N(0) \cup \cdots \cup N(l)$*, given that the QBD starts in state (*l*,* i*), and* $\mathbf{G} = (g_{ij})_{(n-1)\times(n-1)}$*, the entry* g_{ij} *(*$1 \leq i,j \leq n-1$*) of matrix* $\mathbf{G}$ *is the probability that the QBD starts from state (*l*,* i*) and visits state (*$l-1$*,* j*) in a finite time.*

Due to the special structure of $\mathbf{A_2}$*, which is the product of a column vector* $\mathbf{B_2}$ *by*

a row vector $\mathbf{v_0}$*, matrix* $\mathbf{G}$ *can be calculated as*

$$\mathbf{G} = \mathbf{1v_0} \tag{4.37}$$

Based on the results in [64], the expected number of packets $\overline{L}_2$ *of network-queue is given by*

$$\overline{L}_2 = \frac{\mathbf{y_1}(\mathbf{I}-\mathbf{R})^{-2}\mathbf{1}}{\phi}, \tag{4.38}$$

where $\mathbf{y_1}$ *and* ϕ *are determined by (4.24) and (4.25), respectively.*

Finally, by applying Little's Theorem [65], (4.20) follows. This finishes the proof of Theorem IV.2.

4.5 Numerical Results

To validate the QBD-based theoretical results on expected end-to-end delay and per node throughput capacity, a customized C++ simulator has been developed to simulate packet generating, distributing and delivering processes in the considered MANET[1]. In the simulator, not only the i.i.d. node mobility model but also the typical random walk [34] and random waypoint [31] mobility models have been implemented.

- **Random Walk Model:** At the beginning of each time slot, each node first independently selects a cell with equal probability 1/9 among its current cell and its 8 neighboring cells; it then moves into that cell and stays in it until the end of that time slot.

[1]The program of our simulator is now available online at [66]. Similar to [67], the guard-factor is set as $\Delta = 1$.

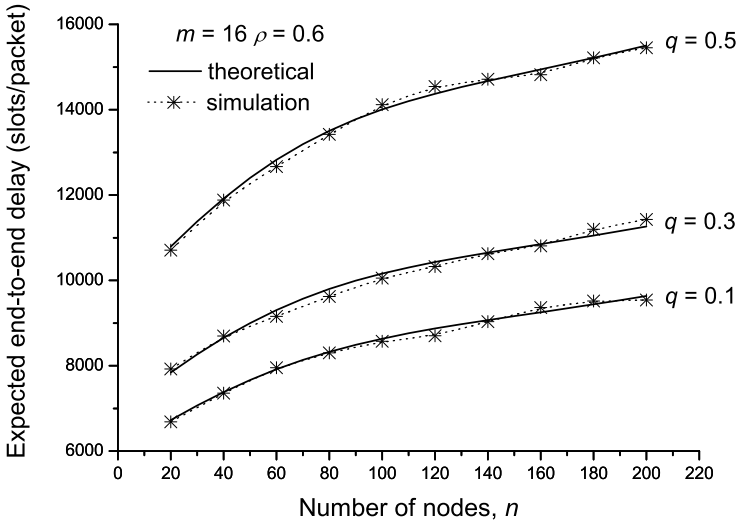

Figure 4.2: Expected packet end-to-end delay VS. number of nodes n in MANET.

- **Random Waypoint Model:** At the beginning of each time slot, each node first independently generates a two-element vector $[x, y]$, where both elements x and y are uniformly drawn from $[1/m, 3/m]$; it then moves along the horizontal and vertical direction of distance x and y, respectively.

4.5.1 End-to-End Delay Validation

For networks of different size n, Fig. 4.2 shows both theoretical and simulation results on packet end-to-end delay under the settings of $m = 16$, system load $\rho = 0.6$ ($\rho = \lambda/\mu$) and packet-broadcast probability $q = \{0.1, 0.3, 0.5\}$. Unless otherwise mentioned, simulation results are reported with small 95% confidence intervals. The results in Fig. 4.2 show clearly that in a wide range of network scenarios considered here, theoretical results match very nicely with simulated ones, indicating that our QBD-based theoretical modeling is really efficient in capturing the expected packet end-to-end delay behavior of concerned MANETs. From Fig. 4.2 we can also see that as network size n increases, packet end-to-end delay increases as well. This is because

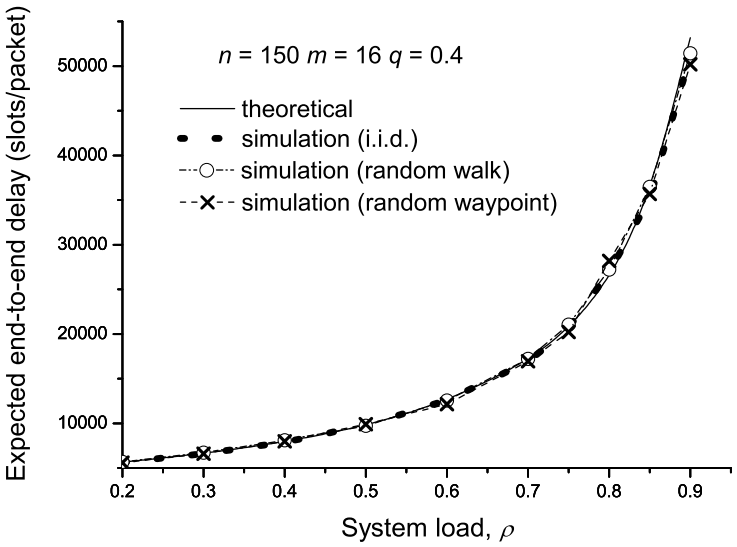

Figure 4.3: Expected packet end-to-end delay VS. system load ρ in MANET.

that in the concerned MANET with fixed unit area and fixed setting of $m = 16$, as n increases the contention for wireless channel access becomes more intensive, resulting in a lower packet delivery opportunity and thus a longer packet end-to-end delay.

For the setting of $n = 150, m = 16$ and $q = 0.4$, Fig. 4.3 shows both the theoretical and simulation results on packet end-to-end delay when system load ρ changes from $\rho = 0.2$ to $\rho = 0.9$. In addition to the i.i.d. mobility model considered in this paper, the corresponding simulation results for the random walk and random waypoint mobility models have also been included in Fig. 4.3 for comparison. Again, we can see from Fig. 4.3 that our theoretical delay model is very efficient. It is interesting to see from Fig. 4.3 that although our theoretical framework is developed under the i.i.d. mobility model, it can also nicely capture the general packet end-to-end delay behavior under more realistic random walk and random waypoint mobility models.

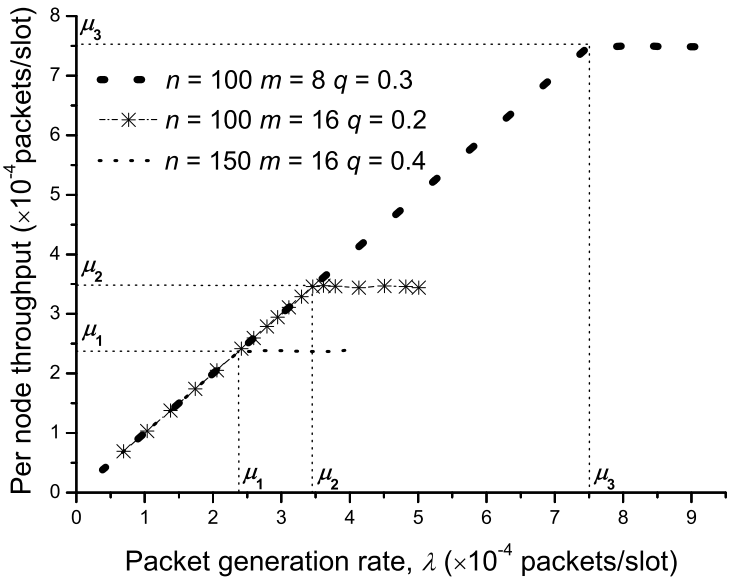

Figure 4.4: Per node throughput VS. packet generation rate λ in MANET.

4.5.2 Throughput Capacity Validation

Another observation of Fig. 4.3 is that the packet end-to-end delay increases sharply as system load ρ approaches 1.0 (i.e., as packet generation rate λ approaches per node throughput capacity μ), which serves as an intuitive verification of our theoretical per node throughput capacity result. To further validate our theoretical model on throughput capacity, Fig. 4.4 provides the simulation results on the achievable per node throughput, i.e., the average rate of packet delivery to destination, when packet generation rate λ increases gradually, where the results of three network scenarios with different throughput capacity $\{n = 150, m = 16, q = 0.4, \mu_1 = 2.37 \times 10^{-4}\}$, $\{n = 100, m = 16, q = 0.2, \mu_2 = 3.46 \times 10^{-4}\}$ and $\{n = 100, m = 8, q = 0.3, \mu_3 = 7.52 \times 10^{-4}\}$ are presented. We can see from Fig. 4.4 that for each network scenario there, the corresponding per node throughput first increases monotonously as λ increases before λ reaches the corresponding throughput capacity (μ_1, μ_2 and μ_3), and then per node throughput remains a constant and does not increase anymore when

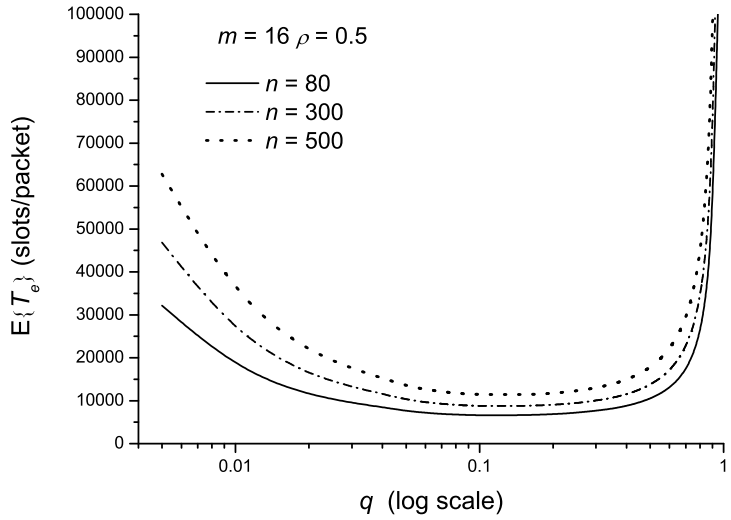

Figure 4.5: Expected packet end-to-end delay T_e VS. 2HR parameter q.

packet generation rate λ goes beyond the corresponding theoretical throughput capacity. Thus, our theoretical capacity model is also efficient in depicting the per node throughput capacity behavior of the considered MANET.

4.5.3 Performance Analysis

With the help of the QBD-based theoretical models, we explore how parameter q of 2HR routing will affect the packet end-to-end delay T_e and per node throughput capacity μ under given m, n and ρ. The corresponding numerical results are summarized in Figs. 4.5 and 4.6.

We first examine the impact of q on T_e. For network settings of $m = 16$, $\rho = 0.5$ and $n = \{80, 300, 500\}$, Fig. 4.5 shows that for a given network its delay T_e always first decreases and then increases as q increases. This phenomenon can be explained as follows. The end-to-end delay experienced by a packet consists of the time it spends in the source-queue and the time it spends in the network-queue. An increase in q has two-fold effects on T_e: on one hand, it decreases the time a packet spends in the source-queue, because source S has more chance to do packet-broadcast for

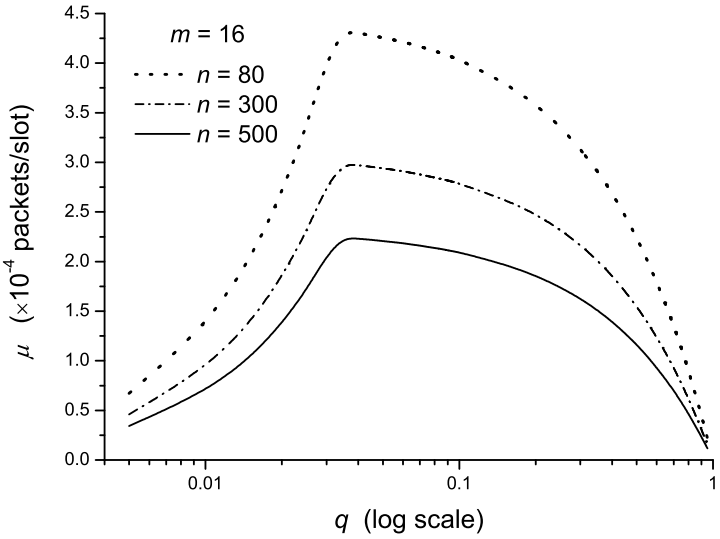

Figure 4.6: Per node throughput capacity μ VS. 2HR parameter q.

packets in its source-queue, which makes the queue to be served more quickly; on the other hand, it increases the time a packet spends in the network-queue, because each relay has less chance to do packet-delivery to deliver a packet to destination D, which makes the network-queue to be served more slowly. Thus, T_e decreases as q increases when the first effect dominates the second one, while T_e increases as q increases when the second effect dominates the first one.

We next explore how parameter q affects μ. For network settings of $m = 16$ and $n = \{80, 300, 500\}$, Fig. 4.6 shows that for a given network its capacity μ always first increases and then decreases as q increases. Notice that μ is determined by the minimum of service rates of the source-queue and network-queue. When q is small, μ is determined by the service rate of source-queue, which increases as q increases. When q is large, μ is determined by the service rate of network-queue, which decreases as q increases. Another observation from Fig. 4.6 is that the capacity μ of $n = 80$ is the largest among different n there. This is because that for a MANET with fixed $m = 16$, a larger number of nodes there will cause a more intensive wireless channel

contention, which decrease opportunities of packet transmission and thus the per node throughput capacity.

4.6 Summary

The main finding of this chapter is that the Quasi-Birth-and-Death (QBD) process can be a promising theory to tackle the challenging issue of analytical end-to-end delay modeling in MANETs. We demonstrated through a two-hop relay MANET that QBD theory can help us: 1) to develop a novel theoretical framework to capture the complicated network state transitions in the highly dynamic MANET, 2) to analytically model the expected end-to-end delay and also the per node throughput capacity of the network, and 3) to enable many important network dynamics like node mobility, wireless channel contention, interference and traffic contention to be jointly considered in the delay modeling process. It is expected that this work will shed light on end-to-end delay modeling in general MANETs also.

CHAPTER V

Throughput Capacity for MAC-TG MANETs

In this chapter, we explore the exact throughput capacity for MAC-TG MANETs in two steps: 1) We first determine a general throughput capacity upper bound for these networks under the condition of network stability. This upper bound holds for any feasible packet routing algorithm in MAC-TG MANETs. 2) We then prove that the considered networks could be stabilized as long as traffic input rate is within the determined throughput capacity upper bound, indicating that the upper bound is just the throughput capacity of such networks.

5.1 Related Works and Their Limitations

The order sense throughput capacity study for MANETs, which mainly focuses on exploring capacity scaling laws of such networks, has been extensively addressed in the last decade. Grossglauser and Tse [68] first showed that by adopting mobile relay nodes, a $\Theta(1)$ per node throughput capacity is achievable under the i.i.d. mobility model[1]. Later, it was proved that the $\Theta(1)$ throughput capacity also holds

[1]In this paper, we adopt the following Knuth's notations [69]:

$$f(n) = O(g(n)) \;\leftrightarrow\; \limsup_{n\to\infty} \frac{f(n)}{g(n)} < \infty,$$
$$f(n) = \Theta(g(n)) \;\leftrightarrow\; f(n) = O(g(n)) \text{ and } g(n) = O(f(n)).$$

under various mobility models, such as Brownian mobility model [70], random walk model [34], uniform mobility model [60] and restricted mobility model [71]. The order sense trade-off between throughput capacity and delay was examined in [16], which indicates that under the i.i.d. mobility model a necessary trade-off between them is *delay / capacity* $\geq O(n)$. Perevalov *et al.* [72] also considered the i.i.d. model, and showed that the delay-limited throughput capacity grows approximately by $d^{2/3}$ for a moderate delay constraint d. More recently, Lin *et al.* [70] proved that for the Brownian mobility model with parameter σ_n^2 and for any $\alpha < 0$, the throughput capacity and packet delay will be $O(1/\sqrt{n})$ and $O(n^{\alpha}/\sigma_n^2)$, respectively. Sharma *et al.* [11] further studied how to trade delay for improved network capacity under hybrid random walk and discrete random direction, two general mobility models that cover many previous mobility models as special cases.

Although order sense results help us to understand how MANET throughput capacity scales with network size, they reveal little about the exact throughput capacity. A thorough understanding of the exact throughput capacity, however, is of great importance for practical design and protocol evaluation of MANETs. Some initial works are now available on the exact throughput capacity study of MANETs. Neely *et al.* [13, 16] established the exact throughput capacity of cell partitioned MANETs under both i.i.d. mobility model and more general Markovian mobility model, where it was assumed that the transmission range of each node is fixed and interference among simultaneous link transmissions can be avoided by using orthogonal channels between adjacent cells. Recently, Liu *et al.* [35, 73] explored the exact throughput capacity for MANETs adopting a specified two-hop relay algorithm with limited packet redundancy for packet delivery.

It is notable that available MANET throughput capacity studies explored either the order sense capacity scaling laws, the exact throughput capacity under some specific algorithm [35, 73], or the exact throughput capacity without a careful considera-

tion of critical wireless interference and transmission range issues in MANETs [13,16]. In this chapter, we study the exact throughput capacity for MAC-TG MANETs, where we adopt TG based scheduling to schedule simultaneous link transmissions for interference avoidance and allow the transmission range of each node to be adjusted.

5.2 System Assumptions

Transmission range: We consider nodes having a general transmission range $r = \sqrt{2}\upsilon/m$ such that all the cells in the transmission range of a node (say S as illustrated in Fig. 5.1) have a horizontal and vertical distance of no more than $\upsilon - 1$ cells away from S's current cell, where $1 \leq \upsilon < \lfloor \frac{m+1}{2} \rfloor$ and $\lfloor \cdot \rfloor$ is the floor function. Thus, a transmitter could cover $(2\upsilon - 1)^2$ cells around it. From now on, we call the $(2\upsilon - 1)^2$ cells covered by S the coverage cells of S and also the coverage cells of its current cell. Under this general transmission range, the MAC-TG parameter α could be determined correspondingly as

$$\alpha = \min\{\lceil (1 + \Delta) \cdot \sqrt{2}\upsilon + \upsilon \rceil, m\}. \tag{5.1}$$

Traffic Pattern: Similar to [13, 16], we assume n is even and there are n unicast traffic flows with source-destination pairing as follows[2]: $1 \leftrightarrow 2$, $3 \leftrightarrow 4$, $\cdots$, $(n-1) \leftrightarrow n$. Based on this traffic model, each node is the source of a traffic flow and at the same time the destination of another traffic flow. For example, node 1 generates packets destined for node 2 and at the same time node 2 generates packets destined for node 1. The local packets generated at any source node i is assumed to follow an i.i.d. process $A_i(t)$, which has the same average packet input rate as $\mathbb{E}\{A_i(t)\} = \lambda$ and a bounded second moment for all time slot t as $\mathbb{E}\{A_i^2(t)\} \leq A_{max}^2 < \infty$.

[2]Our throughput capacity analysis process also applies to any other unicast source-destination pairings as shown later.

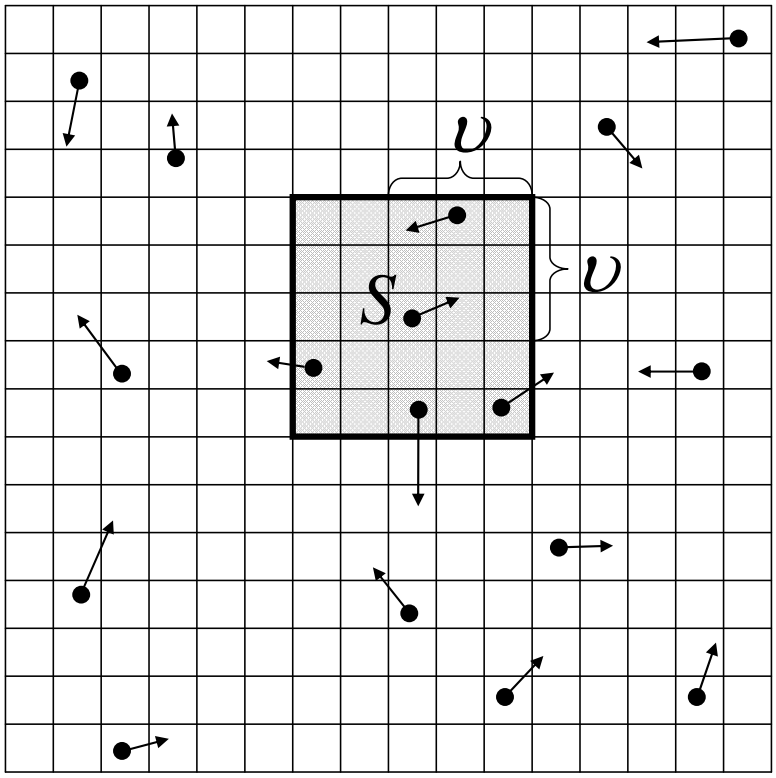

Figure 5.1: A snapshot of a cell partitioned MANET with general transmission range.

5.3 Throughput Capacity Analysis

In this section, we first derive a general throughput capacity upper bound for the concerned MANETs, which holds for any feasible packet delivery algorithm in such networks. We then prove that the throughput capacity upper bound is just the exact throughput capacity of MAC-TG MANETs by constructing a two-hop relay algorithm to stabilize the networks for any input rate within the upper bound.

5.3.1 Throughput Capacity Upper Bound

Before deriving the throughput capacity upper bound, we first introduce the definition of throughput capacity for a MAC-TG MANET.

Throughput Capacity: For a MAC-TG MANET and a given input rate λ (packets/slot) to each node, the network is called stable under this input rate if there exists

a corresponding packet delivery algorithm to ensure the queue length in each node and thus the overall average delay is bounded. The throughput capacity C of such a network is then defined as the maximum value of λ the network can stably support.

We then establish the following lemma regarding the overall transmission opportunities and also the source-destination transmission opportunities an active cell may have at a time slot, which will help us to derive a throughput capacity upper bound in Lemma 2.

Lemma 6 *For a given time slot and a given active cell c of a MAC-TG MANET, let p_0 denote the probability that there are at least two nodes within the coverage cells of c and at least one of those nodes is within c, and let p_1 denote the probability that there are at least one source-destination pair within the coverage cells of c and for each such pair, at least one of its two nodes is within c, then we have*

$$p_0 = \frac{1}{m^{2n}}\Big\{m^{2n} - \big(m^2-1\big)^n - n\big(m^2-h\big)^{n-1}\Big\} \tag{5.2}$$

$$p_1 = \frac{1}{m^{2n}}\Big\{m^{2n} - \big(m^4-2h+1\big)^{n/2}\Big\} \tag{5.3}$$

where $h = (2v-1)^2$.

Proof 9 *The proof of Lemma 6 is given in C.1.*

Remark 5 *From the definitions of p_0 and p_1, it is easy to see that $p_0 > p_1$.*

Based on the probabilities p_0 and p_1, which define the potential transmission opportunities each active cell may have, we can now determine a general throughput capacity upper bound for MAC-TG MANETs.

Lemma 7 *Consider a cell partitioned MANET with n nodes and m^2 cells, where nodes move according to i.i.d. mobility model, MAC-TG protocol is adopted to schedule simultaneous link transmissions and the transmission range of each node can be*

adjusted to cover a set of cells with horizontal and vertical distance of no more than $\upsilon - 1$ *cells away from the node's current cell. A throughput capacity upper bound* μ *for such a network is given by*

$$\begin{aligned}\mu &= \frac{K(p_0 + p_1)}{2n} \\ &= \frac{K}{2nm^{2n}}\Big\{2m^{2n} - \big(m^2-1\big)^n - n\big(m^2-h\big)^{n-1} - \big(m^4-2h+1\big)^{n/2}\Big\} \end{aligned} \tag{5.4}$$

where $K = \lfloor m^2/\alpha^2 \rfloor$ *and* $h = (2\upsilon - 1)^2$.

Proof 10 *Since this lemma can be proved by an approach similar to that adopted in [13, 16], we omit the detailed proof process here and just provide a sketch of the overall proof. By the definition of* p_0*, we know that on average there are* p_0 *overall transmission opportunities for an active cell and a time slot, which holds for any feasible packet delivery algorithm in the network. Notice also that with MAC-TG MANET, there are* K *active cells in each time slot. Thus, during time slot interval* $[0, T]$*, on average* Kp_0T *overall transmission opportunities are available, among them there are* Kp_1T *source-destination transmission opportunities. Since one hop transmission consumes a transmission opportunity, each packet should go through as few hop(s) as possible to reach its destination. Therefore, these* Kp_1T *source-destination transmission opportunities should be dedicated to packets that can reach their destinations in only one hop, and the remaining* $Kp_0T - Kp_1T$ *opportunities can deliver at most* $(Kp_0T - Kp_1T)/2$ *packets, because other packets need at least two hops to reach their destinations.*

Suppose that every node generates packets with average input rate λ*, then during time slot* $[0, T]$*, the average packets to the network will be* $n\lambda T$*. To stabilize the network, for arbitrarily small* $\epsilon > 0$*, there should exist sufficiently large* T *such that the difference between the average total input rate* $n\lambda$ *and the total output rate* $Kp_1 +$

$(Kp_0 - Kp_1)/2$ *should be within* ϵ. *Thus, we have*

$$n\lambda - Kp_1 - \frac{Kp_0 - Kp_1}{2} \leq \epsilon \tag{5.5}$$

or equivalently

$$\lambda \leq \frac{K(p_0 + p_1)}{2n} + \frac{\epsilon}{n} \tag{5.6}$$

Since ϵ *can be arbitrarily small, the upper bound (5.4) then follows.*

5.3.2 Throughput Capacity Proof

In this section, we will prove that the throughput capacity upper bound μ in (5.4) is just the exact throughput capacity for the concerned MANETs. The basic idea of our proof is to first construct a so called 2HR-q algorithm (two-hop relay with parameter $q = \frac{(n-2)\rho+2}{2n}$, $\rho = \frac{\lambda}{\mu}$, where parameter q is the probability with which a transmitter conducts source-to-relay transmission), and then show that this algorithm can stabilize the networks for any input rate $\lambda < \mu$.

The 2HR-q algorithm is defined in Algorithm 1.

Remark 6 *According to Algorithm 1, each node can only conduct one of the following transmissions if possible, namely, source-to-destination transmission, source-to-relay transmission and relay-to-destination transmission. A general packet takes at most two hop transmissions to reach its destination.*

The following lemma reveals some basic properties of the 2HR-q algorithm.

Lemma 8 *In a MAC-TG MANET, average per node input rate* λ *and 2HR-q algorithm, we denote by* p_{sd}, p_{sr} *and* p_{rd} *the probabilities that a node conducts a source-to-destination transmission, source-to-relay transmission and relay-to-destination trans-*

Procedure 5 2HR-q algorithm

1: At any time slot, for an active cell c, first check whether c can schedule a source-destination pair for data transmission.
2: **if** There exists such pairs **then**
3: With equal probability randomly select a pair to do source-to-destination transmission.
4: **if** The transmitter has packets for its destination **then**
5: The transmitter transmits a packet to its destination.
6: **else**
7: The transmitter stays idle for this time slot.
8: **end if**
9: **else**
10: Check whether c can schedule two nodes for data transmission.
11: **if** There exists such nodes **then**
12: With equal probability randomly select one node in c as the transmitter.
13: Randomly select another node within the transmission range of c as its receiver.
14: With probability q, the transmitter does source-to-relay transmission and with probability $1-q$ does relay-to-destination transmission.
15: **if** The transmitter has packets for the receiver **then**
16: The transmitter transmits a packet to the selected receiver.
17: **else**
18: The transmitter stays idle for this time slot.
19: **end if**
20: **end if**
21: **end if**

mission at a time slot, respectively. Then we have

$$p_{sd} = \frac{K}{n} p_1 \tag{5.7}$$

$$p_{sr} = \frac{qK}{n}(p_0 - p_1) \tag{5.8}$$

$$p_{rd} = \frac{(1-q)K}{n}(p_0 - p_1) \tag{5.9}$$

Proof 11 *At a time slot, each node conducts packet transmissions with probability $p_{sd} + p_{sr} + p_{rd}$, so on average there are $n(p_{sd} + p_{sr} + p_{rd})$ nodes conducting packet transmissions at each time slot. Based on the definition of p_0 we know that the average number of nodes that conduct packet transmissions at each time slot is also*

determined as $\sum_{c=1}^{K} p_0$*, where* c *is an index representing the* c*-th active cell in the current active group. Thus,*

$$n(p_{sd} + p_{sr} + p_{rd}) = \sum_{c=1}^{K} p_0 \tag{5.10}$$

Similarly,

$$np_{sd} = \sum_{c=1}^{K} p_1 \tag{5.11}$$

According to the 2HR-q algorithm, we have

$$\frac{p_{sr}}{p_{rd}} = \frac{q}{1-q} \tag{5.12}$$

From (5.10), (5.11) and (5.12), we then have (5.7), (5.8) and (5.9).

We now show that for any feasible input rate $\lambda < \mu$, the network can be stabilized and average packet delay can be bounded under the corresponding 2HR-q algorithm.

Theorem V.1 *In a cell partitioned MANET with* n *nodes and* m^2 *cells, where nodes move according to i.i.d. mobility model, MAC-TG protocol is adopted to schedule simultaneous link transmissions for interference avoidance and the transmission range of each node is adjusted to cover a set of cells with horizontal and vertical distance of no more than* $\upsilon - 1$ *cells away, if the local packet generation process at each node* i *follows an i.i.d. process* $A_i(t)$ *with* $\mathbb{E}\{A_i(t)\} = \lambda(\lambda = \rho\mu, 0 < \rho < 1)$ *and* $\mathbb{E}\{A_i^2(t)\} \leq A_{max}^2 < \infty$*, then the network is stabilized by adopting the 2HR-q algorithm and the corresponding average packet delay* $\overline{D}$ *is upper bounded as:*

$$\overline{D} \leq \frac{B_0}{B_1(1-\rho)\lambda\mu} \tag{5.13}$$

where

$$B_0 = \big(nA_{max}^2 + K - 2K\lambda\big)\big(p_0^2 - p_1^2\big) + 2n\mu\big(p_0 + np_1 - p_1\big) \tag{5.14}$$

$$B_1 = 4(p_0 + np_1 - p_1)(p_0 - p_1) \tag{5.15}$$

Proof 12 *According to the 2HR-q algorithm, each node should have two kinds of queues, one source-queue and $n-2$ relay-queues. The source-queue at a node holds its locally generated packets destined for its own destination and its $n-2$ relay-queues store packets destined for other $n-2$ nodes (i.e., nodes except the current node and its own destination node), respectively. Thus, there are n source-queues and $n(n-2)$ relay-queues in the concerned MANET.*

We need the following notations in our proof:

- $Q_k^{(i,d_i)}$*: For $k = i$, $Q_i^{(i,d_i)}$ represents the source-queue in node i. For $k \neq i$, $Q_k^{(i,d_i)}$ represents a relay-queue in node k storing packets destined for node d_i.Notice that a node sinks packets destined for itself, no queue is needed for such packets and thus $k \neq d_i$.*

- $Q_k^{(i,d_i)}(t)$*: It is the queue length of $Q_k^{(i,d_i)}$ at time slot t, i.e., the number of packets stored in queue $Q_k^{(i,d_i)}$ at time slot t.*

- $A_k^{(i,d_i)}(t)$*: For $k = i$, $A_i^{(i,d_i)}(t)$ is just $A_i(t)$, i.e. the number of packet generated locally at source node i in time slot t. For $k \neq i$, $A_k^{(i,d_i)}(t)$ is an indicator function, taking the value of 1 if relay node k receives a packet destined for d_i from source node i at time slot t and taking the value of 0 otherwise. If relay k receives such a packet (i.e. $A_k^{(i,d_i)}(t) = 1$), the packet will be stored in the corresponding relay-queue $Q_k^{(i,d_i)}$ in node k.*

- $I_{k,in}^{(i,d_i)}(t)$*: It is an indicator function, taking the value of 1 if relay node k is selected as the receiver by source node i to receive a packet destined for d_i and*

taking the value of 0 *otherwise.*

- $D_k^{(i,d_i)}(t)$*: It is an indicator function, taking the value of* 1 *if node* k *sends out a packet from the queue* $Q_k^{(i,d_i)}$ *at time slot* t*,* $k \neq d_i$*, and taking the value of* 0 *otherwise.*

- $I_{k,out}^{(i,d_i)}(t)$*: It is an indicator function, taking the value of* 1 *if node* k *is selected as the transmitter to send out one packet from the queue* $Q_k^{(i,d_i)}$ *at time slot* t*,* $k \neq d_i$*, and taking the value of* 0 *otherwise.*

Under 2HR-q algorithm, we have the followings:

$$A_k^{(i,d_i)}(t) \leq I_{k,in}^{(i,d_i)}(t) \quad , \text{ if } k \neq i \tag{5.16}$$

$$\left(A_k^{(i,d_i)}(t)\right)^2 = A_k^{(i,d_i)}(t) \quad , \text{ if } k \neq i \tag{5.17}$$

$$D_k^{(i,d_i)}(t) = 0 \qquad , \text{ if } Q_k^{(i,d_i)}(t) = 0 \tag{5.18}$$

$$A_k^{(i,d_i)}(t) \cdot D_k^{(i,d_i)}(t) = 0 \qquad , \text{ if } k \neq i \tag{5.19}$$

$$\left(D_k^{(i,d_i)}(t)\right)^2 = D_k^{(i,d_i)}(t) \tag{5.20}$$

$$Q_k^{(i,d_i)}(t) \cdot D_k^{(i,d_i)}(t) = Q_k^{(i,d_i)}(t) \cdot I_{k,out}^{(i,d_i)}(t) \tag{5.21}$$

The above expressions hold as explained in the followings.

For $k \neq i$*, we can see from the definitions of* $A_k^{(i,d_i)}(t)$ *and* $I_{k,in}^{(i,d_i)}(t)$ *that if* $I_{k,in}^{(i,d_i)}(t) = 0$ *then* $A_k^{(i,d_i)}(t) = 0$*, if* $I_{k,in}^{(i,d_i)}(t) = 1$ *then* $A_k^{(i,d_i)}(t)$ *could be either* 1 *or* 0*. Notice that even if* $I_{k,in}^{(i,d_i)}(t) = 1$*, it may happen that source node* i *currently has no packet destined for* d_i *to transmit, resulting in* $A_k^{(i,d_i)}(t) = 0$*. Thus, (5.16) follows.*

(5.17) and (5.20) follow from the fact that $A_k^{(i,d_i)}(t)$ *takes value from* $\{0, 1\}$ *when* $k \neq i$*, and* $D_k^{(i,d_i)}(t)$ *also takes value from* $\{0, 1\}$*. (5.18) holds due to the fact that if queue* $Q_k^{(i,d_i)}(t) = 0$ *in node* k*, then node* k *has no packet to send out.*

From the definitions of $D_k^{(i,d_i)}(t)$ *and* $A_k^{(i,d_i)}(t)$ *we know that for* $k \neq i$*,* $D_k^{(i,d_i)}(t)$ *indicates whether relay node* k *sends out a packet at time slot* t*, while* $A_k^{(i,d_i)}(t)$ *indi-*

cates whether relay node k receives a packet at time slot t. Notice that according to 2HR-q algorithm relay node k can not send out a packet and receive a packet at the same time slot, so at least one of $D_k^{(i,d_i)}(t)$ and $A_k^{(i,d_i)}(t)$ is 0. Thus, (5.19) holds.

From the definitions of $I_{k,out}^{(i,d_i)}(t)$ and $D_k^{(i,d_i)}(t)$ we can see that when $I_{k,out}^{(i,d_i)}(t) = 0$, then $D_k^{(i,d_i)}(t) = 0$. Thus, (5.21) holds for the case that $I_{k,out}^{(i,d_i)}(t) = 0$. We now consider the case that $I_{k,out}^{(i,d_i)}(t) = 1$, which indicates that node k is selected as the transmitter to send out one packet from the queue $Q_k^{(i,d_i)}$ at time slot t, $k \neq d_i$. First, if $Q_k^{(i,d_i)}(t) \neq 0$ at slot t under the case $I_{k,out}^{(i,d_i)}(t) = 1$, then $D_k^{(i,d_i)}(t) = 1$ and thus (5.21) holds. Second, if $Q_k^{(i,d_i)}(t) = 0$ under the case $I_{k,out}^{(i,d_i)}(t) = 1$, then both sides of (5.21) become 0. To sum up, (5.21) always holds.

All queues in a MANET, including source-queues and relay-queues, evolve with time as follows:

$$Q_k^{(i,d_i)}(t+1) = Q_k^{(i,d_i)}(t) - D_k^{(i,d_i)}(t) + A_k^{(i,d_i)}(t) \tag{5.22}$$

At any time slot t, the state of all source-queues in the concerned MANET can be collected into a n-dimension vector

$$\widehat{Q_0}(t) = \left(Q_1^{(1,d_1)}(t), Q_2^{(2,d_2)}(t), \cdots, Q_i^{(i,d_i)}(t), \cdots, Q_n^{(n,d_n)}(t)\right) \tag{5.23}$$

Similarly, the state of all relay-queues in the MANET can be represented by a $n(n-2)$-dimension vector

$$\begin{aligned}\widehat{Q_1}(t) = \Big(&Q_1^{(3,d_3)}(t), \cdots Q_1^{(n,d_n)}(t), \cdots, Q_k^{(i,d_i)}(t), \\ &\cdots, Q_n^{(1,d_1)}(t), \cdots, Q_n^{(n-2,d_{n-2})}(t)\Big)\end{aligned} \tag{5.24}$$

where $k \neq i, d_i$.

Define a quadratic Lyapunov function of source-queue vector $\widehat{Q_0}(t)$ *as*

$$L\big(\widehat{Q_0}(t)\big) = \sum_{k=1}^{n} \Big(Q_k^{(k,d_k)}(t)\Big)^2 \tag{5.25}$$

Then the conditional Lyapunov Drift of source-queues satisfies

$$\begin{aligned}
&\mathbb{E}\Big\{L\big(\widehat{Q_0}(t+1)\big) - L\big(\widehat{Q_0}(t)\big)\Big|\widehat{Q_0}(t)\Big\} \\
&\leq nA_{max}^2 + (1-2\lambda)\mathbb{E}\Big\{\sum_{k=1}^{n} D_k^{(k,d_k)}(t)\Big|\widehat{Q_0}(t)\Big\} \\
&\quad - 2\mathbb{E}\Big\{\sum_{k=1}^{n} Q_k^{(k,d_k)}(t)\Big(I_{k,out}^{(k,d_k)}(t) - A_k(t)\Big)\Big|\widehat{Q_0}(t)\Big\}
\end{aligned} \tag{5.26}$$

The derivation process of (5.26) is given in C.2.

Notice that in the MAC-TG MANET, we have K *active cells at any time slot to schedule simultaneous data transmissions. Thus,*

$$\sum_{k=1}^{n} D_k^{(k,d_k)}(t) \leq K \tag{5.27}$$

According to the 2HR-q algorithm and the definition of $I_{k,out}^{(i,d_i)}(t)$*, we know that* $I_{k,out}^{(k,d_k)}(t)$ *indicates that at time slot* t *whether node* k *can send out one packet from its source-queue* $Q_k^{(k,d_k)}$*, either directly to its own destination through a source-to-destination transmission or to a relay node through a source-to-relay transmission. Thus, we have*

$$\mathbb{E}\Big\{I_{k,out}^{(k,d_k)}(t)\Big\} = p_{sd} + p_{sr} = \frac{K}{n}(qp_0 + p_1 - qp_1) \tag{5.28}$$

Substituting (5.27) and (5.28) into (5.26), we have

$$\begin{aligned}&\mathbb{E}\Big\{L\big(\widehat{Q_0}(t+1)\big)-L\big(\widehat{Q_0}(t)\big)\big|\widehat{Q_0}(t)\Big\}\\&\leq nA_{max}^2+(1-2\lambda)K-2\epsilon_0\sum_{k=1}^{n}Q_k^{(k,d_k)}(t)\end{aligned}\tag{5.29}$$

where $\epsilon_0=\frac{K}{n}(qp_0+p_1-qp_1)-\lambda$.

Define a quadratic Lyapunov function of relay-queue vector $\widehat{Q_1}(t)$ *as*

$$L(\widehat{Q_1}(t))=\sum_{k=1}^{n}\sum_{\substack{i\neq k,\\ d_i\neq k}}\Big(Q_k^{(i,d_i)}(t)\Big)^2$$

Then the conditional Lyapunov Drift of relay-queues satisfies

$$\begin{aligned}&\mathbb{E}\Big\{L\big(\widehat{Q_1}(t+1)\big)-L\big(\widehat{Q_1}(t)\big)\big|\widehat{Q_1}(t)\Big\}\\&\leq\mathbb{E}\Big\{\sum_{k=1}^{n}\sum_{\substack{i\neq k,\\ d_i\neq k}}\Big(A_k^{(i,d_i)}(t)+D_k^{(i,d_i)}(t)\Big)\Big|\widehat{Q_1}(t)\Big\}\\&\quad-2\mathbb{E}\Big\{\sum_{k=1}^{n}\sum_{\substack{i\neq k,\\ d_i\neq k}}Q_k^{(i,d_i)}(t)\Big(I_{k,out}^{(i,d_i)}(t)-I_{k,in}^{(i,d_i)}(t)\Big)\Big|\widehat{Q_1}(t)\Big\}\end{aligned}\tag{5.30}$$

(5.30) follows after similar derivation process of (5.26).

Due to the same reason with (5.27), we have

$$\sum_{k=1}^{n}\sum_{\substack{i\neq k,\\ d_i\neq k}}\Big(A_k^{(i,d_i)}(t)+D_k^{(i,d_i)}(t)\Big)\leq K\tag{5.31}$$

Recall that when $k\neq i$, $I_{k,out}^{(i,d_i)}(t)$ *indicates that at time slot* t *whether node* k *can send out one packet from its relay-queue* $Q_k^{(i,d_i)}$. *According to the 2HR-q algorithm, node* k *conducts relay-to-destination transmissions for* $n-2$ *destinations with equal*

probability, thus

$$\mathbb{E}\Big\{I_{k,out}^{(i,d_i)}(t)\Big\} = \frac{p_{rd}}{n-2} = \frac{(1-q)K}{(n-2)n}(p_0 - p_1). \tag{5.32}$$

Similarly, we have

$$\mathbb{E}\Big\{I_{k,in}^{(i,d_i)}(t)\Big\} = \frac{p_{sr}}{n-2} = \frac{qK}{(n-2)n}(p_0 - p_1). \tag{5.33}$$

Combining (5.30), (5.31), (5.32) and (5.33) together, we get

$$\begin{aligned} &\mathbb{E}\Big\{L\big(\widehat{Q_1}(t+1)\big) - L\big(\widehat{Q_1}(t)\big)\big|\widehat{Q_1}(t)\Big\} \\ &\leq K - 2\epsilon_1 \sum_{k=1}^{n} \sum_{\substack{i\neq k,\\ d_i\neq k}} Q_k^{(i,d_i)}(t) \end{aligned} \tag{5.34}$$

where $\epsilon_1 = \frac{K}{(n-2)n}(1-2q)(p_0 - p_1)$.

Regarding the parameter q of 2HR-q algorithm, we set

$$q = \frac{(n-2)\rho + 2}{2n} \tag{5.35}$$

then

$$\epsilon_0 = \frac{2(1-\rho)(p_0 + np_1 - p_1)}{n(p_0 + p_1)} \cdot \mu > 0 \tag{5.36}$$

$$\epsilon_1 = \frac{K(1-\rho)}{n^2}(p_0 - p_1) > 0 \tag{5.37}$$

From (5.29), (5.36) and Lemma 4.1 of [74], we draw the conclusion that all source-

queues are stable by adopting 2HR-q algorithm, where

$$\begin{aligned}&\limsup_{T\to\infty}\frac{1}{T}\sum_{t=0}^{T-1}\sum_{k=1}^{n}\mathbb{E}\Big\{Q_k^{(k,d_k)}(t)\Big\}\\&\leq\frac{n(nA_{max}^2+K-2\lambda K)(p_0+p_1)}{4(p_0+np_1-p_1)(1-\rho)\mu}\end{aligned}\tag{5.38}$$

From (5.34), (5.37) and Lemma 4.1 of [74], we draw the conclusion that all relay-queues are stable by adopting 2HR-q algorithm, where

$$\limsup_{T\to\infty}\frac{1}{T}\sum_{t=0}^{T-1}\sum_{k=1}^{n}\sum_{\substack{i\neq k,\\ d_i\neq k}}\mathbb{E}\Big\{Q_k^{(i,d_i)}(t)\Big\}\leq\frac{n^2}{2(p_0-p_1)(1-\rho)}\tag{5.39}$$

From (5.38) and (5.39), we have that the aggregate length of all network queues satisfies

$$\limsup_{T\to\infty}\frac{1}{T}\sum_{t=0}^{T-1}\sum_{\substack{k,i,\\ d_i\neq k}}\mathbb{E}\Big\{Q_k^{(i,d_i)}(t)\Big\}\leq\frac{nB_0}{B_1(1-\rho)\mu}\tag{5.40}$$

where

$$\begin{aligned}B_0&=\big(nA_{max}^2+K-2K\lambda\big)\big(p_0^2-p_1^2\big)+2n\mu\big(p_0+np_1-p_1\big)\\B_1&=4(p_0+np_1-p_1)(p_0-p_1)\end{aligned}$$

Notice that the total network input rate is $n\lambda$, after applying Little's Theorem [65] we know that the average packet delay $\overline{D}$ is upper bounded as

$$\overline{D}\leq\frac{B_0}{B_1(1-\rho)\lambda\mu}\tag{5.41}$$

This finishes the proof of Theorem V.1.

Now we are ready to derive the throughput capacity of MAC-TG MANETs and

general transmission range.

Theorem V.2 *In a cell partitioned MANET with n nodes and m^2 cells, where nodes move according to i.i.d. mobility model, MAC-TG protocol is adopted to schedule simultaneous link transmissions for interference avoidance and the transmission range of each node is adjusted to cover a set of cells with horizontal and vertical distance of no more than $\upsilon - 1$ cells away, if the local packet generation process at each node i follows an i.i.d. process $A_i(t)$ with $\mathbb{E}\{A_i(t)\} = \lambda(\lambda = \rho\mu, 0 < \rho < 1)$ and $\mathbb{E}\{A_i^2(t)\} \leq A_{max}^2 < \infty$, then the throughput capacity C of MAC-TG MANETs is determined as*

$$\begin{aligned} C &= \mu \\ &= \frac{K}{2nm^{2n}}\Big\{2m^{2n} - \big(m^2-1\big)^n - n\big(m^2-h\big)^{n-1} - \big(m^4-2h+1\big)^{n/2}\Big\} \end{aligned} \tag{5.42}$$

where $K = \lfloor m^2/\alpha^2 \rfloor$ and $h = (2\upsilon - 1)^2$.

Proof 13 *From Lemma 7 and Theorem V.1, we can see that for any input rate $\lambda < \mu$, the network is stable under the corresponding 2HR-q algorithm, i.e., the queue length of all queues in the network will not grow to infinity and thus we have a bounded average packet delay. According to the definition of throughput capacity of the concerned MANETs, the maximum input rate μ is just the exact throughput capacity of MAC-TG MANETs* [3]*. This completes the proof of Theorem V.2.*

5.4 Numerical Results

In this section, we first provide validation of our theoretical results of throughput capacity and packet delay bound, then explore how transmission range υ and node density (n/m^2) affect the network throughput capacity.

[3]From now on we call μ the network throughput capacity.

5.4.1 Throughput Capacity Validation

We developed a dedicated C++ simulator to simulate the packet delivery process in the concerned MANETs with i.i.d. node mobility, MAC-TG protocol, general transmission range and 2HR-q algorithm [4]. Similar to [67], we set the protocol guard factor as $\Delta = 1$. We assume that the local packet generation process in each source node follows the Poisson process with average input rate λ (packets/slot). For comparison, another two realistic mobility models, the random walk model [34] and random waypoint model [31], were also implemented in the simulator. Under three different mobility models, the MANET topology changes in the following ways:

- **i.i.d. Model:** At the beginning of each time slot, every node independently and uniformly chooses a cell among all cells in the MANET to move into, and then stays in it until the end of that time slot.

- **Random Walk Model:** At the beginning of each time slot, with equal probability 1/9 every node independently chooses a cell among its current cell and its 8 neighboring cells to move into, and then stays in it until the end of that time slot.

- **Random Waypoint Model:** At the beginning of each time slot, every node independently decides a two-element vector $[x, y]$, where both elements x and y are uniformly generated from $[1/m, 3/m]$. The node then moves along the horizontal and vertical direction of distance x and y, respectively.

Extensive simulations have been conducted to validate our throughput capacity and packet delay bound, and some results under network scenarios of $n = 100, m = 8, \upsilon = \{1, 3\}$ and $n = 250, m = 16, \upsilon = \{1, 5\}$ are summarized in Figs. 5.2 and 5.3. All simulation results are reported with 95% confidence interval.

[4]The simulator is available online at [75].

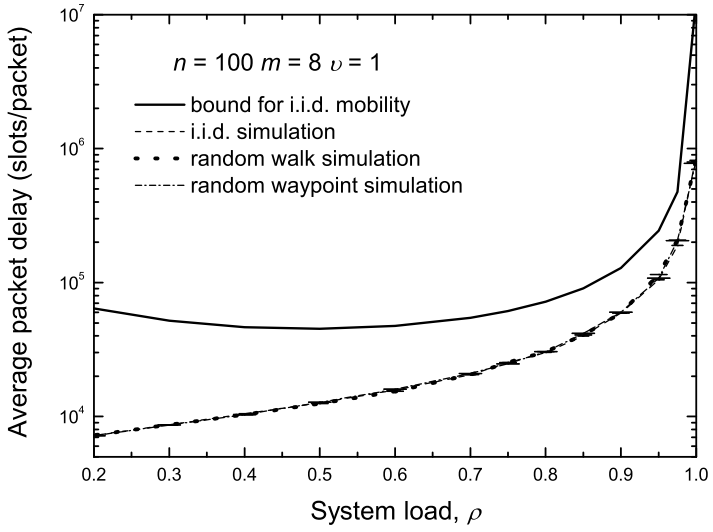

(a) Network scenario ($n = 100, m = 8, \upsilon = 1$) with throughput capacity $\mu = 9.53 \times 10^{-3}$(packets/slot).

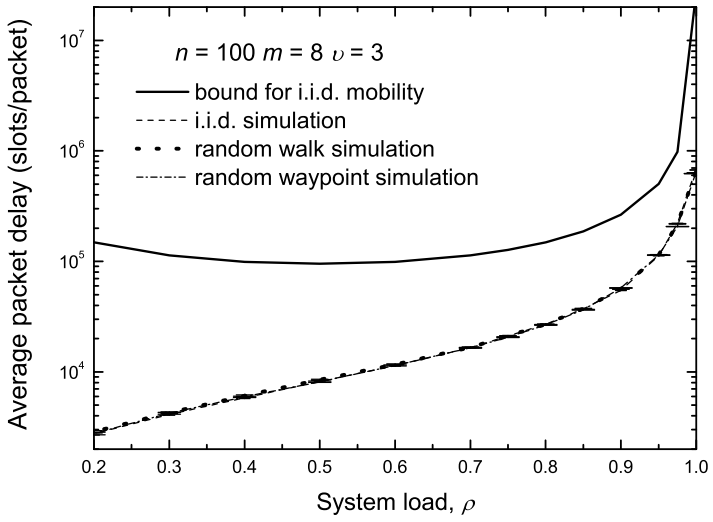

(b) Network scenario ($n = 100, m = 8, \upsilon = 3$) with throughput capacity $\mu = 6.23 \times 10^{-3}$(packets/slot).

Figure 5.2: Average packet delay for network scenarios with $n = 100, m = 8$ and different transmission range υ under the 2HR-q algorithm.

We can see from Figs. 5.2 and 5.3 that in general the packet delay monotonously increases as the system load $\rho(\rho = \lambda/\mu)$ increases. It is notable that as the system load

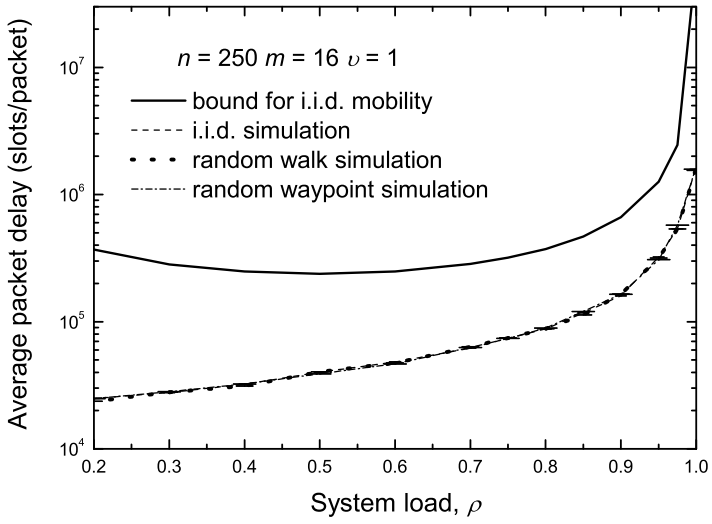

(a) Network scenario $(n = 250, m = 16, \upsilon = 1)$ with throughput capacity $\mu = 8.24 \times 10^{-3}$(packets/slot).

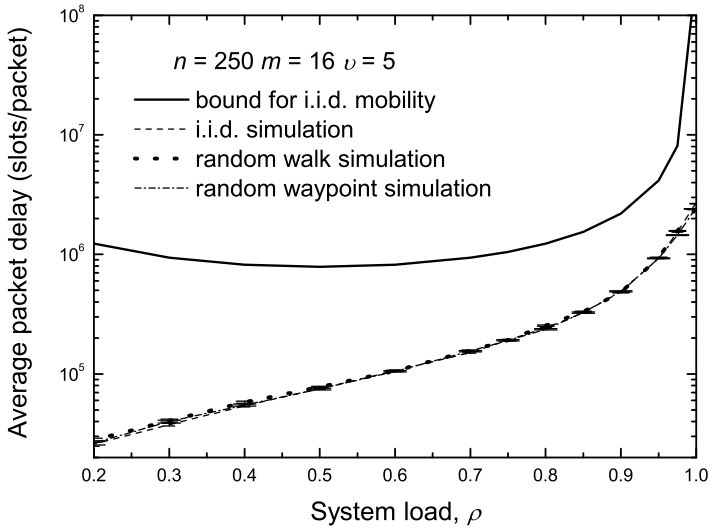

(b) Network scenario $(n = 250, m = 16, \upsilon = 5)$ with throughput capacity $\mu = 1.78 \times 10^{-3}$(packets/slot).

Figure 5.3: Average packet delay for network scenarios with $n = 250, m = 16$ and different transmission range υ under the 2HR-q algorithm.

approaches 1, i.e., as the input rate λ at each node approaches network throughput capacity μ, the packet delay increases sharply and becomes extremely sensitive to

the variation of input rate. This phenomenon indicates clearly that the exact network throughput capacity we developed nicely captures the capacity performance of MAC-TG MANETs. We can also observe from Figs. 5.2 and 5.3 that our derived packet delay upper bound safely bounds the packet delay for any input rate $\lambda < \mu$, indicating that the network is stabilized under the 2HR-q algorithm. Figs. 5.2 and 5.3 also indicate that the packet delay of MANETs under the random walk model and random waypoint model has very similar behaviors to that of MANETs under the i.i.d. mobility model. This indicates that packet delay upper bound, although derived under the i.i.d. mobility model, may also apply to other more realistic mobility models (like the random walk and random waypoint).

Remark 7 *Please notice that the main purpose of providing a theoretical delay bound in this paper is to validate the derived throughput capacity as discussed in the proof of Theorem V.2, i.e., for any feasible input rate less than the derived throughput capacity the corresponding delay can be upper bounded. It is notable that the wide difference between theoretical bound and simulation results comes from the loose upper bounds (5.16), (5.27) and (5.31) adopted in the derivation process of the theoretical delay bound. The loose upper bounds (5.27) and (5.31) are due to the fact that in every time slot there are K active cells according to the MAC-TG protocol, but the total number of successful data transmissions in that time slot may be less than K since some transmitters may not have packets for receivers in that time slot. Thus, applying these loose bounds in the derivation process of theoretical delay bound results in a wide difference between theoretical delay bound and simulation results.*

Remark 8 *It is notable that the simulation results are almost the same under three mobility models, indicating that throughput capacity does not depend on the three mobility models. Actually, throughput capacity will be independent of mobility models as long as these mobility models share the same steady-state location distribution*

[16]. Based on the random walk theory, it can be shown that the resulting steady-state location distributions of the three mobility models considered all follow uniform distribution over all cells in the MANET (please see [16] and references therein). Thus, our derived throughput capacity holds for the i.i.d. model, random walk model and random waypoint model.

5.4.2 Throughput Capacity Illustration

With the help of new throughput capacity result, we explore how transmission range υ and node density (n/m^2) will affect the final network throughpu capacity. For networks with fixed cell partition of $m = 16$, Figs. 5.4a and 5.4b show how network throughput capacity varies with transmission range υ and number of nodes n.

From Fig. 5.4a we can see that as υ grows from 1 to 3, the throughput capacity for networks with $n = \{500, 800\}$ always decreases while the throughput capacity for networks with $n = \{50, 100\}$ first increases and then decreases. This is due to following reasons: when node density (i.e., n/m^2) is low (e.g., $n = \{50, 100\}$), there are not enough relay nodes to help source nodes deliver packets, so a slight increase in transmission range (e.g. from 1 to 2 here) results in an increase in transmission opportunities for source nodes and thus an increase in network throughput capacity; when node density is high (e.g., $n = \{500, 800\}$), however, a larger transmission range will cause a much significant medium contention among nodes and thus a decrease of network throughput capacity. Another observation from Fig. 5.4a is that when $\upsilon \geq 3$, the corresponding throughput capacity μ for all n there slightly increases as υ further increases. This is because that according to the MAC-TG protocol, there is only one active cell to schedule data transmissions at any time slot for MANETs with $m = 16$ and $\upsilon \geq 3$, thus a further increase in transmission range brings more chances for the active cell to schedule a source-destination pair to do source-to-destination

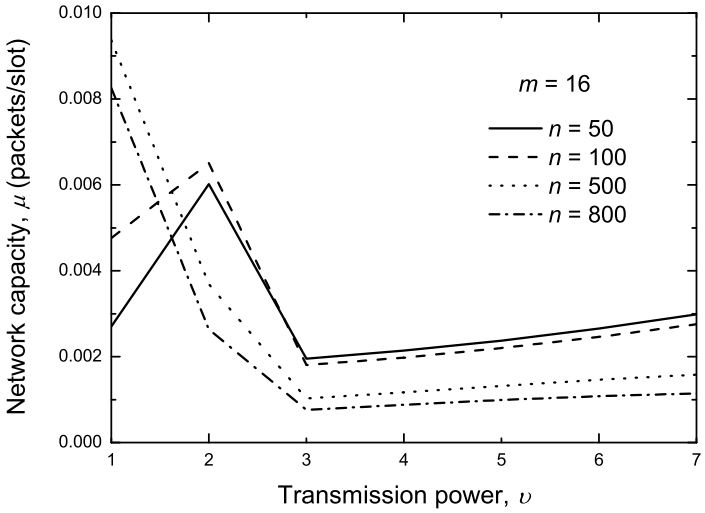

(a) Network throughput capacity μ vs. transmission range υ with fixed node number n.

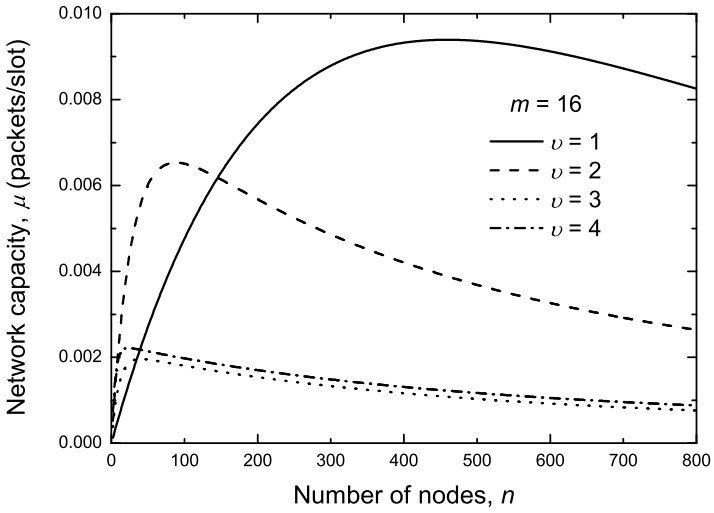

(b) Network throughput capacity μ vs. the number of nodes n with fixed transmission range υ.

Figure 5.4: The network throughput capacity μ of networks with $m = 16$.

transmissions. However, as Fig. 5.4a indicates that this kind of increase in throughput capacity is limited and we can always achieve the maximum network throughput capacity at a low transmission range.

Now we proceed to examine in more details the impact of node density upon network throughput capacity. As we can see from Fig. 5.4b that for a given υ, there always exists an optimal node density (resp.number of nodes) to maximize throughput capacity. This can be explained as follows: on one hand, a higher node density (resp. a greater number of nodes) will result in more chances for an active cell to schedule two nodes to do packet transmissions and thus an increase in transmission rates of source nodes, but on the other hand, a higher node density will introduce more significant medium contentions among source nodes and thus a decrease in their transmission rates. When the former (resp. the latter) factor dominates, network throughput capacity increases (resp. decreases) as node density increases. It is also interesting to see from Fig. 5.4b that when transmission range is smaller, the maximum network throughput capacity will be achieved with a higher node density. For example, for the case of $\upsilon = 1$, the corresponding maximum throughput capacity 9.39×10^{-3} (packets/slot) is achieved when the number of nodes is 460 (resp. when the node density is 1.80). Similarly, the maximum throughput capacity for networks with $\upsilon = 2$ (resp. $\upsilon = 3$ and $\upsilon = 4$) is achieved when the number of nodes is 90 (resp. 40 and 24).

5.5 Summary

This chapter derived the exact throughput capacity for MAC-TG MANETs, which adopt the MAC-TG protocol to schedule simultaneous link transmissions for interference avoidance and allow the transmission range employed by each node to be adjusted to cover a set of cells. First, we identified a throughput capacity upper bound for the considered MANETs. Then, we proved the upper bound is just the throughput capacity of the MANETs by showing that any traffic input rate within the upper bound can be stably supported by adopting a so called 2HR-q algorithm. As verified through extensive simulation studies, our theoretical results nicely char-

acterize the throughput capacity behaviors of the MANETs. Numerical results in this paper indicate that we can usually achieve a high network throughput capacity with a low transmission range and an optimal node density always exists to maximize throughput capacity for a given transmission range.

CHAPTER VI

Conclusion

6.1 Summary of Contributions

In this thesis, we studied the delay and capacity performances for MAC-TG MANETs. The main contributions are summarized as follows.

- For delay performance analysis, we first studied the source delay, which is the time a packet experiences at its source node after it is generated by that source node. We applied the QBD theory to develop a theoretical framework to capture the complex network dynamics in a MANET. The theoretical framework is powerful in the sense it enables complex network dynamics to be incorporated into source delay analysis, like node mobility, medium contention, interference, packet transmitting and packet generating processes. With the help of the theoretical framework, we then derived the cumulative distribution function (CDF) as well as mean and variance of the source delay in the considered MANET. Based on the theoretical source delay models, we further demonstrated how source delay in MANETs is related to network parameters.

- We next studied the end-to-end delay performance for MANETs. We first extended the above QBD-based theoretical framework to efficiently capture the complex network state transitions in MANETs, where main network dynamics

can be jointly taken into considerations. With the help of the theoretical framework, we then showed that we were able to analytically model the expected end-to-end delay and also per node throughput capacity for a two-hop relay MANET. The effects of network parameters on end-to-end delay and throughput capacity were also investigated.

- For throughput capacity analysis of MANETs, we first identified a general throughput capacity upper bound that holds under any feasible packet delivery algorithm in the considered MANETs. We then proved through Lyapunov theory that the upper bound we identified is just the exact throughput capacity for the concerned MANETs by showing that for any traffic input rate within the throughput capacity upper bound, there exists a corresponding two-hop relay algorithm to stabilize such networks. For any traffic input rate within the capacity, a closed-form formula was further derived to upper bound the packet delay under corresponding two-hop relay algorithm. Finally, based on the exact capacity result, we explored how transmission range and node density will affect the MANET throughput capacity.

6.2 Future Works

As shown in this thesis, the Quasi-Birth-and-Death theory and Lyapunov theory are efficient in dealing with complex networks. With the help of these powerful theoretical tools, we conducted delay and capacity studies for MANETs. The future works to extend this thesis are as follows.

- In this thesis, we studied delay performances for MANETs under i.i.d. mobility model, in which all nodes move independently and have no memory of its movement history. However, in reality nodes' movement are usually correlated [20, 32, 76] and they could move from one place only to one adjacent

place. So one possible future work is to take the correlation of node movement into considerations and to study delay performance under markovian mobility models, like random walk mobility model [34,77] and random waypoint mobility model [31, 78].

- We analyzed the expected end-to-end delay for a two-hop relay MAENT, it would be interesting for extend our framework to further study another important aspect of delay performance, i.e., variance. Analyzing the end-to-end delay for MANETs with multi-hop relay routing is another interesting future direction. Furthermore, we may explore how to set network parameters to minimize network end-to-end delay or to meet delay requirements, or what is the best relay routing scheme with regard to delay performance.

- Since our delay and capacity studies are conducted for MANETs with transmission-group based MAC protocol, another one possible extension is to apply our theoretical framework to analyze delay and capacity performances for MANETs with other MAC protocols, such as Aloha protocol [79, 80] and Carrier sense multiple access with collision avoidance (CSMA/CA) protocol [81–83].

- In our work, we assumed that all nodes generate packets at the same rate, i.e., symmetric traffic pattern. Under the symmetric traffic pattern, the network capacity is just one number, the maximum input rate the network could stably support. However, in asymmetric traffic cases, the stably supportable input rates constitute a region. Thus, the network capacity region for MANETs with asymmetric traffic pattern will be of great interest.

APPENDICES

APPENDIX A

Source Delay Analysis

A.1 Proof of Lemma 1

The proof process is similar to that in [35,38]. We omit the proof details here and just outline the main idea of the proof. To derive the probability p_0 (resp. p_1), we first divide the event that S conducts a source-destination transmission (resp. packet-dispatch transmission) in a time slot into following sub-events: 1) S moves into an active cell in the time slot according to the IID mobility model; 2) S successfully accesses the wireless channel after fair contention according to the MAC-EC protocol; 3) S selects to conduct source-destination transmission (resp. packet-dispatch transmission) according to the PD-f scheme. We can then derive probability p_0 (resp. p_1) by combining the probabilities of these sub-events.

A.2 Proof of Lemma 2

To derive the conditional steady state distribution $\boldsymbol{\pi}_{\Omega}^{*}$ of the source-queue under the condition that a packet has just been inserted into the queue, we first study its corresponding transient state distribution $\boldsymbol{\pi}_{\Omega}(t+1)$ at time slot $t+1$.

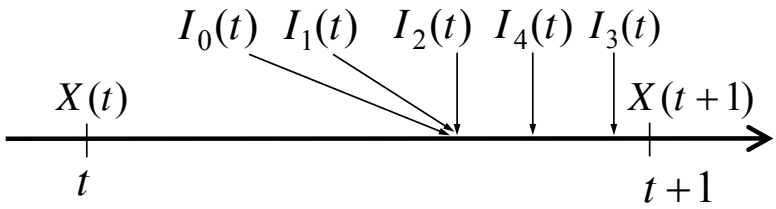

Figure A.1: Illustration for state transition from $\mathbf{X}(t)$ to $\mathbf{X}(t+1)$ during time slot $[t, t+1)$.

Similar to the definition of $\boldsymbol{\pi}_{\Omega}^{*}$, we can see that the $(2+(l-1)f+j)$-th entry of row vector $\boldsymbol{\pi}_{\Omega}(t+1)$, denoted by $[\boldsymbol{\pi}_{\Omega}(t+1)]_{2+(l-1)f+j}$ here, corresponds to the probability that the source-queue is in state $\mathbf{X}(t+1) = (l, j)$ in time slot $t+1$ under the condition that a packet has just been inserted into the source-queue in time slot t, $1 \leq l \leq M, 0 \leq j \leq f-1$. The basic state transition from $\mathbf{X}(t)$ to $\mathbf{X}(t+1)$ is illustrated in Fig. A.1, where $I_0(t)$ through $I_3(t)$ are indicator functions defined in Section III.A, and $I_4(t)$ is a new indicator function, taking value of 1 if the source-queue is not full in time slot t (i.e. the source-queue is in some state in $\big\{\{(0,0)\} \cup \{(l,j)\}; 1 \leq l \leq M-1, 0 \leq j \leq f-1\big\}$), and taking value of 0 otherwise.

From Fig. A.1 we can see that $[\boldsymbol{\pi}_{\Omega}(t+1)]_{2+(l-1)f+j}$ is evaluated as

$$
\begin{aligned}
&[\boldsymbol{\pi}_{\Omega}(t+1)]_{2+(l-1)f+j} && \text{(A.1)}\\
&= Pr\{\mathbf{X}(t+1) = (l,j) | I_4(t) = 1, I_3(t) = 1\} && \text{(A.2)}\\
&= \frac{Pr\{I_4(t) = 1, I_3(t) = 1, \mathbf{X}(t+1) = (l,j)\}}{Pr\{I_4(t) = 1, I_3(t) = 1\}} && \text{(A.3)}\\
&= \frac{Pr\{I_4(t) = 1, I_3(t) = 1, \mathbf{X}(t+1) = (l,j)\}}{\lambda \cdot Pr\{I_4(t) = 1\}}, && \text{(A.4)}
\end{aligned}
$$

where (A.4) follows because the packet generating process is a Bernoulli process independent of the state of the source-queue.

For the probability $Pr\{I_4(t)=1\}$ in (A.4), we have

$$Pr\{I_4(t)=1\} \tag{A.5}$$

$$= \sum_{(l',j')} Pr\{I_4(t)=1, \mathbf{X}(t)=(l',j')\} \tag{A.6}$$

$$= \sum_{(l',j')} Pr\{\mathbf{X}(t)=(l',j')\} Pr\{I_4(t)=1|\mathbf{X}(t)=(l',j')\} \tag{A.7}$$

where $Pr\{I_4(t)=1|\mathbf{X}(t)=(l',j')\}$ is actually the transition probability from state $\mathbf{X}(t)=(l',j')$ to states in $\big\{\{(0,0)\}\cup\{(l,j)\}; 1\le l\le M-1, 0\le j\le f-1\big\}$. The matrix $\mathbf{P_1}$ of such transition probabilities can be determined based on (3.3) by setting the corresponding sub-matrices according to (3.8)-(3.18). With matrix $\mathbf{P_1}$ and (A.7), we have

$$Pr\{I_4(t)=1\} = \boldsymbol{\pi}_\omega(t)\cdot\mathbf{P_1}\cdot\mathbf{1}, \tag{A.8}$$

where $\boldsymbol{\pi}_\omega(t)=(\boldsymbol{\pi}_{\omega,l,j}(t))_{1\times M\cdot f}$ with $\boldsymbol{\pi}_{\omega,l,j}(t)$ being the probability $Pr\{\mathbf{X}(t)=(l',j')\}$.

For the numerator of (A.4), we have

$$Pr\{I_4(t)=1, I_3(t)=1, \mathbf{X}(t+1)=(l,j)\} \tag{A.9}$$

$$= \sum_{(l',j')} Pr\{\mathbf{X}(t)=(l',j'), I_4(t)=1, I_3(t)=1, \mathbf{X}(t+1)=(l,j)\} \tag{A.10}$$

$$= \sum_{(l',j')} Pr\{\mathbf{X}(t)=(l',j')\} \cdot Pr\{I_4(t)=1, I_3(t)=1, \mathbf{X}(t+1)=(l,j)|\mathbf{X}(t)=(l',j')\}, \tag{A.11}$$

where $Pr\{I_4(t)=1, I_3(t)=1, \mathbf{X}(t+1)=(l,j)|\mathbf{X}(t)=(l',j')\}$ represents the transition probability from state $\mathbf{X}(t)=(l',j')$ to state $\mathbf{X}(t+1)=(l,j)$, with the condition that events $\{I_4(t)=1\}$ and $\{I_3(t)=1\}$ also happen simultaneously. The matrix $\mathbf{P_2}$ of such transition probabilities is determined based on (3.3) by setting the corresponding

sub-matrices according to (3.22)-(3.32). With matrix $\mathbf{P_2}$ and (A.11), we have

$$\begin{aligned} &Pr\{I_4(t)=1, I_3(t)=1, \mathbf{X}(t+1)=(l,j)\} \\ &= [\boldsymbol{\pi}_\omega(t)\mathbf{P_2}]_{2+(l-1)f+j}. \end{aligned} \tag{A.12}$$

After substituting (A.8) and (A.12) into (A.4), we get

$$\begin{aligned} &[\boldsymbol{\pi}_\Omega(t+1)]_{2+(l-1)f+j} \\ &= \frac{[\boldsymbol{\pi}_\omega(t)\mathbf{P_2}]_{2+(l-1)f+j}}{\lambda\boldsymbol{\pi}_\omega(t)\mathbf{P_1 1}}. \end{aligned} \tag{A.13}$$

Thus, in vector form

$$\boldsymbol{\pi}_\Omega(t+1) = \frac{\boldsymbol{\pi}_\omega(t)\mathbf{P_2}}{\lambda\boldsymbol{\pi}_\omega(t)\mathbf{P_1 1}}. \tag{A.14}$$

Taking limits on both sides of (A.14), we get the steady state distribution $\boldsymbol{\pi}^*_\Omega$ as

$$\boldsymbol{\pi}^*_\Omega = \lim_{t\to\infty} \boldsymbol{\pi}_\Omega(t+1) \tag{A.15}$$

$$= \lim_{t\to\infty} \frac{\boldsymbol{\pi}_\omega(t)\mathbf{P_2}}{\lambda\boldsymbol{\pi}_\omega(t)\mathbf{P_1 1}} \tag{A.16}$$

$$= \frac{\boldsymbol{\pi}^*_\omega\mathbf{P_2}}{\lambda\boldsymbol{\pi}^*_\omega\mathbf{P_1 1}}, \tag{A.17}$$

where

$$\boldsymbol{\pi}^*_\omega = \lim_{t\to\infty} \boldsymbol{\pi}_\omega(t). \tag{A.18}$$

This completes the proof of Lemma 2.

A.3 Proof of Lemma 3

Recall that as time evolves, the state transitions of the source-queue form a QBD process shown in Fig. 3.3. From Fig. 3.3, we can see that the QBD process has finite states and all states communicate with other states, so the Markov chain is recurrent. We also see from Fig. 3.3 that every state could transition to itself, indicating that the Markov chain is aperiodic. Thus, the concerned QBD process is an ergodic Markov chain and has a unique limit state distribution $\boldsymbol{\pi}_{\omega}^{*}$ defined in (A.18).

Notice that $\boldsymbol{\pi}_{\omega}^{*}$ must satisfy the following equation

$$\boldsymbol{\pi}_{\omega}^{*} = \boldsymbol{\pi}_{\omega}^{*}\mathbf{P_0}, \tag{A.19}$$

where $\mathbf{P_0}$ is the transition matrix of the QBD process, which can be determined based on (3.3) by setting the corresponding sub-matrices according to (3.44)-(3.50). In particular, for $M = 1$ and $M = 2$, the transition matrix $\mathbf{P_0}$ is given by the following (A.20) and (A.21), respectively.

$$\mathbf{P_0} = \begin{bmatrix} \mathbf{B_1} & \mathbf{B_0} \\ \mathbf{B_2} & \mathbf{A_M} \end{bmatrix}, \tag{A.20}$$

$$\mathbf{P_0} = \begin{bmatrix} \mathbf{B_1} & \mathbf{B_0} & \\ \mathbf{B_2} & \mathbf{A_1} & \mathbf{A_0} \\ & \mathbf{A_2} & \mathbf{A_M} \end{bmatrix}. \tag{A.21}$$

Thus, under the cases of $M = 1$ and $M = 2$, $\boldsymbol{\pi}_{\omega}^{*}$ could be easily calculated by equations (3.33)-(3.35) and (3.36)-(3.39), respectively. Due to the special structure of the matrix $\mathbf{A_2}$, which is the product of a column vector $\mathbf{c}$ by a row vector $\mathbf{r}$ [53], $\boldsymbol{\pi}_{\omega}^{*}$ under the case $M \geq 3$ could be calculated by equations (3.40)-(3.43).

A.4 Proof of Theorem III.1

Suppose that the source-queue is in some state according to the steady state distribution $\boldsymbol{\pi}^*_\Omega$, then the source delay of a packet (say Z) is independent of the packet generating process after Z is inserted into the source-queue and is also independent of the state transitions of the source-queue after Z is removed from the source-queue. Such independence makes it possible to construct a simplified QBD process to study the source delay of packet Z, in which new packets generated after packet Z are ignored, and once Z is removed from the source-queue (or equivalently the source-queue transits to state $(0, 0)$), the source-queue will stay at state $(0, 0)$ forever.

For the above simplified QBD process, its transition matrix $\mathbf{P_3}$ can be determined based on (3.3) by setting the corresponding sub-matrices as follows:

For $M = 1$,

$$\mathbf{B_0} = \mathbf{0}, \tag{A.22}$$

$$\mathbf{B_1} = [1], \tag{A.23}$$

$$\mathbf{B_2} = \mathbf{c}, \tag{A.24}$$

$$\mathbf{A_M} = \mathbf{Q}. \tag{A.25}$$

For $M \geq 2$,

$$\mathbf{B_0} = \mathbf{0}, \tag{A.26}$$

$$\mathbf{B_1} = [1], \tag{A.27}$$

$$\mathbf{B_2} = \mathbf{c}, \tag{A.28}$$

$$\mathbf{A_0} = \mathbf{0}, \tag{A.29}$$

$$\mathbf{A_1} = \mathbf{Q}, \tag{A.30}$$

$$\mathbf{A_2} = \mathbf{c} \cdot \mathbf{r}, \tag{A.31}$$

$$\mathbf{A_M} = \mathbf{Q}. \tag{A.32}$$

By rearranging $\mathbf{P_3}$ as

$$\mathbf{P_3} = \begin{bmatrix} 1 & \mathbf{0} \\ \mathbf{c}^+ & \mathbf{T} \end{bmatrix}, \tag{A.33}$$

we can see that matrices $\mathbf{c}^+$ and $\mathbf{T}$ are determined as (3.57)-(3.60). With matrices $\mathbf{c}^+$, $\mathbf{T}$ and $\boldsymbol{\pi}^*_\Omega$, the probability mass function (3.53) and CDF (3.54) of the source delay follow directly from the theory of Phase-type distribution [53].

Based on the probability mass function (3.53), the mean $\overline{U}$ of the source delay can be calculated by

$$\begin{aligned} \overline{U} &= \sum_{u=1}^{\infty} u \cdot Pr\{U = u\} \\ &= \sum_{u=1}^{\infty} u \boldsymbol{\pi}^-_\Omega \mathbf{T}^{u-1} \mathbf{c}^+ \\ &= \boldsymbol{\pi}^-_\Omega \left(\sum_{u=1}^{\infty} u \mathbf{T}^{u-1} \right) \mathbf{c}^+ \end{aligned} \tag{A.34}$$

Let

$$f(\mathbf{T}) = \sum_{u=1}^{\infty} u\mathbf{T}^{u-1}, \tag{A.35}$$

and use $f(x)$ to denote its corresponding numerical series

$$f(x) = \sum_{u=1}^{\infty} ux^{u-1} \tag{A.36}$$

$$= (1-x)^{-2}, \quad \text{for} \quad x < 1. \tag{A.37}$$

Since above simplified QBD process is actually an absorbing Markov Chain with transition matrix $\mathbf{P_3}$, we know from Theorem 11.3 in [84] that

$$\lim_{k\to\infty} \mathbf{T}^k = \mathbf{0}. \tag{A.38}$$

Based on the property (A.38) and the Theorem 5.6.12 in [85], we can see that the spectral radius $\rho(\mathbf{T})$ of matrix $\mathbf{T}$ satisfies following condition

$$\rho(\mathbf{T}) < 1. \tag{A.39}$$

From (A.35), (A.37) and (A.39), it follows that the matrix series $f(\mathbf{T})$ converge as

$$f(\mathbf{T}) = \lim_{g\to\infty} \sum_{u=1}^{g} u\mathbf{T}^{u-1} \tag{A.40}$$

$$= (\mathbf{I} - \mathbf{T})^{-2} \tag{A.41}$$

After substituting (A.41) into (A.34), (3.55) then follows.

The derivation of the variance of source delay (3.56) could be conducted in a similar way and thus is omitted here.

APPENDIX B

End-To-End Delay Analysis

B.1 Proof of Lemma 5

Calculation of p_b: The event corresponding to p_b happens iff the following sub-events happen simultaneously:

1) S moves into an active cell; j out of the remaining $n-1$ nodes move into the same cell with S, $0 \leq j \leq n-1$; other nodes move into cells other than that active cell;

2) S becomes transmitter after fair wireless channel contention;

3) S selects to do packet-broadcast after traffic contention (i.e. conducting packet-broadcast or packet-delivery).

Notice that in a time slot, every node moves according to the i.i.d. mobility model. Thus, we have

$$p_b = \frac{1}{\alpha^2} \sum_{j=0}^{n-1} \binom{n-1}{j} \left(\frac{1}{m^2}\right)^j \left(\frac{m^2-1}{m^2}\right)^{n-1-j} \frac{1}{j+1} q \tag{B.1}$$

$$= \frac{qm^2}{\alpha^2 n} \left\{ 1 - \left(\frac{m^2-1}{m^2}\right)^n \right\} \tag{B.2}$$

Calculation of $p_c(j)$: According to the definition of $p_c(j)$, it is a conditional probability determined as

$$p_c(j) = \frac{p_b(j)}{p_b} \tag{B.3}$$

where $p_b(j)$ is the probability that j copies of a packet exist in the network after S becomes transmitter and selects to do packet-broadcast for that packet, $1 \leq j \leq n-1$. The event corresponding to $p_b(j)$ happens iff the following sub-events happen:

1) S moves into in an active cell; $j-1$ out of the remaining $n-2$ nodes other than S and D move into the coverage cells of S, among which k nodes are in the same cell with S and the remaining $j-1-k$ nodes are in other coverage cells of S, $0 \leq k \leq j-1$; other nodes move into cells other than the coverage cells of S;

2) S becomes transmitter after fair channel contention;

3) S selects to do packet-broadcast.

Notice that D could move either into the same cell with S or any cell other than that active cell, we have

$$\begin{aligned} p_b(j) = & \frac{1}{\alpha^2}\Bigg\{\frac{1}{m^2}\binom{n-2}{j-1}\sum_{k=0}^{j-1}\binom{j-1}{k}\left(\frac{1}{m^2}\right)^k\left(\frac{8}{m^2}\right)^{j-1-k} \\ & \cdot\left(\frac{m^2-9}{m^2}\right)^{n-1-j}\frac{1}{k+2}q \\ & + \frac{m^2-1}{m^2}\binom{n-2}{j-1}\sum_{k=0}^{j-1}\binom{j-1}{k}\left(\frac{1}{m^2}\right)^k \\ & \cdot\left(\frac{8}{m^2}\right)^{j-1-k}\left(\frac{m^2-9}{m^2}\right)^{n-1-j}\frac{1}{k+1}q\Bigg\} \end{aligned} \tag{B.4}$$

$$\begin{aligned} = & \frac{q}{\alpha^2}\binom{n-2}{j-1}\left(\frac{m^2-9}{m^2}\right)^{n-1-j} \\ & \cdot\left\{\frac{m^2-9}{m^{2j}}f(j) + \frac{1}{m^{2j}}f(j+1)\right\} \end{aligned} \tag{B.5}$$

where

$$f(x) = \frac{9^x - 8^x}{x} \tag{B.6}$$

After substituting (B.5) and (B.2) into (B.3) and conducting some basic algebraic calculations, we have

$$p_c(j) = \frac{n\binom{n-2}{j-1}(m^2-9)^{n-1-j}}{m^{2n} - (m^2-1)^n}\Big\{(m^2-9)f(j) + f(j+1)\Big\} \tag{B.7}$$

Calculation of $p_r(j)$: Notice that in a time slot, D could only receive the packet it is currently requesting from one of the j nodes carrying copies of that packet. Thus, after similar arguments to the calculation of p_b, we have

$$p_r(j) = \frac{j(1-q)m^2}{\alpha^2 n(n-1)}\left\{1 - \left(\frac{m^2-1}{m^2}\right)^n - \frac{n}{m^2}\left(\frac{m^2-9}{m^2}\right)^{n-1}\right\} \tag{B.8}$$

To calculate the remaining probabilities, we need to construct the arrival process of network-queue. From Lemma 4, we know that the arrival process of network-queue is a Bernoulli process with probability λ. The arrival process of network-queue can be constructed as follows: once source node S becomes transmitter and selects to do packet-broadcast (with probability p_b), S successfully conducts packet-broadcast for one packet with probability λ',

$$\lambda' = \frac{\lambda}{p_b} \tag{B.9}$$

Thus, after S becomes transmitter and selects to do packet-broadcast, S will successfully distribute out one packet with probability λ'.

Calculation of $p_0(j)$: The event corresponding to $p_0(j)$ happens iff the following sub-events happen:

1) S moves into an active cell; D moves into any cell other than that active cell; $j-1$ out of the remaining $n-2$ nodes move into the coverage cells of S, among which k nodes are in the same cell with S and the remaining $j-1-k$ nodes are in other coverage cells of S, $0 \leq k \leq j-1$; other nodes move into cells other than the coverage cells of S;

2) S becomes transmitter after fair contention;

3) S selects to do packet-broadcast and S distributes out a packet.

Then, we have

$$\begin{aligned} p_0(j) =& \frac{1}{\alpha^2}\frac{m^2-9}{m^2}\binom{n-2}{j-1}\sum_{k=0}^{j-1}\binom{j-1}{k}\left(\frac{1}{m^2}\right)^k\left(\frac{8}{m^2}\right)^{j-1-k} \\ & \cdot\left(\frac{m^2-9}{m^2}\right)^{n-1-j}\frac{1}{k+1}q\lambda' \qquad \text{(B.10)} \\ =& \frac{\lambda\cdot q\cdot\binom{n-2}{j-1}(m^2-9)^{n-j}}{\alpha^2 m^{2n-2}p_b}f(j) \qquad \text{(B.11)} \end{aligned}$$

Calculation of $p_0(0)$: From the definition of $p_0(0)$, we know that

$$p_0(0) = 1 - \sum_{j=1}^{n-1} p_0(j) \qquad \text{(B.12)}$$

After substituting (B.11) into (B.12), we have

$$p_0(0) = 1 - \frac{\lambda\cdot q\cdot(m^2-9)}{\alpha^2(n-1)p_b}\left\{1-\left(\frac{m^2-1}{m^2}\right)^{n-1}\right\} \qquad \text{(B.13)}$$

Calculation of $p_b^+(j)$: The event corresponding to $p_b^+(j)$ is composed of $j-1$ exclusive sub-events, each of which is that: in a time slot S becomes transmitter, selects to do packet-broadcast for one packet; at the same time D receives the packet it is requesting from a specific relay node (say R) carrying a copy of that packet. If

we denote by p_b^+ the probability that one such sub-event occurs in a time slot, then

$$p_b^+(j) = (j-1)p_b^+ \tag{B.14}$$

The event corresponding to p_b^+ happens iff the following sub-events happen:

1) S moves into an active cell; R moves into another active cell; D moves into either the same active cell with R or other coverage cells of R; k out of the remaining $n-3$ nodes move into the coverage cells of R, among which $i \geq 0$ nodes are in the same cell with R; $t \geq 0$ of the remaining $n-3-k$ nodes are in the same active cell with S; other nodes move into cells other than the active cell of S and the coverage cells of R;

2) S and R both become transmitters after fair contention in their respective active cells;

3) S selects to do packet-broadcast and S distributes out a packet; R selects to do packet-delivery and D is selected as its receiver.

Then, we have

$$\begin{aligned} p_b^+ =& \frac{1}{\alpha^2}\frac{m^2-\alpha^2}{m^2\alpha^2}\sum_{k=0}^{n-3}\binom{n-3}{k}\Bigg\{\sum_{i=0}^{k}\binom{k}{i}\left(\frac{1}{m^2}\right)^i\left(\frac{8}{m^2}\right)^{k-i} \\ & \cdot \sum_{t=0}^{n-3-k}\binom{n-3-k}{t}\left(\frac{1}{m^2}\right)^t\left(\frac{m^2-10}{m^2}\right)^{n-3-k-t} \\ & \cdot\left(\frac{1}{m^2}\frac{1}{i+2}\frac{1}{k+1}+\frac{8}{m^2}\frac{1}{i+1}\frac{1}{k+1}\right)(1-q)\frac{1}{t+1}q\lambda'\Bigg\} \qquad \text{(B.15)} \\ =& \frac{\lambda(q-q^2)(m^4-m^2\alpha^2)}{\alpha^4 n(n-1)(n-2)p_b} \\ & \cdot\Bigg\{1-2\left(\frac{m^2-1}{m^2}\right)^n+\left(\frac{m^2-2}{m^2}\right)^n \\ & -\frac{n}{m^2}\left(\frac{m^2-9}{m^2}\right)^{n-1}+\frac{n}{m^2}\left(\frac{m^2-10}{m^2}\right)^{n-1}\Bigg\} \qquad \text{(B.16)} \end{aligned}$$

From (B.16) and (B.14), (4.6) follows.

Calculation of $p_b^-(j)$: From the definitions of $p_b^-(j)$ and $p_b^+(j)$, we know that $p_b^-(j) + p_b^+(j)$ is the probability that in a time slot S becomes transmitter, selects to do packet-broadcast and also successfully conducts packet-broadcast for one packet. This probability is just λ according to the arrival process of network-queue. Thus, $p_b^-(j)$ can be calculated as

$$p_b^-(j) = \lambda - p_b^+(j) \tag{B.17}$$

Calculation of $p_f^+(j)$: By the definition of $p_r(j)$, it is easy to see that $p_f^+(j)$ can be calculated as

$$p_f^+(j) = p_r(j) - p_b^+(j) \tag{B.18}$$

Calculation of $p_f^-(j)$: From the definitions of $p_b^+(j)$, $p_b^-(j)$, $p_f^+(j)$ and $p_f^-(j)$, we know that

$$p_b^+(j) + p_b^-(j) + p_f^+(j) + p_f^-(j) = 1 \tag{B.19}$$

Thus, (4.9) follows.

APPENDIX C

Throughput Capacity Analysis

C.1 Proof of Lemma 6

From the definition of p_0 we know that the event corresponding to p_0 can be decoupled into following two exclusive sub-events. 1) there is only one node in c itself and there are i nodes ($1 \leq i \leq n-1$) within the other $(2v-1)^2-1$ coverage cells of c, while the remaining $n-i-1$ nodes are within cells other than the $(2v-1)^2$ coverage cells of c ; 2) there are i nodes ($2 \leq i \leq n$) in c itself and the remaining $n-i$ nodes are within cells other than the active cell c. Notice that according to the IID mobility model, in a time slot each node randomly and independently chooses a cell to move into at the beginning of the time slot and then stays in it for the remaining whole slot. Thus, for a given time slot, the probability of sub-event 1 can be calculated as

$$\frac{n}{m^2}\sum_{i=1}^{n-1}\binom{n-1}{i}\left(\frac{(2v-1)^2-1}{m^2}\right)^i\cdot\left(\frac{m^2-(2v-1)^2}{m^2}\right)^{n-i-1} \tag{C.1}$$

and the probability of sub-event 2 can be calculated as

$$\sum_{i=2}^{n} \binom{n}{i} \left(\frac{1}{m^2}\right)^i \left(\frac{m^2-1}{m^2}\right)^{n-i} \tag{C.2}$$

Since the event corresponding to p_0 is composed of the exclusive sub-event 1 and sub-event 2, we then have

$$\begin{aligned} p_0 = & \frac{n}{m^2} \sum_{i=1}^{n-1} \binom{n-1}{i} \left(\frac{(2v-1)^2-1}{m^2}\right)^i \cdot \left(\frac{m^2-(2v-1)^2}{m^2}\right)^{n-i-1} \\ & + \sum_{i=2}^{n} \binom{n}{i} \left(\frac{1}{m^2}\right)^i \left(\frac{m^2-1}{m^2}\right)^{n-i} \\ = & \frac{1}{m^{2n}} \Big\{ m^{2n} - \big(m^2-1\big)^n - n\big(m^2-(2v-1)^2\big)^{n-1} \Big\} \end{aligned} \tag{C.3}$$

Based on the definition of p_1 we can easily see that the event corresponding to p_1 can be determined as follows: among all $\frac{n}{2}$ node pairs defined in Section 5.2 (Notice that source-destination pairs $1 \leftrightarrow 2$ are regarded as one node pair here), there are i pairs ($1 \leq i \leq \frac{n}{2}$) within the coverage cells of active cell c and for each such pair, at least one of its two nodes is within c. Again, since in a time slot each node randomly and independently chooses its cell according to the i.i.d. mobility model, the probability p_1 can be calculated as

$$\begin{aligned} p_1 = & \sum_{i=1}^{\frac{n}{2}} \binom{\frac{n}{2}}{i} \left(\frac{2\big((2v-1)^2-1\big)}{m^4} + \frac{1}{m^4}\right)^i \\ & \cdot \left(1 - \frac{2\big((2v-1)^2-1\big)}{m^4} - \frac{1}{m^4}\right)^{\frac{n}{2}-i} \\ = & \frac{1}{m^{2n}} \Big\{ m^{2n} - \big(m^4 - 2(2v-1)^2 + 1\big)^{n/2} \Big\} \end{aligned} \tag{C.4}$$

C.2 Derivaion of Expression (5.26)

The derivation of (5.26) starts from the following conditional *Lyapunov Drift*

$$\mathbb{E}\Big\{L\big(\widehat{Q_0}(t+1)\big) - L\big(\widehat{Q_0}(t)\big)\big|\widehat{Q_0}(t)\Big\} \tag{C.5}$$

By applying Lyapunov function (5.25) to (C.5) and conducting some basic algebraic operations, we have

$$\begin{aligned}
&\mathbb{E}\Big\{L\big(\widehat{Q_0}(t+1)\big) - L\big(\widehat{Q_0}(t)\big)\big|\widehat{Q_0}(t)\Big\} \\
&= \mathbb{E}\Big\{\sum_{k=1}^{n}\Big(\Big(Q_k^{(k,d_k)}(t+1)\Big)^2 - \Big(Q_k^{(k,d_k)}(t)\Big)^2\Big)\Big|\widehat{Q_0}(t)\Big\} \\
&= \mathbb{E}\Big\{\sum_{k=1}^{n}\Big(Q_k^{(k,d_k)}(t+1) - Q_k^{(k,d_k)}(t)\Big)^2\Big|\widehat{Q_0}(t)\Big\} \\
&\quad +2\mathbb{E}\Big\{\sum_{k=1}^{n}Q_k^{(k,d_k)}(t)\Big(Q_k^{(k,d_k)}(t+1) - Q_k^{(k,d_k)}(t)\Big)\Big|\widehat{Q_0}(t)\Big\}
\end{aligned} \tag{C.6}$$

After substituting (5.22) into (C.6), we have

$$\begin{aligned}
&\mathbb{E}\Big\{L\big(\widehat{Q_0}(t+1)\big) - L\big(\widehat{Q_0}(t)\big)\big|\widehat{Q_0}(t)\Big\} \\
&= \mathbb{E}\Big\{\sum_{k=1}^{n}\Big(A_k^{(k,d_k)}(t) - D_k^{(k,d_k)}(t)\Big)^2\Big|\widehat{Q_0}(t)\Big\} \\
&\quad +2\mathbb{E}\Big\{\sum_{k=1}^{n}Q_k^{(k,d_k)}(t)\Big(A_k^{(k,d_k)}(t) - D_k^{(k,d_k)}(t)\Big)\Big|\widehat{Q_0}(t)\Big\}
\end{aligned} \tag{C.7}$$

For the first term of (C.7), we have

$$\begin{aligned}
&\mathbb{E}\Big\{ \sum_{k=1}^{n} \Big(A_k^{(k,d_k)}(t) - D_k^{(k,d_k)}(t) \Big)^2 \Big| \widehat{Q_0}(t) \Big\} \\
&= \mathbb{E}\Big\{ \sum_{k=1}^{n} \Big(A_k(t) \Big)^2 \Big| \widehat{Q_0}(t) \Big\} + \mathbb{E}\Big\{ \sum_{k=1}^{n} \Big(D_k^{(k,d_k)}(t) \Big)^2 \Big| \widehat{Q_0}(t) \Big\} \\
&\quad - 2\mathbb{E}\Big\{ \sum_{k=1}^{n} A_k(t) \cdot D_k^{(k,d_k)}(t) \Big| \widehat{Q_0}(t) \Big\} \qquad \text{(C.8)}
\end{aligned}$$

(C.8) follows from the definition of $A_k^{(i,d_i)}(t)$ that $A_k^{(k,d_k)}(t) = A_k(t)$ for $k = i$.

Notice that local packet generation process $A_k(t)$ is an i.i.d. process, so it is independent of the state of $\widehat{Q_0}(t)$ and $D_k^{(k,d_k)}(t)$. Thus, we have

$$\begin{aligned}
&2\mathbb{E}\Big\{ \sum_{k=1}^{n} A_k(t) \cdot D_k^{(k,d_k)}(t) \Big| \widehat{Q_0}(t) \Big\} \\
&= 2\sum_{k=1}^{n} \mathbb{E}\Big\{ A_k(t) \cdot D_k^{(k,d_k)}(t) \Big| \widehat{Q_0}(t) \Big\} \\
&= 2\sum_{k=1}^{n} \mathbb{E}\Big\{ A_k(t) \Big| \widehat{Q_0}(t) \Big\} \cdot \mathbb{E}\Big\{ D_k^{(k,d_k)}(t) \Big| \widehat{Q_0}(t) \Big\} \\
&= 2\sum_{k=1}^{n} \mathbb{E}\Big\{ A_k(t) \Big\} \cdot \mathbb{E}\Big\{ D_k^{(k,d_k)}(t) \Big| \widehat{Q_0}(t) \Big\} \\
&= 2\lambda\ \mathbb{E}\Big\{ \sum_{k=1}^{n} D_k^{(k,d_k)}(t) \Big| \widehat{Q_0}(t) \Big\} \qquad \text{(C.9)}
\end{aligned}$$

Substituting (C.9) and (5.20) into (C.8), we have

$$\begin{aligned}
&\mathbb{E}\Big\{\sum_{k=1}^{n}\Big(A_k^{(k,d_k)}(t)-D_k^{(k,d_k)}(t)\Big)^2\Big|\widehat{Q_0}(t)\Big\}\\
&=\mathbb{E}\Big\{\sum_{k=1}^{n}\Big(A_k(t)\Big)^2\Big|\widehat{Q_0}(t)\Big\}\\
&\quad+(1-2\lambda)\mathbb{E}\Big\{\sum_{k=1}^{n}D_k^{(k,d_k)}(t)\Big|\widehat{Q_0}(t)\Big\}\\
&\le nA_{max}^2+(1-2\lambda)\mathbb{E}\Big\{\sum_{k=1}^{n}D_k^{(k,d_k)}(t)\Big|\widehat{Q_0}(t)\Big\} \qquad \text{(C.10)}
\end{aligned}$$

For the second term of (C.7), we have

$$\begin{aligned}
&2\mathbb{E}\Big\{\sum_{k=1}^{n}Q_k^{(k,d_k)}(t)\Big(A_k^{(k,d_k)}(t)-D_k^{(k,d_k)}(t)\Big)\Big|\widehat{Q_0}(t)\Big\}\\
&=2\mathbb{E}\Big\{\sum_{k=1}^{n}\Big(Q_k^{(k,d_k)}(t)A_k(t)-Q_k^{(k,d_k)}(t)D_k^{(k,d_k)}(t)\Big)\Big|\widehat{Q_0}(t)\Big\} \qquad \text{(C.11)}\\
&=2\mathbb{E}\Big\{\sum_{k=1}^{n}\Big(Q_k^{(k,d_k)}(t)A_k(t)-Q_k^{(k,d_k)}(t)I_{k,out}^{(k,d_k)}(t)\Big)\Big|\widehat{Q_0}(t)\Big\} \qquad \text{(C.12)}
\end{aligned}$$

where (C.12) follows from substituting (5.21) into (C.11).

Finally, by subtituting (C.12) and (C.10) into (C.7),

$$\begin{aligned}
&\mathbb{E}\Big\{L\big(\widehat{Q_0}(t+1)\big)-L\big(\widehat{Q_0}(t)\big)\big|\widehat{Q_0}(t)\Big\}\\
&\le nA_{max}^2+(1-2\lambda)\mathbb{E}\Big\{\sum_{k=1}^{n}D_k^{(k,d_k)}(t)\Big|\widehat{Q_0}(t)\Big\}\\
&\quad-2\mathbb{E}\Big\{\sum_{k=1}^{n}Q_k^{(k,d_k)}(t)\Big(I_{k,out}^{(k,d_k)}(t)-A_k(t)\Big)\Big|\widehat{Q_0}(t)\Big\} \qquad \text{(C.13)}
\end{aligned}$$

BIBLIOGRAPHY

BIBLIOGRAPHY

[1] A. Goldsmith, *Wireless Communications*. Cambridge University Press, 2005.

[2] D. Tse and P. Viswanath, *Fundamentals of Wireless Communication*. Cambridge University Press, 2005.

[3] M. Mauve, J. Widmer, and H. Hartenstein, "A survey on position-based routing in mobile ad hoc networks," *IEEE Network*, vol. 15, no. 6, pp. 30–39, Nov.-Dec. 2001.

[4] J. Andrews, S. Shakkottai, R. Heath, N. Jindal, M. Haenggi, R. Berry, D. Guo, M. J. Neely, S. Weber, S. Jafar, and A. Yener, "Rethinking information theory for mobile ad hoc networks," *IEEE Communications Magazine*, vol. 46, no. 12, pp. 94–101, December 2008.

[5] A. Goldsmith, M. Effros, R. Koetter, M. Mdard, and L. Zheng, "Beyond shannon: the quest for fundamental performance limits of wireless ad hoc networks," *IEEE Communications Magazine*, vol. 49, no. 5, pp. 195–205, May 2011.

[6] Information Theory for Mobile Ad Hoc Networks. http://www.mit.edu/ medard/itmanet/.

[7] Future and Emerging Technologies. http://cordis.europa.eu/fp7/ict/fet-open/.

[8] R. Groenevelt, P. Nain, and G. Koole, "The message delay in mobile ad hoc networks," *Performance Evaluation*, vol. 62, no. 1-4, pp. 210–228, October 2005.

[9] J. Liu, X. Jiang, H. Nishiyama, N. Kato, and X. Shen, "End-to-end delay in mobile ad hoc networks with generalized transmission range and limited packet redundancy," in *WCNC*, 2012.

[10] A. E. Gamal, J. Mammen, B. Prabhakar, and D. Shah, "Throughput-delay trade-off in wireless networks," in *INFOCOM*, 2004.

[11] G. Sharma, R. Mazumdar, and N. B. Shroff, "Delay and capacity trade-offs for mobile ad hoc networks: A global perspective," *IEEE/ACM Transactions on Networking*, vol. 15, no. 5, pp. 981–992, October 2007.

[12] P. Gupta and P. Kumar, "The capacity of wireless networks," *IEEE Transactions on Information Theory*, vol. 46, no. 2, pp. 388–404, March 2000.

[13] R. Urgaonkar and M. J. Neely, "Network capacity region and minimum energy function for a delay-tolerant mobile ad hoc network," *IEEE/ACM Transactions on Networking*, vol. 19, no. 4, pp. 1137–1150, August 2011.

[14] G. Sharma and R. Mazumdar, "Delay and capacity trade-off in wireless ad hoc networks with random mobility," in *Dept. Elect. Comput. Eng., Purdue Univ.,West Lafayette, IN*, 2005. [Online]. Available: https://ece.uwaterloo.ca/˜mazum/adhoc_mobility.pdf

[15] M. Grossglauser and D. N. Tse, "Mobility increases the capacity of ad hoc wireless networks," *IEEE/ACM Transactions on Networking*, vol. 10, no. 4, pp. 477–486, August 2002.

[16] M. J. Neely and E. Modiano, "Capacity and delay tradeoffs for ad-hoc mobile networks," *IEEE Transactions on Information Theory*, vol. 51, no. 6, pp. 1917–1936, June 2005.

[17] Y. Wu, P. A. Chou, and S.-Y. Kung, "Minimum-energy multicast in mobile ad hoc networks using network coding," *IEEE Transactions on Communications*, vol. 53, no. 11, pp. 1906–1918, November 2005.

[18] L. H. II and R. Tafazolli, "A survey of qos routing solutions for mobile ad hoc networks," *IEEE Communications Surveys and Tutorials*, vol. 9, no. 2, pp. 50–70, 2nd Quarter 2007.

[19] L. Chen and W. B. Heinzelman, "A survey of routing protocols that support qos in mobile ad hoc networks," *IEEE Network*, vol. 21, no. 6, pp. 30–38, November-December 2007.

[20] T. Camp, J. Boleng, and V. Davies, "A survey of mobility models for ad hoc network research," *Wireless Communication & Mobile Computing*, vol. 2, no. 5, pp. 483–502, 2002.

[21] R. Hekmat and P. V. Mieghem, "Interference in wireless multi-hop ad-hoc networks and its effect on network capacity," *Wireless Networks*, vol. 10, no. 4, pp. 389–399, July 2004.

[22] P. Cardieri, "Modeling interference in wireless ad hoc networks," *IEEE Communications Surveys & Tutorials*, vol. 12, no. 4, pp. 551–572, 2010.

[23] S. Kumar, V. S. Raghavan, and J. Deng, "Medium access control protocols for ad hoc wireless networks: a survey," *Ad Hoc Networks*, vol. 4, no. 3, p. May 2006, 2004.

[24] L. Huang, S. Moeller, M. J. Neely, and B. Krishnamachari, "Lifo-backpressure achieves near optimal utility-delay tradeoff," *IEEE/ACM Transactions on Networking*, vol. 21, no. 3, pp. 831–844, June 2013.

[25] M. J. Neely, "Delay analysis for max weight opportunistic scheduling in wireless systems," *IEEE Transactions on Automatic Control*, vol. 54, no. 9, pp. 2137–2150, September 2009.

[26] L. B. Le, K. Jagannathan, and E. Modiano, "Delay analysis of maximum weight scheduling in wireless ad hoc networks," in *Annual Conference on Information Sciences and Systems*, 2009.

[27] H. Xiong, R. Li, A. Eryilmaz, and E. Ekici, "Delay-aware cross-layer design for network utility maximization in multi-hop networks," *IEEE Journal on Selected Areas in Communications*, vol. 29, no. 5, pp. 951–959, May 2011.

[28] D. Xue and E. Ekici, "Delay-guaranteed cross-layer scheduling in multi-hop wireless networks," *IEEE/ACM Transactions on Networking*, December 2012.

[29] X. Wang, W. Huang, S. Wang, J. Zhang, and C. Hu, "Delay and capacity tradeoff analysis for motioncast," *IEEE/ACM Transactions on Networking*, vol. 19, no. 5, pp. 1354–1367, October 2011.

[30] G. Sharma and R. Mazumdar, "On achievable delay/capacity trade-offs in mobile ad hoc networks," in *Wiopt*, 2004.

[31] S. Zhou and L. Ying, "On delay constrained multicast capacity of large-scale mobile ad-hoc networks," in *INFOCOM*, 2010.

[32] D. Ciullo, V. Martina, M. Garetto, and E. Leonardi, "Impact of correlated mobility on delay-throughput performance in mobile ad hoc networks," *IEEE/ACM Transactions on Networking*, vol. 19, no. 6, pp. 1745–1758, December 2011.

[33] P. Li, Y. Fang, J. Li, and X. Huang, "Smooth trade-offs between throughput and delay in mobile ad hoc networks," *IEEE Transactions on Mobile Computing*, vol. 11, no. 3, pp. 427–438, March 2012.

[34] A. E. Gamal, J. Mammen, B. Prabhakar, and D. Shah, "Optimal throughput-delay scaling in wireless networks-part i: The fluid model," *IEEE Transactions on Information Theory*, vol. 52, no. 6, pp. 2568–2592, June 2006.

[35] J. Liu, X. Jiang, H. Nishiyama, and N. Kato, "Delay and capacity in ad hoc mobile networks with f-cast relay algorithms," *IEEE Transactions on Wireless Communications*, vol. 10, no. 8, pp. 2738 – 2751, August 2011.

[36] ——, "Generalized two-hop relay for flexible delay control in manets," *IEEE/ACM Transactions on Networking*, vol. 20, no. 6, pp. 1950–1963, December 2012.

[37] L. Ying, S. Yang, and R. Srikant, "Optimal delay-throughput trade-offs in mobile ad hoc networks," *IEEE Transactions on Information Theory*, vol. 54, no. 9, pp. 4119–4143, September 2008.

[38] J. Liu, J. Gao, X. Jiang, H. Nishiyama, and N. Kato, "Capacity and delay of probing-based two-hop relay in manets," *IEEE Transactions on Wireless Communications*, vol. 11, no. 11, pp. 4172–4183, November 2012.

[39] S. R. Kulkarni and P. Viswanath, "A deterministic approach to throughput scaling in wireless networks," *IEEE Transactions on Information Theory*, vol. 50, no. 6, pp. 1041–1049, June 2004.

[40] G. Dommety and R. Jain, "Potential networking applications of global positioning systems (gps)," Computer Science Department, The Ohio State University, Tech. Rep., April 1996.

[41] Y.-B. Ko and N. H. Vaidya, "Location-aided routing (lar) in mobile ad hoc networks," *Wireless Networks*, vol. 6, no. 4, pp. 307–321, July 2000.

[42] J. Gao and X. Jiang, "Delay modeling for broadcast-based two-hop relay manets," in *11th International Symposium on Modeling and Optimization in Mobile, Ad Hoc, and Wireless Networks (WiOpt)*, 2013.

[43] A. A. Hanbali, P. Nain, and E. Altman, "Performance of ad hoc networks with two-hop relay routing and limited packet lifetime (extended version)," *Performance Evaluation*, vol. 65, no. 6-7, pp. 463–483, June 2008.

[44] T. Small and Z. Hass, "Resource and performance tradeoffs in delay-tolerant wireless networks," in *Proc. ACM SIGCOMM workshop on Delay-tolerant networking (WDTN)*, 2005, pp. 260–267.

[45] A. Panagakis, A. Vaios, and I. Stavrakakis, "Study of two-hop message spreading in dtns," in *WiOpt*, 2007.

[46] M. Ibrahim, A. A. Hanbali, and P. Nain, "Delay and resource analysis in manets in presence of throwboxes," *Performance Evaluation*, vol. 64, no. 9-12, pp. 933–947, October 2007.

[47] A. A. Hanbali, A. A. Kherani, and P. Nain, "Simple models for the performance evaluation of a class of two-hop relay protocols," in *Proc. IFIP Networking*, 2007, pp. 191–202.

[48] T. Spyropoulos, K. Psounis, and C. S. Raghavendra, "Efficient routing in intermittently connected mobile networks: The multiple-copy case," *IEEE/ACM Transactions on Networking*, vol. 16, no. 1, pp. 77–90, February 2008.

[49] F. Baccelli and B. Blaszczyszyn, "A new phase transitions for local delays in manets," in *INFOCOM*, 2010.

[50] M. Haenggi, "The local delay in poisson networks," *IEEE Transactions on Information Theory*, vol. 59, no. 3, pp. 1788–1802, March 2013.

[51] Z. Gong and M. Haenggi, "The local delay in mobile poisson networks," [Online]. Available: http://www3.nd.edu/~mhaenggi/pubs/.

[52] B. Williams and T. Camp, "Comparison of broadcasting techniques for mobile ad hoc networks," in *MobiHoc*, 2002.

[53] G. Latouche and V. Ramaswamy, *Introduction to Matrix Analytic Methods in Stochastic Modeling*. ASA-SIAM Series on Statistics and Applied Probability, 1999.

[54] C++ simulator for PD-f MANETs. [Online]. Available: http://researchplatform.blogspot.jp/.

[55] M. Alresaini, M. Sathiamoorthy, and M. J. Neely, "Backpressure with adaptive redundancy (bwar)," in *INFOCOM*, 2012.

[56] O. H. Florin Ciucu and P. Hui, "Non-asymptotic throughput and delay distributions in multi-hop wireless networks," in *Annual Allerton Conference on Communicaiton, Control, and Computing (Allerton)*, 2010.

[57] F. Ciucu, "Non-asymptotic capacity and delay analysis of mobile wireless networks," in *SIGMETRICS*, 2011.

[58] A. A. Hanbali, R. de Haan, R. J. Boucherie, and J.-K. van Ommeren, "A tandem queueing model for delay analysis in disconnected ad hoc networks," in *Proceedings of the 15th international conference on Analytical and Stochastic Modeling Techniques and Applications (ASMTA)*, 2008, pp. 189–205.

[59] A. Jindal and K. Psounis, "Contention-aware performance analysis of mobility-assisted routing," *IEEE Transactions on Mobile Computing*, vol. 8, no. 2, pp. 145–161, February 2009.

[60] R. M. de Moraes, H. R. Sadjadpour, and J. Garcia-Luna-Aceves, "Taking full advantage of multiuser diversity in mobile ad hoc networks," *IEEE Transactions on Communications*, vol. 55, no. 6, pp. 1202 – 1211, June 2007.

[61] E. Altman, T. Basar, and F. D. Pellegrini, "Optimal control in two-hop relay routing," *IEEE Transactions on Automatic Control*, vol. 56, no. 3, pp. 670–675, March 2011.

[62] M. J. Neely and R. Urgaonkar, "Optimal backpressure routing for wireless networks with multi-receiver diversity," *Ad Hoc Networks*, vol. 7, no. 5, pp. 862–881, July 2009.

[63] H. Daduna, *Queueing Networks with Discrete Time Scale: Explicit Expressions for the Steady State Behavior of Discrete Time Stochastic Networks*. Springer, 2001.

[64] A. S. Alfa, *Queueing Theory for Telecommunications: Discrete Time Modelling of a Single Node System.* Springer, 2010.

[65] D. P. Bertsekas and R. G. Gallager, *Data Networks.* New Jersey: Prentice-Hall, Inc., 1992.

[66] C++ simulator for the 2HR-B MANETs. [Online]. Available: http://researchplatform.blogspot.jp/.

[67] The network simulator ns-2. [Online]. Available: http://www.isi.edu/nsnam/ns/.

[68] M. Grossglauser and D. N. Tse, "Mobility increases the capacity of ad hoc wireless networks," in *INFOCOM*, 2001.

[69] D. E. Knuth, *The Art of Computer Programming.* Addison-Wesley, 1998.

[70] X. Lin, G. Sharma, R. R. Mazumdar, and N. B. Shroff, "Degenerate delay-capacity tradeoffs in ad hoc networks with brownian mobility," *IEEE Transactions on Information Theory*, vol. 52, no. 6, pp. 2777–2784, June 2006.

[71] J. Mammen and D. Shah, "Throughput and delay in random wireless networks with restricted mobility," *IEEE Transactions on Information Theory*, vol. 53, no. 3, pp. 1108–1116, March 2007.

[72] E. Perevalov and R. Blum, "Delay-limited throughput of ad hoc networks," *IEEE Transactions on Communications*, vol. 52, no. 11, pp. 1957–1968, November 2004.

[73] J. Liu, X. Jiang, H. Nishiyama, and N. Kato, "Exact throughput capacity under power control in mobile ad hoc networks," in *INFOCOM*, 2012.

[74] L. Georgiadis, M. J. Neely, and L. Tassiulas, "Resource allocation and cross-layer control in wireless networks," *Foundations and Trends in Networking*, vol. 1, no. 1, pp. 1–149, 2006.

[75] C++ simulator for the 2HR-q MANETs. http://distplat.blogspot.com.

[76] X. Hong, M. Gerla, G. Pei, and C.-C. Chiang, "A group mobility model for ad hocwireless networks," in *ACM international workshop on Modeling, analysis and simulation of wireless and mobile systems*, 1999.

[77] C. Zhao and M. L. Sichitiu, "Contact time in random walk and random waypoint: Dichotomy in tail distribution," *Ad Hoc Networks*, vol. 9, no. 2, pp. 152–163, March 2011.

[78] C. Bettstetter, G. Resta, and P. Santi, "The node distribution of the random waypoint mobility model for wireless ad hoc networks," *IEEE Transactions on Mobile Computing*, vol. 2, no. 3, pp. 257–269, 2003.

[79] F. Baccelli, B. Blaszczyszyn, and P. Muhlethaler, "An aloha protocol for multihop mobile wireless networks," *IEEE Transactions on Information Theory*, vol. 52, no. 2, pp. 421–436, February 2006.

[80] S. Kompalli and R. Mazumdar, "On the stability of finite queue slotted aloha protocol," *IEEE Transactions on Information Theory*, vol. 59, no. 10, pp. 6357–6366, October 2013.

[81] L. Jiang and J. Walrand, "A distributed csma algorithm for throughput and utility maximization in wireless networks," *IEEE/ACM Transactions on Networking*, vol. 18, no. 3, pp. 960–972, June 2010.

[82] J. Hwang and S.-L. Kim, "Cross-layer optimization and network coding in csma/ca-based wireless multihop networks," *IEEE/ACM Transactions on Networking*, vol. 19, no. 4, pp. 1028–1042, August 2011.

[83] R. Laufer and L. Kleinrock, "On the capacity of wireless csma/ca multihop networks," in *INFOCOM*, 2013.

[84] C. M. Grinstead and J. L. Snell, *Introduction to Probability: Second Revised Edition.* American Mathematical Society, 1997.

[85] R. A. Horn and C. R. Johnson, *Matrix Analysis.* Cambridge University Press, 1990.

Publications

Jounal Articles

[1] Juntao Gao, Jiajia Liu, Xiaohong Jiang, Osamu Takahashi, and Norio Shiratori. Throughput Capacity of MANETs with Group-Based Scheduling and General Transmission Range., *IEICE Transactions on Communications*, vol.E96-B no.7, pp.1791-1802, July 2013.

[2] Jiajia Liu, Juntao Gao, Xiaohong Jiang, Hiroki Nishiyama and Nei Kato. Capacity and Delay of Probing-Based Two-Hop Relay in MANETs. *IEEE Transactions on Wireless Communications*, vol.11, no. 11, pp.4172-4183, November 2012.

[3] Juntao Gao, Yulong Shen and Xiaohong Jiang. End-to-End Delay Modeling for Mobile Ad Hoc Networks: A Quasi-Birth-and-Death Approach. *Ad Hoc and Sensor Wireless Networks*, *Submitted*, 2013.

[4] Juntao Gao, Yulong Shen, Xiaohong Jiang and Jie Li. Source Delay in Mobile Ad Hoc Networks. *Ad Hoc Networks*, *Submitted*, 2013.

[5] Bin Yang, Juntao Gao, Yuezhi Zhou and Xiaohong Jiang. Delay Control in MANETs with Erasure Coding and f-cast Relay. *Wireless Networks*, *Submitted*, 2013.

Conference Papers

[6] Juntao Gao and Xiaohong Jiang. Delay Modeling for Broadcast-Based Two-Hop Relay MANETs. IEEE 11th International Symposium on Modeling and Optimization in Mobile, Ad Hoc, and Wireless Networks (WiOpt), Tsukuba Science City, Japan, 13-17 May, 2013.

[7] Juntao Gao, Jiajia Liu, Xiaohong Jiang, Osamu Takahashi and Norio Shiratori. Exact Capacity Study for A Class of MANETs. IEEE/CIC International Conference on Communications in China (ICCC), Beijing, China, 15-18 August, 2012.

[8] Bin Yang, Juntao Gao, Yuezhi Zhou and Xiaohong Jiang. Two-Hop Relay Algorithm with Packet Redundancy and Erasure Coding in MANETs. IEEE/CIC International Conference on Communications in China (ICCC), Xi'an, China, 12-14 August, 2013.

[9] Jiajia Liu, Juntao Gao, Xiaohong Jiang, Hiroki Nishiyama and Nei Kato. Probing-Based Two-Hop Relay with Limited Packet Redundancy. IEEE 13th International Conference on High Performance Switching and Routing (HPSR), Belgrade, Serbia, 24-27 June, 2012.